9.05 Water in the Evolution of the Earth and Other Terrestrial Planets

S Karato, Yale University, New Haven, CT, USA

9.05.1 Introduction

The Earth is a unique planet. As far as we know, it is the only planet where life has evolved and where plate tectonics operates. It is generally believed that this is in large part due to the presence of a certain amount of liquid water on its surface for most of its history (e.g., Langmuir and Broecker, 2012). Furthermore, the amount of water that Earth has on its surface appears to be just right for life to evolve: if Earth had much more or less water, then life would not have evolved or would have been more difficult to evolve (e.g., Maruyama et al., 2013). Consequently, one of the important questions in the study of the Earth as a terrestrial planet is how did Earth get that amount of water and how has Earth kept the ocean on its surface for such a long time? To what extent is it a natural consequence of formation and evolution of planets, and to what extent did it happen by chance?

To answer these questions, one needs to understand the physics and chemistry of behavior of water and other volatiles during planetary formation and evolution and analyze geologic, geochemical, and geophysical observations to obtain some

observational constraints. The purpose of this chapter is to review these two issues.

Planets are formed as a by-product of star formation (e.g., Hayashi et al., 1985; Safronov, 1972). Therefore, the source materials of planets are essentially the same as that of a star with which they are associated. In the case of the solar system, the composition of the Sun can be estimated from the spectroscopic studies of its outer convective layer and is dominated by the volatile elements such as H, He, C, and N (**Figure 1(a)**; Lauretta, 2011). These are the source materials from which planets were formed. Some of them (H, C, O, N, P, and K) are the key elements of life and others are essential ingredients of rocks (Mg, Si, O, Fe, Ca, and Al). The theory of formation of elements shows that the presence of these elements is a natural consequence of nucleosynthesis during the Big Bang and subsequent star evolution (Burbidge et al., 1957; Langmuir and Broecker, 2012). Indeed, the chemical composition of one of the most primitive materials in the solar system (carbonaceous chondrite) shows a similarity to the solar composition except for the volatile elements that are depleted relative to the solar abundance (**Figure 1(b)**).

Therefore, it is critical to understand how and to what extent volatile elements are depleted during planetary formation and evolution. Recall that the amount of volatile elements to make a 'wet' planet like the Earth is not large. The mass of the ocean on Earth is ~0.023 wt% of the total mass (~0.033 wt% of the mantle). This means that even 99% of depletion of water from the carbonaceous chondrite (likely the source materials for terrestrial planets in the solar system) still makes a planet 'wet' (~5 ocean mass of water). Note that even a small amount (~0.01–0.1 wt%) of volatiles such as hydrogen affects two of the key properties of rocky materials, namely, rheological properties (e.g., Karato and Jung, 2003; Mei and Kohlstedt, 2000a,b) and melting relationships (e.g., Dasgupta and Hirschmann, 2006; Hirschmann, 2006; Inoue, 1994; Kushiro et al., 1968), that control the dynamics and evolution of terrestrial planets. Although a small amount, it is these volatile elements that control the surface conditions of terrestrial planets where life might evolve (e.g., Abe et al., 2011; Langmuir and Broecker, 2012; van Thienen et al., 2007). Consequently, it is critical to understand how much of volatile elements are acquired to a growing planet and how they may be circulated during the long-term evolution of a planet.

Plausible processes that might control the volatile acquisition and circulation in a planet are schematically summarized in **Figure 2** (see also **Table 1**). They include (i) condensation from the primitive solar nebula, (ii) collisions of planetary embryos including later-stage collisions of relatively large planetary bodies ('giant impacts'), (iii) magma ocean formation and crystallization and interaction of magma ocean with the atmosphere, (iv) core formation, and (v) long-term evolution of atmosphere–hydrosphere coupled with mantle convection and core cooling. Each of these processes (or groups of processes) involves microscopic physics and chemistry and meso- to macroscopic processes that control the large-scale distribution of volatiles. **Table 1** provides a brief summary of each process and issues to be discussed in some detail in this article.

Among various volatile elements, hydrogen has strong influence on some of the key physical and chemical properties (e.g., rheological properties of rocks and melting relationships), and consequently, hydrogen distribution has strong feedback to geodynamic processes. The strong influence of hydrogen on

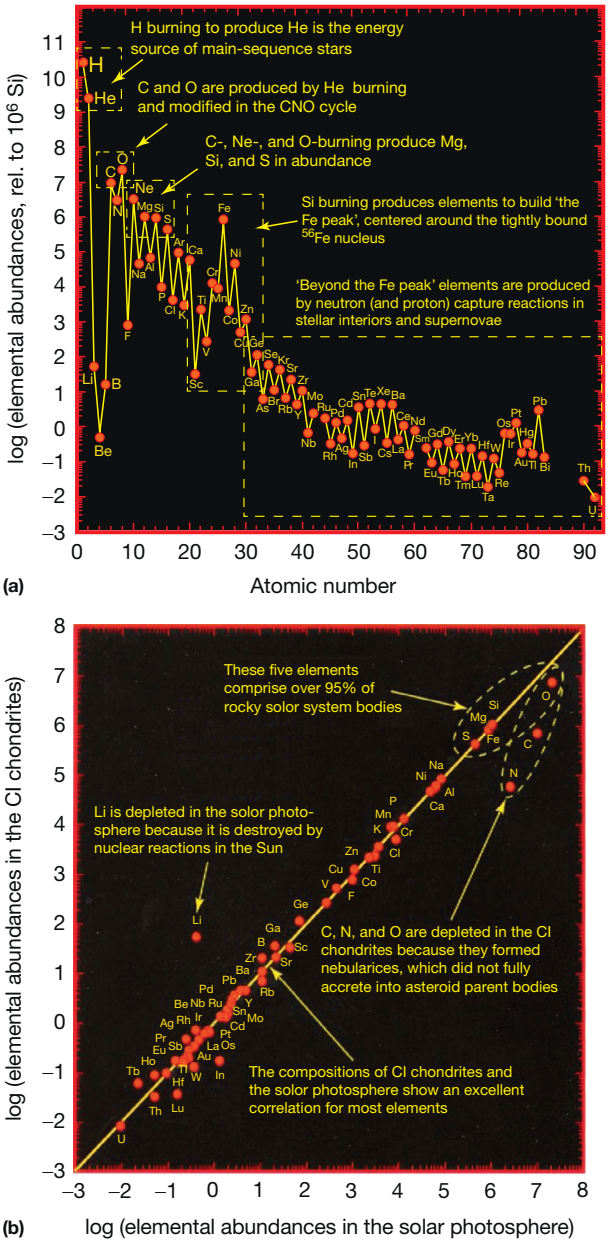

Figure 1 (a) Cosmic abundance of elements. (b) Abundance of element in carbonaceous chondrite. Cosmic abundance reflects processes of element synthesis, while abundance of elements in carbonaceous chondrite shows systematic depletion in volatile elements (elements with low condensation temperature). Reproduced form Lauretta DS (2011) A cosmochemical view of the solar system. *Elements* 7: 11–16.

some physical properties also allows us to infer hydrogen distribution using some geophysical observations (e.g., Karato, 2011). Therefore, the focus will be placed on hydrogen (water). However, a brief discussion on other volatile elements such as carbon will also be presented where appropriate. The factors controlling volatile distribution include equilibrium thermodynamic properties of volatiles such as the partitioning coefficients of volatile elements between two coexisting phases, diffusion coefficients of volatiles in minerals, and the meso- to macroscopic processes by which materials containing volatile elements are transported.

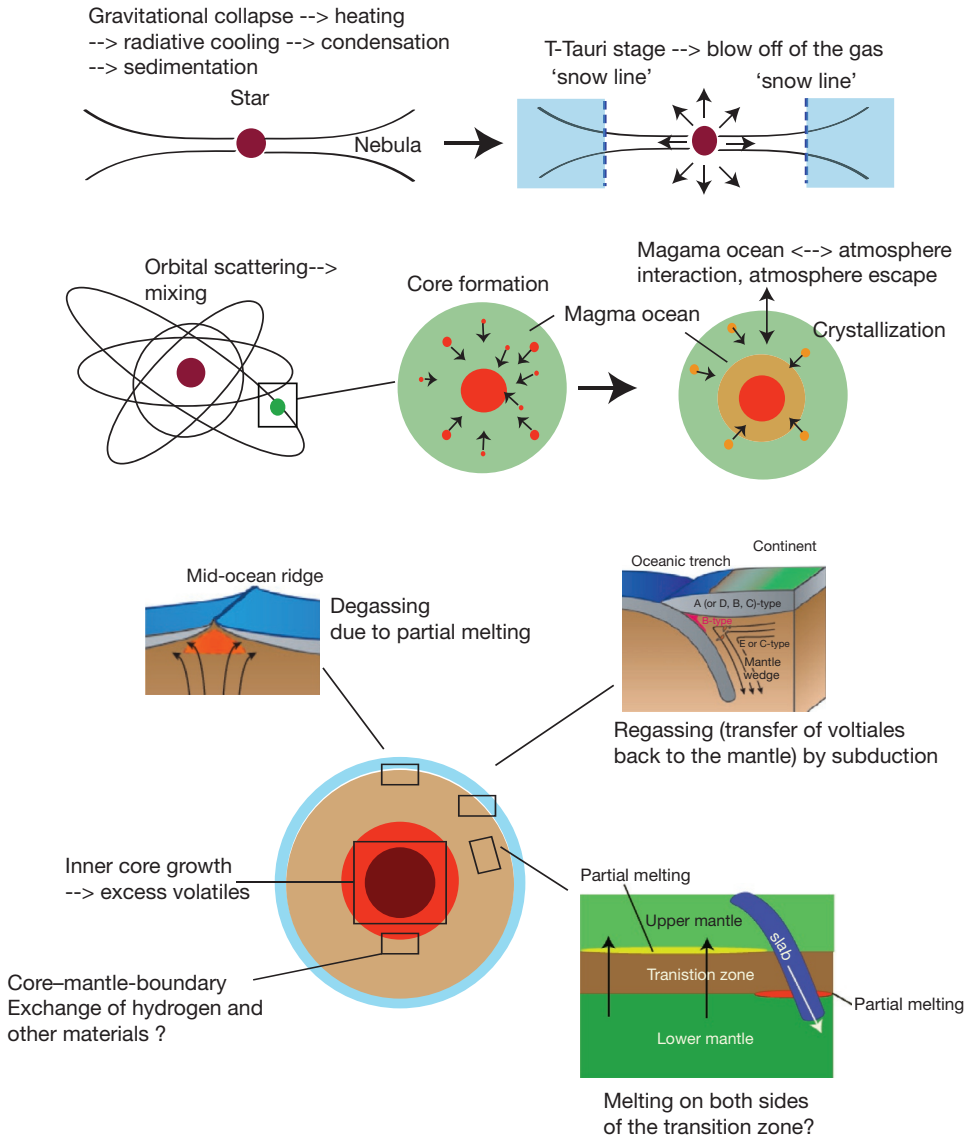

Figure 2 A schematic diagram of possible process controlling the volatile distribution in planets.

There are two aspects in doing such a study. First, it is important to identify the processes by which volatile content (and its distribution) in terrestrial planets might be controlled. Second, it is critical to estimate, based on a range of observations, how much volatiles are in the terrestrial planets and how these volatiles are distributed in space and time (evolution). Because a large amount of data are available for Earth, my discussion will be naturally focused on Earth, but issues of volatiles in other terrestrial planetary bodies including the Moon, Venus, Mars, and meteorites will also be discussed.

9.05.2 Equilibrium and Transport Properties (Processes) Relevant to Volatile Distribution

9.05.2.1 General Introduction

Volatile distribution is affected by phase transformations, notably by those among different states of matter. For a given matter, there are three different states (gas, liquid, and solid), and one can think of transformations among three different combinations of two states: gas↔solid, solid↔liquid, and liquid↔gas (Figure 3). The first one (gas↔solid) is studied in cosmochemistry, while the second one (solid↔liquid) is discussed in geochemistry/petrology. Because the solubility of volatiles is different among different phases (see Section 9.05.2.3), changes in volatile distribution will occur upon these phase transformations. For instance, condensation will reduce the water component unless condensed materials are hydrous minerals such as ice and serpentine. Similarly, by partial melting (solid↔liquid transformation), a substantial amount of volatile is lost from the rock. In contrast to these two processes that have been studied in cosmochemistry and geochemistry (petrology), respectively, the third process, that is, gas↔liquid transformation, has never been studied in detail (except for Ebel and Grossman, 2000). As I will review later (see also Karato, 2013a), the gas↔liquid phase transformation may play an important role in some processes of planetary formation.

Table 1 Various processes in planetary evolution that may control the volatile budget

	Processes	*Questions*
Condensation	Heating by gravitational collapse +radiation from the star Cooling of the protoplanetary nebula Condensation Transport of condensed matter	Where is the 'snow line' (how does it depend on the properties of the star and the nebula)? Do condensed matters ('planetesimals') acquire enough volatiles within the snow line to make a 'wet' planet like the Earth?
Collisions	Degassing by collisions Orbital scattering	How much heating has occurred by collisions? What is the extent of orbital scattering and when?
Magma ocean	Melting Solidification Magma ocean–atmosphere interaction	How does a magma ocean interact with the (proto)atmosphere? To what extent is a planet chemically stratified by the solidification of a magma ocean?
Core formation	Small-scale (equilibrium) separation Large-scale (nonequilibrium) separation	How much volatiles did the core acquire during the core formation? How can we infer the hydrogen content in the core?
Long-term evolution	Mantle convection (phase transformations) Core cooling Degassing (volcanism), regassing (subduction) Atmospheric escape	How are volatile elements distributed in Earth and other terrestrial planets? When was the ocean formed? How has the ocean mass changed with time? How does the regassing (degassing) rate change with time? What is the nature of feedback between mantle convection and mantle (and surface) volatiles? Are there internal processes in the mantle (and core) to regulate the ocean mass? How much is the atmospheric escape (how do we explain D/H of different planetary bodies)?

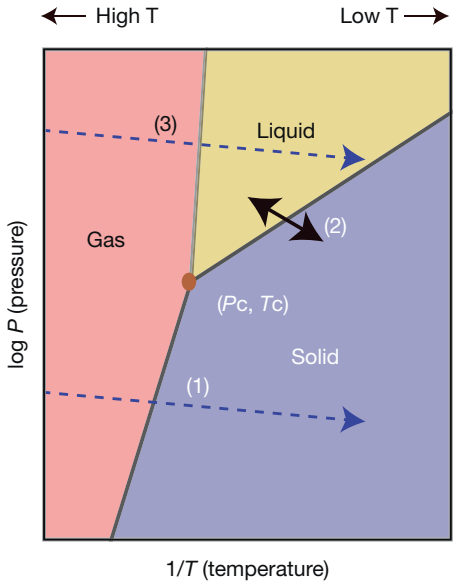

Figure 3 A schematic gas–liquid–solid phase diagram. Gas ↔ solid transitions are usually studied in cosmochemistry. Solid ↔ liquid transitions are usually studied in geochemistry. Gas ↔ liquid transitions are not studied extensively, but will play an important role in a relatively high-pressure environment. Above certain pressure, gas and liquid states become indistinguishable. This condition is referred to as the critical point. This region is not included in this figure because the focus is condensation that occurs at relatively low pressures.

In most cases, the equilibrium properties (e.g., element partitioning coefficients) have important influence on the volatile distribution associated with these processes. Therefore, I will provide a brief review on this subject. However, properties or processes of transport of volatiles must also be considered in order to interpret various observations properly. For example, Keppler and Bolfan-Casanova (2006) and Inoue et al. (2010) discussed that equilibrium partition coefficients of water may control the actual distribution of water, explaining a higher water content in the transition zone than in the upper or the lower mantle by the different hydrogen solubility. Such an argument is unlikely valid, however, because diffusion is very inefficient in transporting elements to a large scale (even hydrogen, the diffusion distance for ~1 Gyr is ~1–10 km in most part of the Earth's mantle). Consequently, without any large-scale mass transport, the distribution of some elements cannot change from one region to another at a scale larger than ~100 km. In other words, if a large difference in composition between different regions (with large size, ~100 km or more) of the Earth (and other terrestrial planets) was identified, it would imply the presence of large-scale processes to segregate materials, for example, partial melting and resultant melt–solid separation.

9.05.2.2 Condensation

At high enough temperatures, all elements assume gaseous state where entropy is large (in various molecular species, H, H_2, CO, SiO, etc.). When a hot gas is cooled, then the energy reduced by forming chemical bonding exceeds the amount of entropy obtained in a gaseous state, and a condensed phase will be formed. Let us consider an element E that condenses from the protoplanetary nebula that is dominated by hydrogen molecules. Let us assume the chemical equilibrium between the gas and a condensed phase containing the element E and also that the element E is a minor element compared with H (hydrogen) and behaves as an ideal gas in the gas phase. Then, applying the law of mass action, one can show that the fraction of condensation of element E, α_E, is related to temperature and total pressure of the gas as (e.g., Grossman and Larimer, 1974; Larimer, 1967)

$$\ln(1-\alpha_E) = -\frac{\Delta G_E}{RT} - \ln f_E - \ln\frac{P_T}{P_o} \quad [1]$$

where f_E is the molar fraction of element E in the gas, ΔG_E is the Gibbs free energy difference of element E between gas state and condensed state (this represents the bonding strength), R is the gas constant, T is temperature, and P_T is the total pressure (P_o is the reference pressure at which ΔG_E is defined). Condensation starts at a certain temperature, T^E_{oo}, where $\frac{\Delta G_E}{RT^E_{oo}} + \ln f_E + \ln\frac{P_T}{P_o} = 0$ and the fraction of condensed matter decreases sharply with further cooling because $\Delta G_E \gg RT$ (Figure 4). In most cases, the *condensation temperature* (T^E_{cond}) of an element E is defined as a temperature at which the fraction of condensed matter is 50% ($\alpha_E = 0.5$):

$$T^E_{cond} = \frac{\Delta G_E}{R\left(0.693 - \ln f_E - \ln\frac{P_T}{P_o}\right)} \quad [2]$$

As one can see from this equation, an element with a small ΔG_E (weak chemical bonding) has a low condensation temperature. These are called volatile elements. Note that the condensation temperature also depends on the total pressure P_T.

Urey was one of the first scientists who studied the physics and chemistry of condensation to understand the chemistry of planets (see Chapter 4 of Urey, 1952). Systematic studies on condensation in the primitive solar nebula were made in the early 1970s (e.g., Grossman, 1972; Grossman and Larimer, 1974; Figure 4). Those calculations were successful in explaining a variety of chemical compositions of meteorites and to some extent the compositions of terrestrial planets (Lewis, 1972, 1974). In particular, Grossman and Larimer (1974) were able to explain a variety of compositions of meteorites including the presence of calcium-rich inclusions in Allende meteorite (carbonaceous chondrite) and the Fe content of some of the meteorites.

However, these calculations are not so successful in explaining the abundance of volatile components. Grossman and Larimer (1974) discussed that the abundance pattern of volatile elements (Ag, Pb, Bi, In, Tl, and Zn) in carbonaceous chondrites cannot be explained by the equilibrium model of condensation by assigning a single condensation temperature and suggested that these meteorites were formed by the mixing of materials with different degrees of volatile depletion (different condensation temperatures). This suggests orbital scattering (variation in the eccentricity of orbits) during the processes of planetary formation as I will discuss later. However, no detailed calculations were made on the condensation of hydrous minerals because of the lack of reliable data on the kinetics of condensation.

There are a few issues on the condensation of volatile elements. The volatility (condensation temperature) of a given element depends on the condensed phase to which the element condenses (for a given element, there are several possible condensed phases). For instance, for hydrogen, if ice (H_2O) is the condensed phase to which hydrogen condenses first, then the condensation temperature for a typical solar nebula conditions is ~170 K (this defines the 'snow line'; see Section 9.05.5). However, hydrogen could condense as other more refractory materials such as serpentine ($Mg_3Si_2O_5(OH)_4$) or brucite ($(Mg(OH)_2$) could. In these cases, the condensation temperature would be much higher, and one would expect to have a nonnegligible amount of water even within the 'snow line.' However, in many of the previous studies, condensation of hydrogen into these hydrous minerals was not included because it was considered that the kinetics to form these phases is slow. Actual condensation temperature of hydrogen is important in understanding how hydrogen is acquired in a growing terrestrial planet. This issue will be discussed later.

By the same token, the volatility (condensation temperature) of S (and Se) depends on the fugacity of hydrogen. Dominant gaseous phase containing S or Se is H_2S or H_2Se, and therefore, at low hydrogen content, the vapor pressure is low that makes S and Se less volatile. Ringwood (1979) explained anomalously high concentration of S and Se in the lunar rocks by a low hydrogen fugacity (compared with the

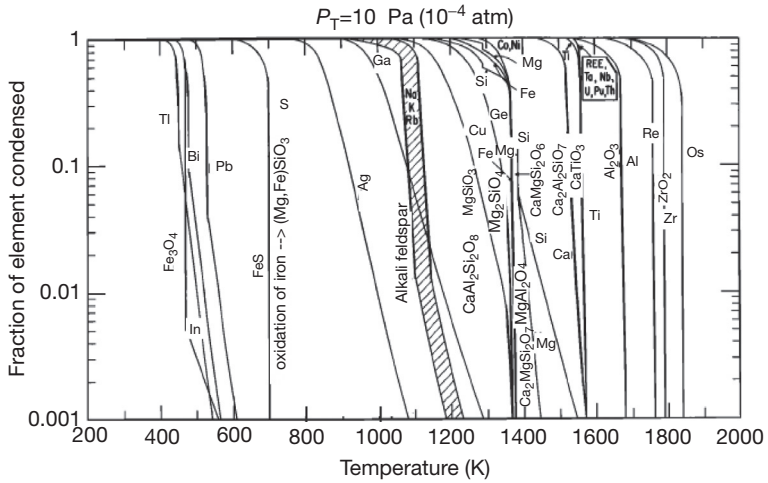

Figure 4 Condensation of various elements. A given element starts to condense at a certain temperature and the fraction of condensed material increases rapidly with decreasing the temperature. 'Condensation temperature' is often defined as a temperature at which 50% of the element is condensed. Reproduced from Grossman L and Larimer JW (1974) Early chemical history of the solar system. *Review of Geophysics and Space Physics* 12: 71–101.

hydrogen fugacity in the primitive solar nebula) in which lunar materials were condensed.

Also important is if one treats the system as an open or a closed system. The question of open versus closed system is partly related to the transport of condensed matter. When condensed materials are formed in the nebula, they will migrate due to gravity and by the pressure caused by radiation. Many of them sink to the equatorial plane but some may migrate to the Sun (e.g., Cassen, 1996). If this migration is effective, then the composition of the system we are considering will change immediately after the condensation of some materials occurs. Orbital scattering changes the eccentricity of orbits of any condensed bodies (particularly the large bodies; Kokubo and Ida, 2000; Morbidelli et al., 2000) and will also affect the composition of planetary materials (see **Section 9.05.5**).

9.05.2.3 Solubility of Volatiles in the Condensed Matter

After a terrestrial planet is formed, the most important processes to redistribute volatile elements are melting and solidification (solid↔liquid transitions) (**Figure 3**). For instance, the magma ocean formed in the early stage of planetary evolution could contain a substantial amount of volatiles. Upon solidification, volatiles will be redistributed, and the way in which volatiles are redistributed is controlled by (i) the partition coefficients (solubility ratios) of volatiles between solids and liquids and by (ii) the mode of solid and liquid separation. Also, after the magma ocean was completely solidified, then partial melting in some regions of the planet will redistribute the volatile elements. Similar to the solidification from the magma ocean, the key factors controlling the volatile distribution upon partial melting are (i) the partition coefficients of volatile elements between solid and liquid and (ii) the mode of liquid–solid separation.

The partition coefficients are the ratio of concentration of an element between two phases and are essentially controlled by the solubility of that element in two phases. Since a gas can dissolve any species to a large degree, the partitioning of an element between the gas phase and a condensed phase (solid or liquid) is essentially controlled by the solubility of that element in the condensed phase. The basic physics of solubility is similar to condensation, but an important difference is that in solubility, we consider an element in a condensed phase as an impurity.

Such a reaction can be written schematically as

$$r{\cdot}Y(\mathrm{X})_{(\mathrm{gas})} + A_{(\mathrm{solid,\ liquid})} \leftrightarrow A(\mathrm{X})_{(\mathrm{solid,\ liquid})} \qquad [3]$$

where Y(X) is a gaseous phase containing a volatile element X (e.g., H_2O), r is a coefficient that depends on the nature of impurity X in the condensed matter and on the dominant volatile species where the element X occurs in the gas, and A(X) is a condensed phase (olivine, basaltic melt, etc.) that contains element X as an impurity. Assuming a small concentration of dissolved element for which the chemical potential of A(X) is given by $\mu_{A(\mathrm{X})} = \mu^0_{A(\mathrm{X})} + RT\log[\mathrm{X}]$, one finds

$$[\mathrm{X}] = B{\cdot}f_{\mathrm{Y}}^{r}(P,T){\cdot}\exp\left(-\frac{\Delta E + P\Delta V}{RT}\right) \qquad [4]$$

where B is a constant, f_Y is the fugacity of the gaseous phase that contains an element X (Y(X)), ΔE (ΔV) is the energy (volume) difference between material A(X) and A, and other symbols have their usual meaning. The exponent r depends on the nature of chemical reaction including the molecular species of the volatile in the gas and the nature of atomic species dissolved in the condensed matter. When hydrogen exists as water in the gas ($Y = H_2O$) and hydrogen is dissolved in the condensed phase as OH, then $r = 1/2$. Both the fugacity of the volatile species ($f_X(P,T)$) and $\exp\left(-\frac{\Delta E + P\Delta V}{RT}\right)$ term strongly depend on pressure and temperature. Consequently, the volatile solubility strongly depends on pressure and temperature.

The solubility of various volatile elements (H, C, etc.) has been determined for both solid minerals and melts. Microscopic mechanisms of dissolution of volatile elements have also been studied using various spectroscopic methods (e.g., infrared spectroscopy) and theoretical calculations, as well as from the parameters in relation [3] (particularly r and ΔV).

The important results are summarized as follows:

(1) Volatile elements such as H and C can be dissolved in condensed phases in a variety of forms (e.g., OH, H_2, H_2O, hydrogen-related point defects, C, CO_2, and carbon-related point defects).
(2) Solubility of volatile elements such as H and C in melts is much higher than that in solids except for hydrous minerals or carbonates (e.g., McMillan, 1994; Ni and Keppler, 2013).
(3) Hydrous minerals and carbonates can contain a large amount of volatiles (to ~10 wt% or more), but they are stable only at relatively low-temperature conditions such as in and/or near subduction zones (**Figure 5**; the actual stability of a given phase depends also on the total chemistry of a rock and could be narrower) (e.g., Ohtani, 2005; Williams and Hemley, 2001).
(4) Under high-temperature and high-pressure conditions, most of H occurs as an impurity (point defects) in 'nominally anhydrous minerals' (minerals that do not have H in their chemical formula, e.g., Mg_2SiO_4) (e.g., Karato, 2008a; Kohlstedt et al., 1996) (**Figure 6**).
(5) The solubility of H in nominally anhydrous minerals is mineral-specific (for review, see Bolfan-Casanova, 2005; Ingrin and Skogby, 2000; Karato, 2008a). For minerals in the Earth's transition zone (~410–660 km depth), the solubility is quite high (to a few wt%). The solubility of H in the upper mantle minerals is up to ~0.1 wt%. The solubility of H in the lower mantle minerals is not precisely known, but for (Mg,Fe)O and (Mg,Fe)SiO_3 perovskite, the solubility of H is comparable with or less than that in the upper mantle minerals. The solubility of H in $CaSiO_3$ perovskite could be higher but not well constrained. As a consequence, there is a marked depth variation in H solubility (**Figure 7**) that promotes partial melting (Bercovici and Karato, 2003; Ohtani et al., 2004). The solubility of H in iron is very large, leading to the molecular ratio of H/Fe ~ 1 (e.g., Fukai and Suzuki, 1986; Okuchi, 1997). The core is potentially the largest hydrogen reservoir on Earth. However, the actual amount of H in the core depends on the processes of core formation, particularly the relative timing of volatile acquisition and core formation (see **Section 9.05.5**; Ohtani et al., 2005; Rubie et al., 2007). Similarly, the actual amount of H in the mantle is likely different from the solubility limit (see **Section 9.05.4**).

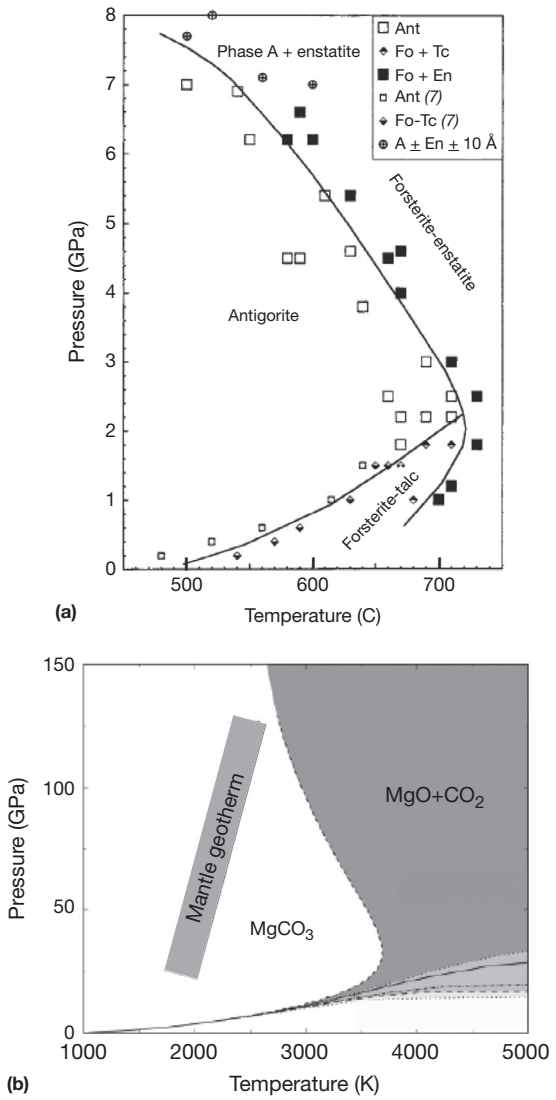

Figure 5 (a) Stability of serpentine (reproduced from Ulmer P and Trommsdorff V (1995) Serpentine stability to mantle depths and subduction-related magmatism. *Science* 268: 858–861). (b) Stability field of magnesite (reproduced from Fiquet G, Guyot F, Kunz M, Matas J, Andrault D, and Hanfland M (2002) Structural refinements of magnesite at very high pressure. *American Mineralogist* 87: 1261–1265).

(6) Hydrogen is dissolved in a mineral in various types of point defects (Nishihara et al., 2008). Hydrogen-related point defects with a small concentration often control the physical properties such as electrical conductivity and rheological properties (Karato, 2006a).

(7) The solubility of carbon in 'nominally ancarbonaceous minerals' (minerals that do not have C in their chemical formula, e.g., Mg_2SiO_4) is much less than that of hydrogen in nominally anhydrous minerals (Shcheka et al., 2006).

(8) The parameters characterizing the solubility (r, ΔE, and ΔV in eqn [3]) depend on the mechanism of dissolution, and consequently, the pressure, temperature, and fugacity dependence of solubility are different among different solubility mechanisms (e.g., Bolfan-Casanova, 2005; Karato, 2008a).

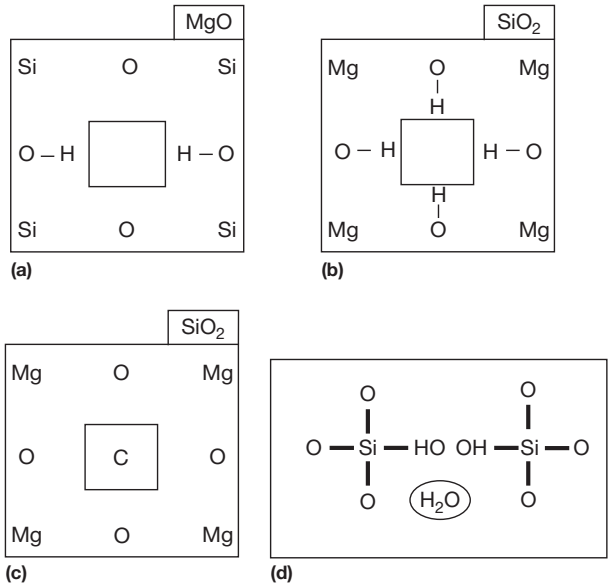

Figure 6 Atomistic models of dissolution of hydrogen and carbon. (a, b) Models of hydrogen dissolution in silicate minerals. (c) A model of carbon dissolution in silicate mineral. (d) Models of dissolution of water in silicate melt (silicate melts could dissolve water either as OH or as H_2O). Reproduced from Karato S (2008a) *Deformation of Earth Materials: Introduction to the Rheology of the Solid Earth*, p. 463. Cambridge: Cambridge University Press.

(9) When two (or more) volatile elements (e.g., H and C) coexist, then the solubility of each element into a condensed phase depends on the nature of chemical reaction among them. In this particular case, because both H and C react with O (oxygen), oxygen fugacity also affects the solubility (Ni and Keppler, 2013).

These results form a basis for any discussions on the volatile distribution in terrestrial planets. For instance, the solubility ratios define the element partitioning coefficients that affect how volatiles are redistributed during various processes in planetary evolution. However, these data themselves do not provide direct constraints on the actual distribution of volatile elements. The actual distribution of volatile elements at a large scale (say, >100 km) depends strongly on the processes of evolution of planets because, in many cases, large-scale (>100 km) distribution of elements in a planetary body is not controlled by thermochemical equilibrium. In fact, a numerical study by Richard et al. (2002) showed little or no influence of large water solubility in the transition zone on the nature of global water circulation. This is due to the fact that their model does not include large-scale processes of water redistribution such as partial melting and subsequent melt segregation. In the next section, I will review some properties and processes that may control the actual distribution of volatile elements in a planet.

9.05.2.4 Transport of Volatiles

9.05.2.4.1 Diffusion

Any elements may be transported by diffusion if there is a chemical potential gradient such as the gradient in

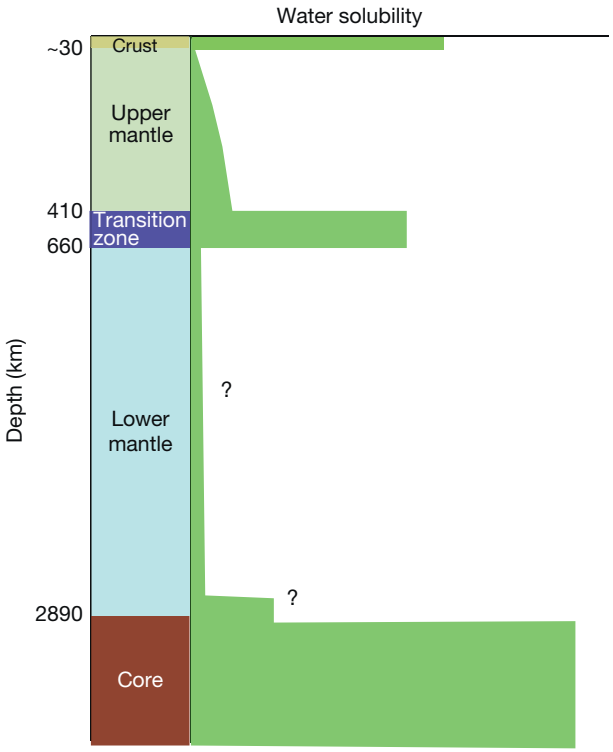

Figure 7 The solubility of water (hydrogen) in the Earth's interior. Water (hydrogen) solubility in minerals changes with depth due to the change in pressure and temperature, chemical layering and to the phase transformations. The water solubility has a peak in the mantle transition zone (~2–3 wt%). The water solubility in the lower mantle minerals is not well constrained. The hydrogen solubility in the core is large. The actual upper limit of hydrogen (water) in minerals can be lower than the solubility if water-bearing phase is not pure water vapor (e.g., a silicate melt). In such a case, the water fugacity in the system is less than the maximum water fugacity of pure water, and the amount of water (hydrogen) that can be present in minerals is smaller. The amount of water (hydrogen) in minerals in these cases is the actual limit of water (hydrogen) content and is often referred to the 'water storage capacity.' The water storage capacity not only is the property of a mineral itself but also depends on the bulk composition of the system.

concentration. Diffusion coefficients of various species in minerals are summarized in Figure 8. Diffusion coefficients vary among various species by as much as ~10 orders of magnitude at the same condition. H (hydrogen) has the fastest diffusion coefficients among them, and hence, in some cases, hydrogen content in minerals corresponds to that at near-equilibrium conditions. However, even for hydrogen, the variation in its concentration at a large scale cannot be controlled by diffusion-controlled chemical equilibrium. To see this, let us calculate the diffusion distance for several atomic species. The length scale of chemical equilibrium attained by diffusion can be given as

$$l \approx 2\sqrt{Dt} \qquad [5]$$

where D is the diffusion coefficient and t is the time. Hydrogen has the highest diffusion coefficients among various elements and hence has the longest diffusion distance.

Figure 9 shows diffusion distance for various elements as a function of timescale. It is seen that in no case diffusion, length becomes larger than ~100 km for the age of the Earth, and it is concluded that chemical heterogeneity with larger than ~100 km space scale will persist and needs to be explained by initial conditions or by transport of matter by processes other than diffusion. However, regarding the chemical equilibrium during partial melting, space scale is different. Here, we consider the exchange of materials at the scale of each grain (several millimeters) when melt–solid separation occurs by percolation. In these cases, chemical equilibrium may be attained for some elements (see Section 9.05.2.4.2).

In defining 'diffusion coefficients,' one should note the difference between isotope (self-) diffusion and chemical diffusion. When hydrogen diffuses from one region of mineral (or rock) to another driven by the concentration gradient, the transport of hydrogen involves the transport of another charged species and it is called chemical diffusion. In such a case, when hydrogen (proton) moves from one region to another, there must be the movement of other species to maintain the charge neutrality. Consequently, the chemical diffusion coefficient is a harmonic average of self-diffusion coefficient of hydrogen and that of another charge-compensating species. In a given mineral, hydrogen can be dissolved in a few different species and each of them has a different diffusion coefficient (mobility). Evidence for multiple hydrogen-bearing species was reported by Nishihara et al. (2008) and the presence of multiple species with different diffusion coefficients explains the observed differences between isotope diffusion of hydrogen (H/D diffusion) and hydrogen-assisted electrical conductivity (see Section 9.05.3.4; Karato, 2013b).

9.05.2.4.2 Melt–solid separation

9.05.2.4.2.1 Compaction

Given the inefficient transport of volatile elements by diffusion even for hydrogen, large-scale transport of volatile elements must involve meso- to macroscopic relative motion of materials. One case is the removal of melt from solid by gravity-induced compaction. When the melt density is different from the solid density, melt tends to be segregated from solid if melt is interconnected. This process is controlled by the melt permeability and plastic deformation of the solid matrix. The processes of melt segregation (compaction) can be characterized by two parameters (e.g., McKenzie, 1984; Ribe, 1985; Richter and McKenzie, 1984): the compaction length,

$$\delta_{\mathrm{comp}} = \sqrt{\frac{k\eta_{\mathrm{s}}}{\eta_{\mathrm{m}}}} \approx 10 \text{ m}, \qquad [6]$$

and the compaction time,

$$\tau_{\mathrm{comp}} = \frac{1}{\Delta\rho \cdot g}\sqrt{\frac{\eta_{\mathrm{m}}\eta_{\mathrm{s}}}{k}} \approx 1 \text{ Myr} \qquad [7]$$

where k is the permeability of melt through solid matrix ($\sim 10^{-17}$ m^2), η_{s} is the viscosity of solid matrix ($\sim 10^{18}$ Pa s), η_{m} is the viscosity of melt (~1 Pa s), $\Delta\rho$ is the density difference between melt and solid (~300 kg m^{-3}), and g is the acceleration due to gravity (~10 m s^{-2}). I conclude that compaction is efficient in most of the cases.

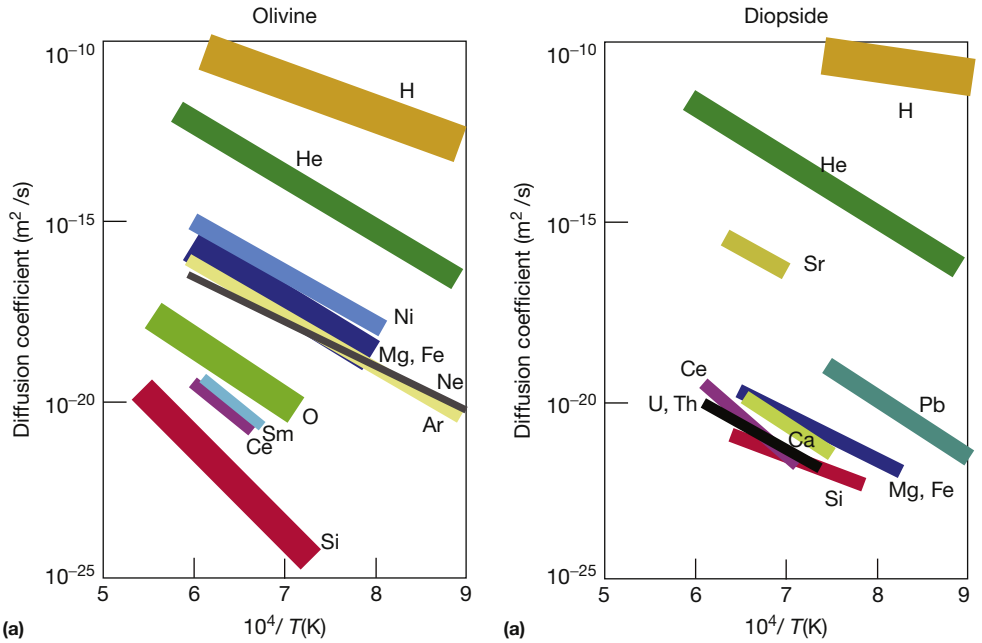

Figure 8 Diffusion coefficients of various elements in olivine ($(Mg,Fe)_2SiO_4$, Fe/(Fe+Mg)$\sim$0.1) and clinopyroxene (diopside ($CaMgSi_2O_6$)) at room pressure or $P\sim1$ GPa. Data: olivine (Baxter, 2010; Chakraborty, 2010; Farver, 2010) and diopside (Baxter, 2010; Cherniak and Dimanov, 2010; Farver, 2010). Results are applicable to shallow regions of the Earth (and other planets, $P<2$–3 GPa). Diffusion coefficients in a mineral depend strongly on diffusing species, and therefore, the degree to which chemical equilibrium is attained during melting (melt segregation) depends on species. Most of 'trace elements' in the upper mantle reside in diopside, and therefore, the diffusion coefficients in diopside control the mode of melt segregation. Hydrogen redistribution upon partial melting is likely controlled by diffusion in olivine (and orthopyroxene).

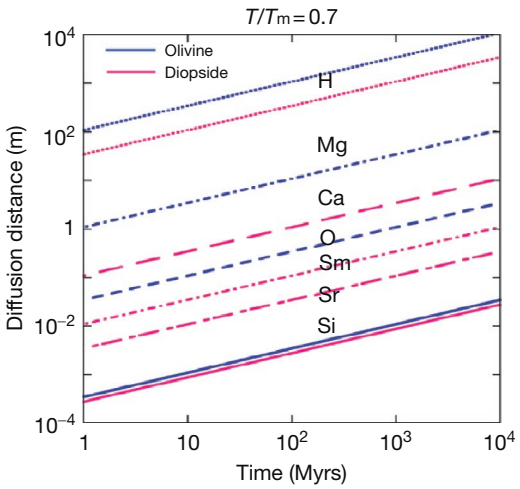

Figure 9 Diffusion distance of various elements in olivine and clinopyroxene (diopside). T, temperature; T_m, melting temperature. $T/T_m=0.7$ is a typical mantle condition. Diffusion distance of hydrogen is plotted as a function of time. In most cases, diffusion distance is small compared to global structures ($\sim$100–1000 km), and any heterogeneity or layering in composition at the global scale implies large-scale material segregation. Diffusion of H at the core–mantle boundary might be an exception. If pressure effects on hydrogen diffusion are small, the diffusion distance of H will be large ($\sim$100 km or more) at the core–mantle boundary and substantial exchange of hydrogen between the core and the mantle.

9.05.2.4.2.2 Chemical equilibrium during melt–solid separation

When melt and solid segregate, chemical equilibrium between them may not be maintained. In order to understand the influence of melt extraction, the mode of melt segregation is often classified into two categories, *batch melting* and *fractional melting*. Batch melting is a process where melt formed from the solid rock migrates slowly in the solid matrix so that whole melt is always in equilibrium with whole solid. So this may be called equilibrium melting. Fractional melting is opposite where melt migrates so fast that chemical equilibrium between melt and solid is attained only locally at the melt–solid interface. Fractional melting can remove incompatible elements (e.g., volatile elements) more efficiently from the original rock. A parameter to characterize the mode of melt segregation is the ratio of diffusion timescale and timescale of melt–solid contact (Iwamori, 1993), that is,

$$\psi \equiv \frac{d^2 \upsilon}{DL} \qquad [8]$$

where d is the grain size, D is the diffusion coefficient of a relevant species, υ is the velocity of solid moving through a partially molten layer, and L is the thickness of the partially molten layer. If $\psi \gg 1$, then diffusion is so slow that melt will migrate through solid without much exchange of materials (fractional melting). If, on the other hand, $\psi \ll 1$, then chemical equilibrium will be attained during the melt separation (batch melting) (Figure 10). It can be seen that the mode of melt segregation strongly depends on diffusion coefficients.

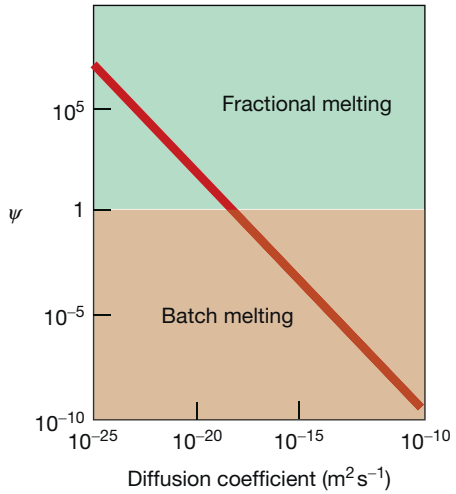

Figure 10 Mode of melt–solid separation. The mode of melting can be classified into batch (equilibrium) melting and fractional (disequilibrium) melting. Whether batch melting or fractional melting occurs is largely controlled by a nondimensional parameter ψ that is a ratio of timescale of diffusion and melt migration through a solid column. If $\psi \ll 1$, then the batch melting occurs; otherwise, fractional melting occurs. Because this parameter depends strongly on the diffusion coefficients and diffusion coefficients vary largely among different species, the mode of melting is likely different among different atomic species. Grain size is 5 mm, velocity of solid material is 5 cm year^{-1}, and the thickness of partially molten layer is 50 km.

An important conclusion is that either batch (equilibrium) or fractional (disequilibrium) melting depends on the atomic species. This figure (also **Figure 9**) shows that for some slow-diffusing species, the melt produced by partial melting may not be as much enriched with these elements even though they are incompatible. These include U, Th, and Ce.

A similar question can be asked as to the mode of solid–liquid separation during freezing of a melt layer (e.g., magma ocean) (or during the core formation (separation of iron from silicates); Karato and Murthy, 1997; Stevenson, 1990). As far as the density of solid is different from that of the melt, separation tends to occur. However, convection current tends to suspend grains if the grain size is small. Such an issue was analyzed by Solomatov (2009) and Tonks and Melosh (1990). If melt–solid separation occurs efficiently during the freezing stage of a magma ocean, then one would expect a substantial layering in composition including the water content (e.g., Elkins-Tanton and Grove, 2011). However, the predicted layering in density for the Moon by Elkins-Tanton and Grove (2011) is not consistent with the observed moment inertia (Konopliv et al., 2001) that indicates that the lunar mantle has nearly homogeneous density.

9.05.2.4.3 Macroscopic segregation involving a melt-rich layer in the midmantle

Somewhat different processes will work if a melt-rich layer is formed inside of the mantle. Such a layer is likely on top of the 410 km and below the 660 km discontinuities in the Earth's interior (e.g., Bercovici and Karato, 2003; Ohtani et al., 2004; Young et al., 1993). In these cases, a thin melt-rich layer (thickness ~ compaction length) will be formed, and the melt will either remain there or be entrained by subducted slabs and carried into the deep mantle (Leahy and Bercovici, 2007). The strongest vertical flow is a downgoing flow associated with subducted slabs, and consequently, these melts or melt-rich materials could go into the deep mantle. The consequence of such a material segregation on the global volatile circulation and hence the evolution of ocean mass will be discussed in **Section 9.05.5**.

9.05.3 Influence of Water on Physical and Chemical Properties

9.05.3.1 Melting

The role of volatiles to enhance melting and to change the composition of melt was already recognized by Bowen (1928). The essential reason for a large influence of volatiles on melting behavior is the large contrast in the solubility of volatile components into liquid and solid. Volatile elements are much more soluble in liquid than solid, and this increases the configurational entropy of liquid thereby reducing its free energy. Consequently, liquid becomes stable relative to solid at high temperatures, enhancing the melting. Assuming the ideal solution model for simplicity, such a behavior can be summarized by the following relationship (e.g., Carmichael et al., 1974):

$$T_m = \frac{T_{mo}}{1 + \frac{RT_{mo}}{\Delta H}\left|\log\frac{1-x_m}{1-x_s}\right|} \quad [9]$$

where T_{mo} is the melting temperature of a volatile-free system, T_m is the melting temperature with x_m being the mole fraction of volatiles in the melt, x_s is the solid, and ΔH is the enthalpy difference between the melt and solid (for a pure system). Because the main cause of the melting temperature depression is the configurational entropy (expressed by the $R\log(1-x)$ term), any impurities would have similar effects as far as their number density is the same.

Extensive experimental studies have been made on the role of volatiles on melting including the role of hydrogen (water) (e.g., Inoue, 1994; Kushiro et al., 1968; Litasov and Ohtani, 2007; **Figure 11**), carbon (e.g., Dasgupta and Hirschmann, 2006; Wyllie and Huang, 1976), and potassium (K) (Wang and Takahashi, 2000).

An important point about melting is that because the melting is enhanced by the presence of volatiles due to the solubility contrast of volatiles between melt and solid, melting caused by volatiles will occur only when the volatile content exceeds a critical value that is proportional to the solubility of volatiles in solids. This means that when there are some solids that can host a large amount of volatiles, melting is difficult. For carbon, its solubility in minerals depends on oxygen fugacity, and hence, a change in oxygen fugacity can change the melting temperature (Rohrbach and Schmidt, 2011). Similarly, if some K-bearing minerals are stable, then K will not enhance melting (Wang and Takahashi, 2000).

After partial melting, one obtains solid and melt whose compositions are different from the composition of the original solid. **Figure 12** is a schematic diagram showing the evolutional trend of composition of coexisting melt and solid. When a material ascends, decreased pressure promotes melting.

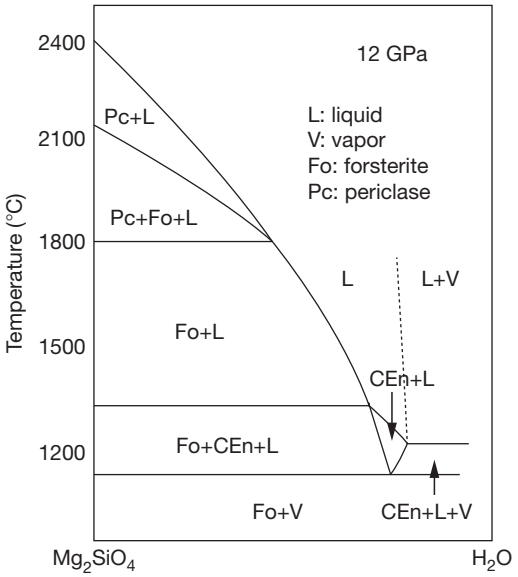

Figure 11 The influence of water on the melting relationship in Mg_2SiO_4. Reproduced from Inoue T (1994) Effect of water on melting phase relations and melt composition in the system Mg_2SiO_4–$MgSiO_3$–H_2O up to 15 GPa. *Physics of Earth and Planetary Interiors* 85: 237–263.

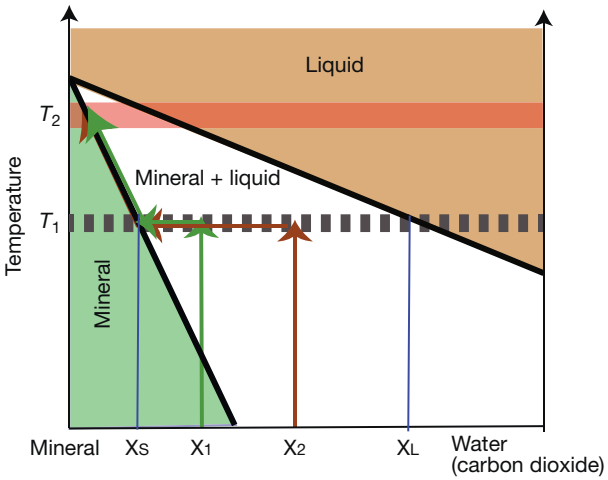

Figure 12 A schematic phase diagram showing volatile-assisted melting. Above the eutectic temperature (T_e), partial melting will occur, if the volatile concentration exceeds the volatile concentration at the solidus. The volatile concentration at the solidus depends on the volatile solubility in the solid. The amount of melt produced by the help of a volatile is determined by the volatile concentration. When a material will move upward below near the surface, the solidus decreases.

When melting involves volatile elements (such as H and C), they will be redistributed because their solubility in melt and solid is different: volatile elements in the solid will be reduced after the melting. However, the volatile content in the solid after the melting will not depend on the initial volatile content so much. Initial volatile content affects the degree of melting but the composition of the residual solid is controlled by the composition of the solidus. Consequently, partial melting homogenizes the composition of the residual solids.

9.05.3.2 Rheological Properties

Griggs and his coworkers were the first to report the strong influence of water (hydrogen) on plastic deformation of minerals. They discovered that the dissolution of hydrogen reduces the creep strength of quartz dramatically (Griggs and Blacic, 1965). A similar phenomenon, although to a lesser degree, was soon observed for olivine (Blacic, 1972). The fundamental reason for the weakening is that the hydrogen dissolved in these minerals makes chemical bonding weak, thereby promoting plastic deformation that requires large-scale relative motion of atoms in a crystal.

Systematic studies on the influence of water on plastic deformation were conducted on several minerals, and the flow law of the following form is usually used to describe the influence of water on plastic deformation (e.g., Karato, 2008a; Kohlstedt, 2009):

$$\dot{\epsilon} = \dot{\epsilon}_{d0} \cdot \sigma^{n_d} \cdot \exp\left(-\frac{H_{cd}^*}{RT}\right) + \dot{\epsilon}_{w0}\left(\frac{C_W}{C_{W0}}\right)^{r_c} \cdot \sigma^{n_w} \cdot \exp\left(-\frac{H_{cw}^*}{RT}\right) \quad [10]$$

where $\dot{\epsilon}$ is the strain rate, $\dot{\epsilon}_{d0(w0)}$ are the preexponential terms for dry (wet) conditions, σ is the stress, $n_{d(w)}$ is the stress exponent, and $H^*_{cd(cw)}$ is the activation enthalpy for dry (wet) conditions. The influence of water to enhance deformation has been demonstrated for all crustal and upper mantle minerals (quartz (Post et al., 1996), olivine (Karato and Jung, 2003), (Mei and Kohlstedt, 2000a), orthopyroxene (Ross and Nielsen, 1978), clinopyroxene (Chen et al., 2006), pyrope garnet (Katayama and Karato, 2008a), and wadsleyite (Kawazoe et al., 2013)). In general, the degree of water weakening is larger for minerals with higher SiO_2 content.

The most detailed studies have been made on olivine, for which water-weakening effect was found for diffusion creep (Karato et al., 1986; Mei and Kohlstedt, 2000a), power-law dislocation creep (high-temperature dislocation creep) (Karato and Jung, 2003; Mei and Kohlstedt, 2000b), and the Peierls mechanism (low-temperature dislocation creep) (Katayama and Karato, 2008b) (**Figure 13**). Water reduces the effective viscosity of olivine up to ~3–4 orders of magnitude for a given stress.

However, water-weakening effect on lower mantle minerals has not been demonstrated. The influence of hydrogen on the diffusion of Mg–Fe in (Mg,Fe)O was studied, but its effect is small at low pressures ($P < 20$ GPa) (Otsuka and Karato, 2013). In lower mantle minerals such as (Mg,Fe)O, the concentration of ferric iron is large and it is unclear if hydrogen has large effects on defect-related properties including plastic deformation and electrical conductivity (Otsuka et al., 2013).

The mechanisms of weakening effects by water (hydrogen) were reviewed by Karato (2008a) and Kohlstedt (2009). Since high-temperature creep is controlled by diffusion-related processes, enhancement of creep by water is partly due to enhanced diffusion (e.g., Costa and Chakraborty, 2008). However, enhancement of diffusion itself cannot explain the strong anisotropy in the water effects on dislocation creep in olivine (Karato, 2010a). A substantial part of water (hydrogen) weakening must be through the modifications to jog/kink densities

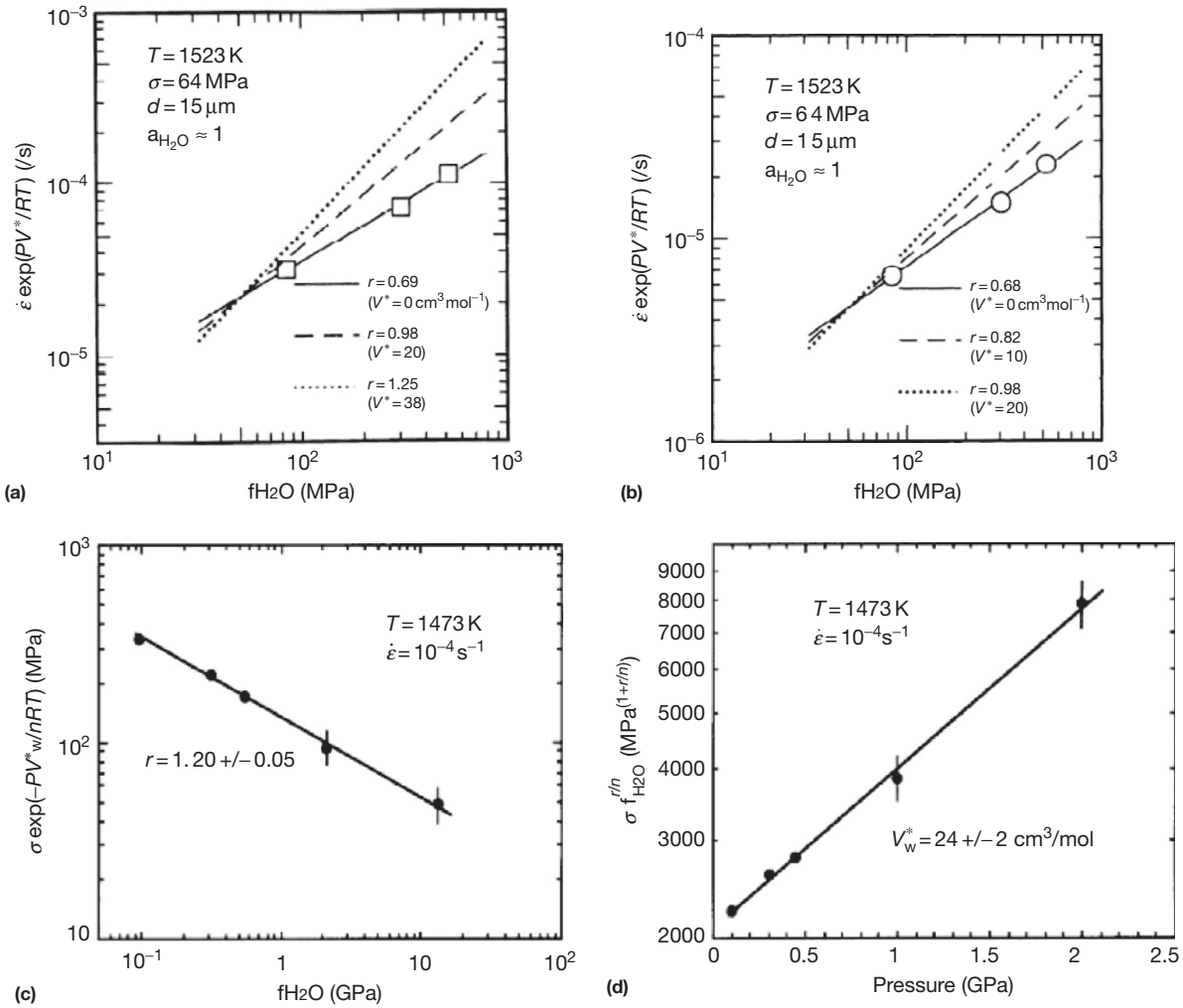

Figure 13 Influence of water on the creep strength of olivine in the (a) dislocation creep regime and (b) diffusion creep regime (after Karato and Jung, 2003; Mei and Kohlstedt, 2000a,b). In the Mei and Kohlstedt (2000a,b) study, experiments were made under water-saturated conditions at low pressures ($P < 0.45$ GPa). Enhancement of deformation with increase of pressure was observed and it was interpreted as a result of increased water fugacity. However, the influence of water fugacity and the intrinsic effect of pressure were not separated, and the key parameters characterizing the water effects were unconstrained (note that the activation volume, V^*, that characterizes the pressure effect remained an arbitrary parameter in their paper). Karato and Jung (2003) conducted deformation experiments at higher pressures (to 2 GPa) and were able to determine the two key parameters (water fugacity exponent (r) and the activation volume (V^*)) for dislocation creep separately. It is necessary to constrain both of these parameters in order to extrapolate these results to the deep upper mantle (deeper than ~30 km) where the influence of water is potentially important (see also Karato, 2010b).

on dislocations. This means that the degree of enhancement of dislocation creep by water is likely larger than the degree of enhancement of diffusion creep.

Influence of other volatile elements such as carbon on plastic deformation is unknown. In olivine, carbon is dissolved in the Si-site (Keppler et al., 2003) and its solubility is low compared with that of hydrogen. However, since Si diffusion likely affects the rheological properties and the concentration of intrinsic defects at Si-site is very small, even a small amount of carbon might have some effects on rheological properties.

The influence of water (hydrogen) to enhance plastic deformation is sometimes anisotropic: hydrogen enhances deformation along one orientation more than along other orientations. Anisotropic water effect can be understood if the influence of water on dislocation properties such as kink/jog density plays an important role (diffusion in olivine is nearly isotropic). This leads to the variation in the lattice-preferred orientation (LPO) (nonrandom distribution of crystallographic orientations of minerals) when plastic deformation occurs by the glide of crystal dislocations (Karato et al., 2008). Consequently, water affects seismic anisotropy in the upper mantle.

Recently, Fei et al. (2013) reported relatively small effects of water on diffusion of Si in Mg_2SiO_4 olivine and argued that creep in olivine is not as much sensitive to water as previously considered. However, such a conclusion is inconsistent with the well-documented large effects of water to enhance creep in olivine ($(Mg,Fe)_2SiO_4$) including anisotropic effects summarized in the preceding text. A more reasonable conclusion from such an observation is either (i) the influence of water is not only through diffusion but also through jog formation

(which results in anisotropic effects) or (ii) the influence of water is different between Mg_2SiO_4 and $(Mg,Fe)_2SiO_4$ olivine.

9.05.3.3 Seismic Wave Propagation

Seismology provides the most detailed information of the Earth's interior (also lunar interior). Water and other volatile elements may affect the seismic wave propagation. If such effects were demonstrated, then water distribution on Earth (and other planets) would be inferred from seismological observations. Based on these ideas, a number of studies have been carried out to investigate how water affects seismic wave propagation. The following aspects of seismic wave propagation have been studied: (i) (average) seismic wave velocities, (ii) topography of velocity discontinuities, (iii) seismic anisotropy, and (iv) seismic wave attenuation.

Dissolution of water (hydrogen) weakens chemical bonding, and hence, one may expect that seismic wave velocities will be reduced by the dissolution of water (hydrogen). However, experimental studies showed that the effects of water on (high-frequency) elastic properties are small (e.g., Jacobsen, 2006; Jacobsen et al., 2008; Mao et al., 2008). In fact, the influence of other factors such as a variation in major element chemistry (e.g., pyrolite versus harzburgite) is much larger than the influence of hydrogen, making it difficult to resolve hydrogen content from seismic wave velocities (Karato, 2011) (**Figure 14**).

High water solubility in transition zone minerals means that the dissolution of water (hydrogen) stabilizes the transition zone minerals relative to the upper or lower mantle minerals. Consequently, the depth of '410 km' or '660 km' discontinuity will be modified by the addition of water. Experimental studies confirmed this (e.g., Chen et al., 2002; Litasov and Ohtani, 2007; Smyth and Frost, 2002), but the magnitude of topography is reduced at high temperatures, and under most of mantle conditions, such topography will be small and hard to detect seismologically (Frost and Dolejš, 2007) (**Figure 15**). In these cases, the actual topography is not much caused by the variation in water content but by the variation in temperature and major element chemistry. Consequently, the inference of water content from these seismological observations is difficult, and sometimes, one finds puzzling results when such a method is used to infer water content (see **Section 9.05.4**).

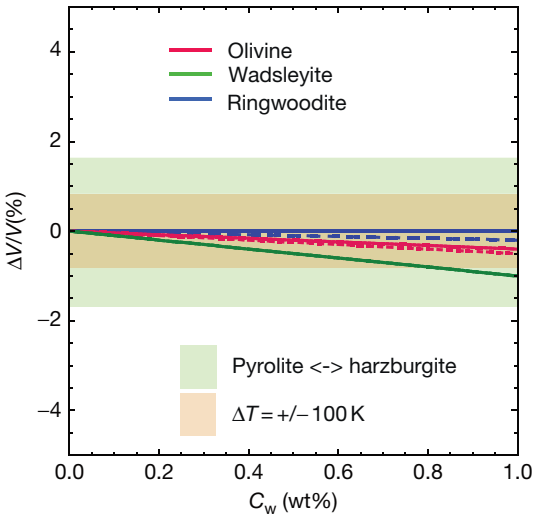

Figure 14 Influence of water on seismic wave velocities at high frequencies. C_w is the water content. Addition of water (hydrogen) reduces seismic wave velocities. However, for plausible water content in the Earth's mantle (<0.1 wt%), its influence is small compared with that of major element chemistry and temperature. The influence of water will be larger at seismic frequencies because of the enhancement of anelastic relaxation.

In contrast, the influence of water on seismic anisotropy in the upper mantle is strong: in some cases, the direction of anisotropy changes substantially (90°). This is caused by the change in the dominant slip system(s) in olivine, and consequently, the distribution of seismic anisotropy can be used to obtain some insight into the distribution of water (Karato et al., 2008) (**Figure 16**).

Also, the addition of water (hydrogen) increases attenuation through the enhanced plastic deformation (decreases Q). This was proposed by Karato (1995) using an analogy with plastic deformation and later confirmed qualitatively by Aizawa et al. (2008) (**Figure 17**). Using essentially the same line of argument, McCarthy et al. (2011) suggested that seismic wave attenuation increases with water content. The functional relationship between seismic wave attenuation and the water content has not been well characterized. However, using the Maxwell time scaling, the following relationship is expected (e.g., Karato, 2006b; McCarthy et al., 2011):

$$Q^{-1} = Q_d^{-1}\exp\left(-\frac{H_{Qd}^*}{RT}\right) + Q_w^{-1}\left(\frac{C_W}{C_{Wo}}\right)^{r_Q}\exp\left(-\frac{H_{Qw}^*}{RT}\right) \quad [11]$$

where Q^{-1} is the fraction of energy loss, $Q_{d(w)}^{-1}$ are the reference values of Q^{-1} for dry (wet) conditions, $H_{Qd(Qw)}^*$ are the activation enthalpy for dry (wet) conditions, and r_Q is a non-dimensional parameter (between 1 and 2).

Shito et al. (2006) developed a method to infer the water content (and temperature and major element chemistry) from the observed velocity and attenuation anomalies. They reported that the deep upper mantle in the Philippine Sea upper mantle has large water content. However, the challenge in using these observations is that the resolution of seismological observations (anisotropy and attenuation) is not as good as the average velocity or topography of discontinuities.

9.05.3.4 Electrical Conductivity

Most minerals are ionic crystals, and therefore, there are always a large number of charged species. However, in an ideal state, most charged species (such as Mg^{2+} and O^{2-}) are strongly bonded to each other, and they do not carry much current except at very high temperatures (close to melting temperature). Impurities such as ferric iron and proton substantially enhance electrical conductivity because electrons attached to ferric iron and protons are both highly mobile (for a review, see Karato and Wang, 2013).

When the concentration of these impurities ('point defects') is increased, electrical conductivity can increase (or decrease) by orders of magnitude. Therefore, electrical conductivity is a good sensor for the physical/chemical state of a planet related to these defects including hydrogen. In many cases, geologic

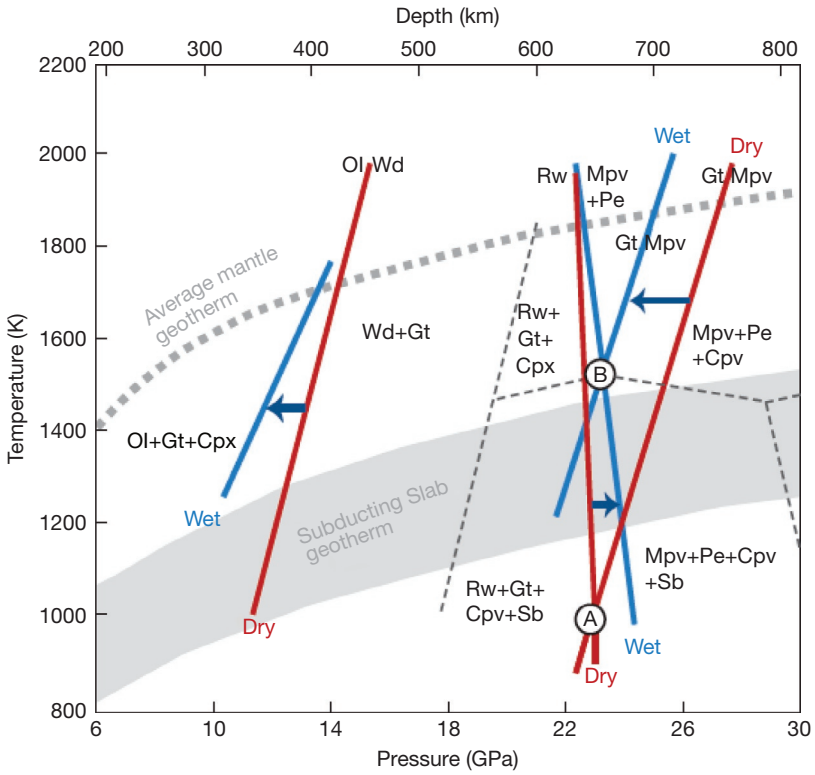

Figure 15 The influence of water on the phase relationship in $(Mg,Fe)_2SiO_4$. Reproduced from Litasov KD and Ohtani E (2007) Effect of water on the phase relations in Earth's mantle and deep water cycle. In: Ohtani E (ed.) *Advances in High-Pressure Mineralogy*, pp. 115–156. Geological Society of America.

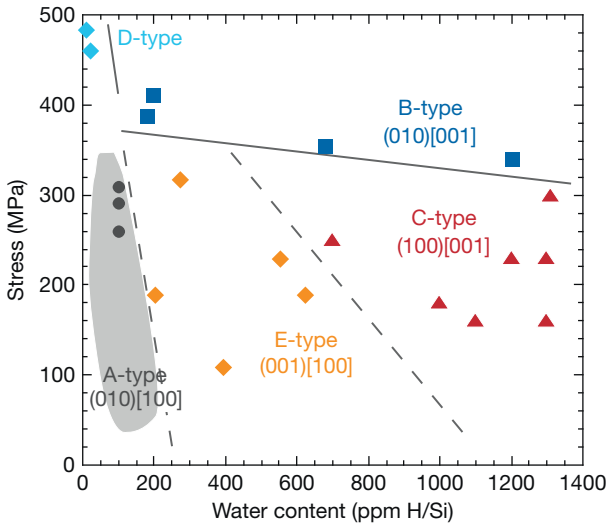

Figure 16 The influence of water (and stress) on the lattice-preferred orientation (LPO) of olivine (after Karato et al., 2008). A, B, C, D, and E types of LPO represent different types of olivine LPO. The LPO of olivine depends on various physical and chemical parameters including water content (water fugacity), stress, temperature, and pressure. The results shown correspond to the LPO at $P < 3$ GPa. At higher pressures, different LPOs might develop. The water content shown is estimated using the Paterson calibration. If SIMS calibration is used, these values should be multiplied by a factor of ~3.

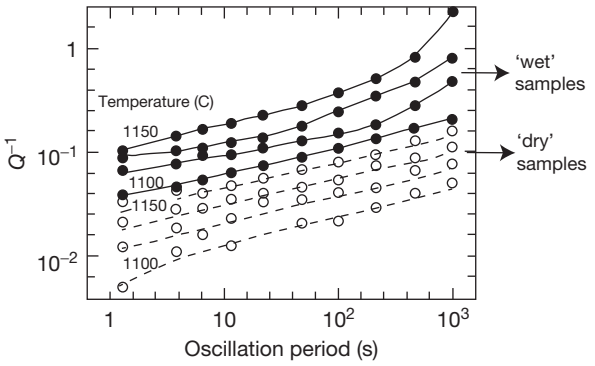

Figure 17 The influence of water on seismic wave attenuation in olivine (Aizawa et al., 2008). Q^{-1} is a measure of seismic wave attenuation (fraction of energy dissipated as heat). 'Wet' samples are those that contain more water than 'dry' due to the use of different jackets. Therefore, the results shown here strongly suggest that water enhances seismic wave attenuation. However, the functional relationship between water content and seismic wave attenuation has not been quantified experimentally.

question we would like to address is the order of magnitude of concentrations of these defects (e.g., hydrogen) as opposed to the precise value of defect concentration. Consequently, although the electrical conductivity of the Earth's interior (or other planetary interiors) cannot be determined as precisely as

seismic wave velocities, even a crude estimate of electrical conductivity provides an important constraint on hydrogen content.

In most minerals, electrical conductivity is caused by two types of impurities, ferric iron and proton (hydrogen). In both cases, the concentration and mobility of charged species are highly dependent on temperature and water content (e.g., Karato, 2008a). Consequently, electrical conductivity of a mineral (σ; not stress!) may be written as

$$\sigma = \sigma_{d0}\exp\left(-\frac{H_{\sigma d}^*}{RT}\right) + \sigma_{w0}\left(\frac{C_W}{C_{W0}}\right)^{r_\sigma}\exp\left(-\frac{H_{\sigma w}^*}{RT}\right) \quad [12]$$

where $\sigma_{d0(w0)}$ is the preexponential term for dry (wet) mechanism, $H^*_{\sigma d(\sigma w)}$ is the activation enthalpy for dry (wet) mechanism, and r_σ is a constant (0.5–1). In most cases, electrical conductivity is also dependent on oxygen fugacity, and in these cases, the influence of oxygen fugacity can be included in the preexponential factor, $\sigma_{d0(w0)}$. Major element chemistry also affects electrical conductivity. Particularly important is the influence of Fe content (in most minerals; Cemič et al., 1980) and Al_2O_3 content in orthopyroxene (Huebner et al., 1979).

Parameters in relation [12] have been determined for some mantle and crustal minerals including plagioclase (Yang et al., 2012), olivine (Wang et al., 2006; Yang, 2012), orthopyroxene (Dai and Karato, 2009a; Yang et al., 2012), clinopyroxene (Yang, 2012), pyrope (Dai and Karato, 2009b), wadsleyite (Dai and Karato, 2009c), and ringwoodite (Huang et al., 2005). Also, the dependence of these parameters on major element chemistry has been determined for some minerals.

The magnitude of the effect of hydrogen is large in comparison with the influence of other factors such as temperature, major element chemistry, and oxygen fugacity (Karato, 2011) (**Figure 18**). Detailed studies on olivine showed that the enhancement of electrical conductivity by the dissolution of hydrogen is not equally caused by all the hydrogen atoms dissolved in a mineral but rather mostly due to a small fraction of dissolved hydrogen with high mobility and that the hydrogen-related species controlling the conductivity changes with temperature (e.g., Dai and Karato, 2014; Karato, 2006a, 2013b; Wang et al., 2006).

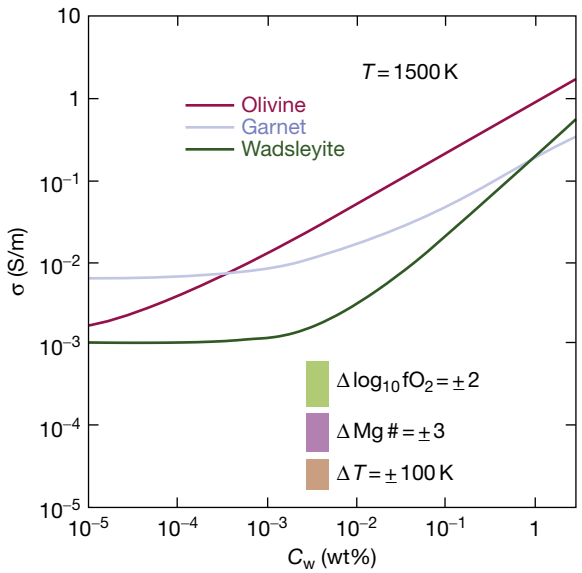

Figure 18 Influence of water on the electrical conductivity of minerals compared with the influence of major element chemistry, temperature, and oxygen fugacity (after Karato, 2011). C_w is the water content. The effect of water (hydrogen) is much larger than the effects of major element chemistry, temperature, and oxygen fugacity for a plausible range of these variables.

The influence of hydrogen on the electrical conductivity has not been studied for the lower mantle minerals. Although there are several studies on the electrical conductivity in lower mantle minerals (e.g., Dobson and Brodholt, 2000; Katsura et al., 1998; Peyronneau and Poirier, 1989; Shankland et al., 1993), the hydrogen content in these samples was not measured, and we do not know if hydrogen has any effect on the electrical conductivity in these minerals (hydrogen was not added in these studies, but some hydrogen is likely dissolved in these minerals). In lower mantle minerals, other defects such as ferric iron and oxygen vacancies contribute to electrical conductivity (e.g., Dobson, 2003), and it is not clear if hydrogen enhances electrical conductivity. It is also noted that most of hydrous minerals do not have high electrical conductivity that is likely due to the low mobility of hydrogen in these minerals (Karato and Wang, 2013).

The influence of carbon on electrical conductivity was discussed by Duba and Shankland (1982). A detailed experimental study was performed by Wang et al. (2013) who showed that when more than ~1 wt% of graphite is present in an olivine aggregate, electrical conductivity is enhanced. The reported high-conductivity regions in the shallow continental lithosphere (e.g., Jones et al., 2003) might represent regions of anomalously high carbon content with low oxygen fugacity.

9.05.3.5 Influence of Partial Melting

Partial melting is ubiquitous in the Earth's mantle when volatile components are present (e.g., Hirschmann, 2010; Kushiro, 2001). Partial melting has effects on various physical properties similar to hydrogen: partial melting makes materials softer (except for the effects of hydrogen removal from minerals that will make materials stronger; see Karato, 1986). Therefore, it is critical to distinguish the influence of volatile element (such as hydrogen) and that of partial melting.

One way to assess the possible contribution from partial melting is to estimate how much melt one needs to explain geophysical anomalies and to address if it is feasible to maintain a required amount of melt. For example, for a given seismic wave velocity reduction, one can estimate the necessary volume fraction of melt that depends on the melt geometry (wetting (dihedral) angle). For the typical asthenosphere (~50–100 km depth in Earth), the dihedral angle is 20–40° (Cooper and Kohlstedt, 1982; Yoshino et al., 2009). For this wetting geometry, the inferred velocity reduction of 5–10% at the lithosphere–asthenosphere boundary requires 3–6% of melt (Takei, 2002). Such a melt fraction is difficult to maintain in a large region from both the static (equilibrium thermodynamics) point of view and dynamic point of view (melt generation and transport) (Karato, 2014b). The essential reasons are (i) because partial melting in many cases in the Earth's mantle is caused by volatiles, the degree of melting is controlled by the amount of volatiles and is small (<0.1%), and

(ii) high melt fraction is difficult to maintain because of the effective compaction (see Section 9.05.2.4.2). An exception is a region where melt completely wets the grain boundaries. In these cases, grain-boundary relaxation would occur that reduces seismic wave velocities by several % (e.g., Karato, 2012). This is a possible case for the deep upper mantle above 410 km where continuous melt production by the upwelling of water-rich materials from the transition zone combined with complete wetting will produce a thick low-velocity region (Karato, 2012; Yoshino et al., 2007).

For electrical conductivity, a smaller melt fraction could explain observed high conductivity if carbonatite melt with a large concentration of alkali ions (Na^+ and K^+) is present (e.g., Gaillard et al., 2008; Naif et al., 2013; Sifré et al., 2014). However, both the magnitude and anisotropy observed by Baba et al. (2006) and Naif et al. (2013) are in good agreement with a hybrid model of hydrogen-assisted conductivity where it is predicted that the conduction mechanism changes at a temperature of ~1300 K to conduction by two protons trapped at M-site and that high anisotropy is consistent with the observed anisotropy (Dai and Karato, 2014; Karato, 2013b). In contrast, the amount of melt needed to explain the observed conductivity exceeds substantially the degree of melting caused by the volatile components (see, e.g., Ni et al., 2011).

It is also noted that a small fraction of melt does not affect the rheological properties strongly under the shallow mantle conditions (Kohlstedt, 2002). The small effect of partial melt is attributed to the wetting geometry of basaltic melt under the shallow upper mantle conditions (Kohlstedt, 2002) and is similar to the small effect on seismic wave velocities. In contrast to these observations, Takei and Holtzman (2009) presented a new theory where they claim a larger effect of a small fraction (~0.1%) of melt for diffusion creep (a factor of 5–10 enhancement of strain rate, still modest compared with the hydrogen effect). However, the validity of their theory is not clear because there is no clear experimental support. (Using an analog material, McCarthy et al. (2011) reported that a small amount (~0.1% or less) of melt has a large effect on deformation. However, the influence of chemical composition is not well corrected in their work and the validity of their conclusion is unclear.) And the stress state calculated in their theory has singularities at grain boundaries that are the transient feature and does not correspond to the true steady-state feature according to the theory by Raj and Ashby (1971). In fact, Raj (1975) and Lifshitz and Shikin (1965) explained transient fast strain rate (by a factor of ~5–10) by such a transient stress state. Furthermore, the dominant mechanism of deformation in most of the asthenosphere is dislocation creep as inferred from strong seismic anisotropy (e.g., Karato et al., 2008); in which case, the influence of partial melt will be even smaller.

In summary, I conclude that although partial melting is ubiquitous in the Earth's mantle due to the presence of volatile elements, partial melting is unlikely to affect physical properties (seismic wave velocities, electrical conductivity, and rheological properties) so much because melt does not completely wet grain boundaries and the melt fraction is small (<0.1%). A region above the 410 km discontinuity is an exception where a substantial reduction in seismic wave velocities is expected (see Coutier and Revenaugh, 2006, 2007; Gao et al., 2006; Tauzin et al., 2010). It is possible that this region has a low viscosity that might decouple convection current across the 410 km discontinuity.

9.05.4 Distribution of Volatile Elements on Earth

A large amount of volatile elements on Earth occurs on its surface (atmosphere, ocean, and sedimentary rocks), but there must be some volatile elements in its deep interior (mantle and core) as seen by the eruption of volcanic gases. The total amount of volatile elements on Earth and their spatial distribution are the key constraints in developing a model of volatile circulation and the evolution of the ocean (Section 9.05.6.3). In this section, I will provide a review on the inferences of volatile distribution.

9.05.4.1 Geochemical Inference of Water and Other Volatile Element Distribution on Earth

The distribution of volatile elements such as hydrogen and carbon can be inferred from the samples from the Earth's interior. These samples include volcanic gases and rock samples (e.g., Bell and Rossman, 1992; Dixon et al., 2002; Ito et al., 1983; Marty, 2012; Peslier, 2010).

Two approaches are used to infer the distribution of volatiles on Earth from rock samples (Figure 19). One is to measure the volatile content in mantle or crustal rock specimens (e.g., Bell and Rossman, 1992; Ingrin and Skogby, 2000; Peslier, 2010). This is a direct approach. In many cases, the temperature and pressure conditions at which a given sample established the last chemical equilibrium can be inferred. Consequently, one can obtain some ideas about the depth variation in the volatile content from these samples (e.g., Peslier et al., 2010). However, there are two limitations with this approach. First, the range of planetary interior that one can explore by this approach is limited by the availability of samples. In the Earth, most of mantle rocks are from depths shallower than ~200 km. Occasionally, some deep samples coming from the transition zone or deeper are identified (Haggerty and Sautter, 1990; Harte, 2010; Walter et al., 2011), but these are very rare (recently, Pearson et al. (2014) reported a high water content (~1 wt%) of ringwoodite (a transition zone mineral) in one of the diamond inclusions, but the relevance of such an observation to the water distribution at the global scale is unclear). Second, even if one can determine the water content from these limited samples, the significance of such results on the water content in the mantle is unclear. This is because hydrogen content in these samples is likely modified (either hydrogen loss or hydrogen gain) during their transport to the surface. In much of the published literature, only hydrogen loss is examined (e.g., Demouchy et al., 2006), but hydrogen (or other volatile elements) may also be gained from the volatile-rich kimberlite magma during the transport of these samples (e.g., Karato, 2010b).

Alternatively, hydrogen (and other volatile) distribution in the mantle can be estimated from the concentration of these elements in the basalts. This is an indirect method for inferring the water content in the mantle because basalts themselves are not mantle rocks. However, this is an important approach

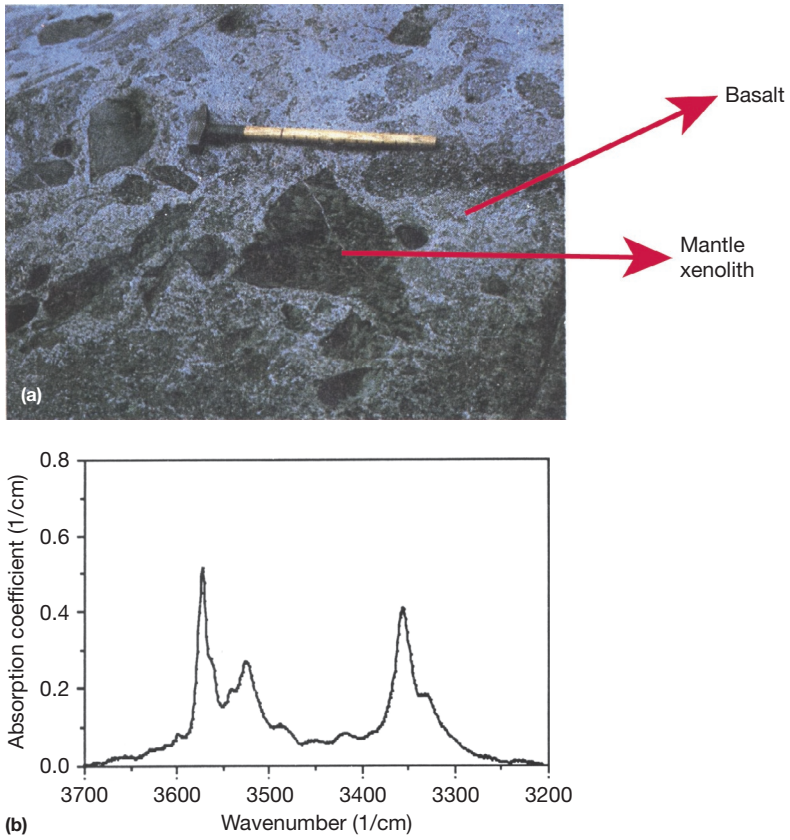

Figure 19 Geochemical (geologic) approach for estimating water (volatile) distribution. (a) A rock specimen containing both basalt and mantle xenoliths. (b) An example of infrared absorption spectrum from which water content in a sample can be estimated. The distribution of volatile elements is to measure the concentration of volatile elements from rock samples (geochemical approach). This method provides direct constraints on the volatile content, but the regions that one can explore is limited and often poorly constrained. Also, the volatile content of rock specimens collected from the Earth's surface may not necessarily represent the volatile content in the Earth's interior. One needs a careful examination of the influence of transport processes of rocks on the volatile content to infer the volatile content in the Earth's interior.

because basaltic magmas are generated at the global scale by partial melting of mantle materials, and hence, their composition reflects mantle composition at a broad space scale (e.g., Hofmann, 1997). In particular, mid-ocean ridge basalt (MORB) is formed by the partial melting of the asthenosphere materials and its chemical composition is nearly homogeneous (Hofmann, 1997). Also, the degree of melting associated with MORB formation (~10%) and hydrogen partitioning between basaltic melt and upper mantle minerals are well known (e.g., Hauri et al., 2006). Consequently, the hydrogen content in MORB provides a robust estimate of water content in the asthenosphere. In contrast, the interpretation of water content of ocean island basalt (OIB) is more complicated because the source regions and the processes of partial melting of OIB are not well understood (e.g., Hofmann, 1997).

Ito et al. (1983) and Dixon et al. (2002) determined the water content in various basalts and inferred the water content in their source regions (**Table 2(a)**). The source regions of MORB, that is, the asthenosphere of the Earth, contain ~0.01 wt% of water (with a factor of ~2 uncertainties). This corresponds to ~4% of the ocean mass, and if this concentration were homogeneous throughout the mantle, the total water content would be ~30% of the ocean mass. The source regions of OIB have a variety of water content, but a common component of OIB source regions, referred to as FOZO (Focus Zone), contains much higher water content (by a factor of ~5–10) than the source region of MORB. This suggests that the deep mantle contains higher water content than the upper mantle. However, because the source regions (particularly their volume) of OIB are unknown, both the total amount of water in the mantle and its distribution are unconstrained from such a geochemical approach. For example, Rüpke et al. (2006) considered that the volume of water-rich FOZO is only ~7% of the mantle, leading to a relatively small total water content of the mantle (~30% of ocean mass). In their model, the mantle is treated as a single component, and therefore, the volume of OIB that has different water content than the MORB source region cannot be large (otherwise, its assumption would be invalidated). Korenaga (2008) obtained a similar conclusion where he assumed that the whole mantle has the same composition as the asthenosphere. A small total water content (also a small content of radioactive elements, i.e., a small Urey ratio (the ratio of heat generation to heat loss of the Earth)) in the mantle in these models is a consequence of the assumption of homogeneous (not layered) mantle chemistry and not a conclusion required from the observations. However, the validity

Table 2 Geochemical estimates of volatile contents[a]

(a) Water contents in the various regions of the Earth's mantle inferred from basalts (after Dixon et al., 2002)

	Depleted mantle[b] (ppm wt)	*FOZO[b] (ppm wt)*	*EM[b] (ppm wt)*
H_2O	100	750	<400

(b) A comparison between the volatile content of the Earth's interior and other objects in the solar system (after Marty, 2012)

	Solar (mol g^{-1})	*Carbonaceous chondrite (mol g^{-1})*	*Depleted mantle (mol g^{-1})*	*Depleted mantle (ppm wt)*	*Bulk Earth (mol g^{-1})*	*Bulk Earth (ppm wt)*
^{12}C	8.6×10^{-11}	2.9×10^{-3}	1.7×10^{-6}	14	6.4×10^{-5}	530
^{14}N	1.8×10^{-11}	1.1×10^{-4}	6.4×10^{-9}	0.12	9.0×10^{-8}	1.7
H_2O	1.2×10^{-10}	6.6×10^{-3}	8.3×10^{-6}	110	2.0×10^{-4}	2700
^{36}Ar	6.3×10^{-13}	3.5×10^{-11}	2.7×10^{-15}	10^{-7}	7.8×10^{-14}	3×10^{-6}

[a]Uncertainties are typically ~50%.
[b]'Depleted mantle' is the upper mantle (source region of mid-ocean ridge basalt (MORB)) that is depleted with volatiles. FOZO is a common component of the source regions of ocean island basalt (OIB). These regions are likely located in the deep mantle. EM is an 'enriched mantle' that is a source region of some of the OIB with large concentrations of various incompatible elements.

of such an assumption is not clear, and there are some observations that suggest that this assumption is not correct, as I will discuss later in the text.

Marty (2012) used a somewhat different approach in which he used the ratio of the concentrations of volatile elements to that of ^{40}Ar in the basaltic rocks (and other samples) (**Table 2(b)**). ^{40}Ar is a highly volatile element produced by the radioactive decay of ^{40}K, and there is essentially no ^{40}Ar in the primordial atmosphere and mantle. Also, as shown in **Figure 8** (also **Figure 9**), ^{40}Ar has relatively high diffusion coefficient, and therefore, most of ^{40}Ar will be removed from solid by partial melting together with volatile elements that in general have high diffusion coefficients (this is not the case for other incompatible elements such as Ce that have low diffusion coefficient). (The H/Ce ratio is often assumed to be a constant and used to infer the hydrogen content (e.g., Dixon et al., 2002). If Ce is not completely removed from minerals by partial melting due to slow diffusion (**Figure 8**), such a method introduces a systematic bias. Also, there is no guarantee that the partitioning coefficients of H and Ce are the same for various pressure and temperature conditions.)) Consequently, when a rock is degassed near the surface, almost all ^{40}Ar must be degassed from the original rock similar to all other volatile elements (H, C, N, Ne, etc.). Therefore, their ratios, for example, $H/^{40}Ar$, reflect their ratios in the mantle. If the concentration of K in the mantle is known, ^{40}Ar content in the mantle can be calculated from the measured ^{40}Ar content in the atmosphere. Marty (2012) used the geoneutrino observations (Gando et al., 2011) to estimate K content and inferred that the Earth's water content is 0.27 ± 0.13 wt% of the total mass, $\sim10\pm5$ ocean mass. The geoneutrino inference of K content has a large uncertainty, but high concentration of K and other volatile elements in the deep mantle was also inferred by Allègre et al. (1996) and Halliday (2013) from geochemical considerations. The higher concentration of incompatible elements such as H and K in the deep mantle than that in the upper mantle is a natural consequence of transition zone partial melting (Bercovici and Karato, 2003).

This value is in good agreement (within a factor of ~2) with the estimate by Karato (2011) using geophysical observations as will be discussed in the next section that shows that the water content in the transition zone and the lower mantle is much larger than that in the upper mantle. However, these estimates differ considerably from those by Hirschmann (2006), Hirschmann and Dasgupta (2009), and Rüpke et al. (2006) who assumed that the water content in the deep mantle is similar to that in the upper mantle except for very small water-rich regions as a source for OIB.

Distribution of other volatile elements such as C (carbon) can also be estimated from rock samples. For example, the carbon content in the mantle was estimated by Dasgupta and Hirschmann (2010), Marty (2012), and Wood et al. (1996) from geochemical observations. In particular, based on the composition of MORB and OIB, Hirschmann and Dasgupta (2009) inferred that H/C ratio in the upper mantle is larger than that in the deep mantle (transition zone and below), implying that the lower mantle has a relatively high carbon content. The abundance of other volatiles such as S, N, Ne, and Ar was also estimated (e.g., Marty, 2012). Marty (2012) showed that the concentrations of most of volatile elements are higher in the deep mantle than those in the upper mantle (depleted mantle), and the total amount of volatile elements in the Earth is on the order of 1–3% of those in carbonaceous chondrite (**Table 2(b)**) (a similar conclusion was obtained by Allègre et al., 1986/1987).

9.05.4.2 Geophysical Inference of Water Distribution

Although the geochemical approach for estimating the volatile distribution is more direct, its major limitations are the difficulties in locating where those volatile elements are present and in estimating the volume of each region ('reservoir') except for the source region of MORB, that is, the asthenosphere. For example, direct sampling from the deep interior of planets is difficult, and even for the Earth, there is little consensus as to the location and the size of the source regions of OIB. In fact,

some assume that the composition of most of the deep mantle is the same as that of the asthenosphere (e.g., Hirschmann, 2006; Korenaga, 2008; Rüpke et al., 2006), whereas there is some geochemical evidence that the deep mantle contains much higher volatile contents (e.g., Allègre et al., 1996; Marty, 2012). As I will discuss in **Section 9.05.5**, these models lead to very different views of global volatile circulation.

In view of these limitations, a geophysical approach, that is, remote sensing, is an alternative approach to be explored (Karato, 2006b; **Figure 20**). Various remote sensing techniques have been developed to explore planetary interiors including (i) geodesy (gravity, shape of planets, and orbit), (ii) seismology (elastic and anelastic properties), and (iii) geomagnetic induction (electrical conductivity). In these methods, one uses the observations obtained outside of a planet that are related to some physical (and chemical) properties of planetary interiors. If one knows a relation between these observable properties and volatile content, then one can infer volatile distribution in a planet. A major advantage of this approach is that in most cases, these measurements provide information of distribution of physical properties in the entire planet and sometimes provide three-dimensional models.

However, unlike geochemical approach where volatile content is directly measured on rock samples, geophysical approach is indirect. In order to provide useful constraints on the volatile distribution from geophysical approach, one needs to identify which properties one may use and to establish a relationship between the volatile content and these physical properties. Various physical properties depend not only on volatile content but also on other parameters. As I discussed in **Section 9.05.3**, hydrogen is exceptional among various volatile elements in influencing some of the geophysically observable properties to the extent that one can place important constraints on its distribution. This is due to the weak chemical bonding of hydrogen with other atoms such as oxygen and relatively large solubility of hydrogen in most minerals. Therefore, hereafter in this section, I will focus on the estimate of hydrogen content. If the ratio of hydrogen content to the content of other volatile elements is known, then one can use hydrogen as a geophysical tracer to infer the distribution of other elements.

The dependence of a physical property, X, on various parameters may be symbolically written as

$$X = X(C_W, T; \xi) \quad [13]$$

where C_W is the water content, T is the temperature, and ξ are 'other factors' such as the major element chemistry (pressure effect is not included here. If needed, temperature could be interpreted as a homologous temperature, $T/T_m(P)$ ($T_m(P)$, melting temperature), to include the pressure effect). Since all of them can vary in a planetary interior, if a property can be used to infer water content, its sensitivity to 'other factors' (major element chemistry) and temperature must be weak or well characterized. As I will discuss later in the text, some physical properties such as electrical conductivity and seismic attenuation (tidal dissipation) are relatively insensitive to the major element chemistry (or one can infer the influence of major element chemistry with sufficient accuracy). In these cases, one can infer combinations of C_W (water content) and T (temperature) that explain geophysical observations. In a case where temperature can be estimated using other approaches (this is the case for the Earth's mantle), water content can be inferred from such a geophysical observation.

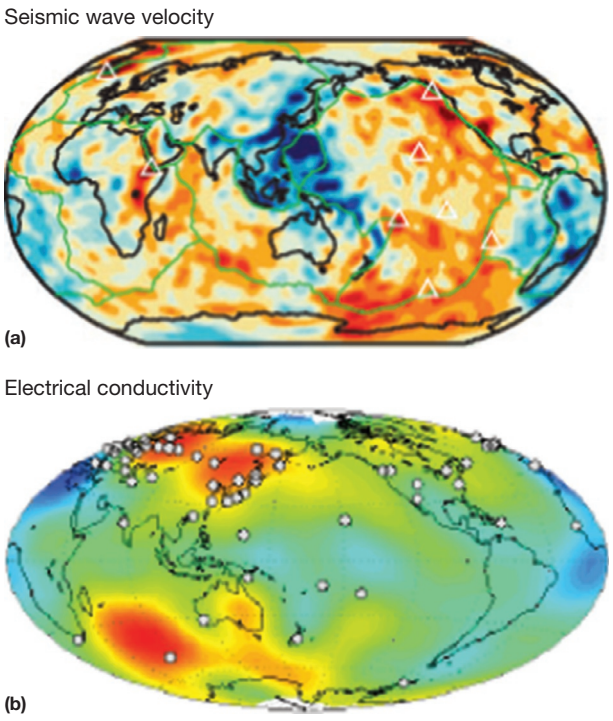

Figure 20 Data that could be used in geophysical remote sensing of volatiles. (a) Anomalies in seismic shear wave velocity in the transition zone (Ritsema et al., 2011). (b) Anomalies in electrical conductivity in the transition zone (Kelbert et al., 2009). The distribution of volatile elements can be inferred from geophysical observations if some geophysically measurable properties are sensitive to volatile content and if geophysical observations with sufficient resolution are available. In order to apply these methods, one needs careful studies on the influence of volatile elements on geophysical properties. Only hydrogen is known to produce its presence in geophysical properties such as electrical conductivity, seismic attenuation, and anisotropy. From this approach, one can investigate the spatial distribution of volatile content better than the geochemical approach.

9.05.4.2.1 From seismological observations

Seismology provides high-resolution images of the Earth's interior (there are some data on the Moon as well; Garcia et al., 2011). Among others, seismic wave velocities can be determined with the highest precision and provide the best constraints on the composition of the Earth's interior (e.g., Dziewonski, 2000). Also, in some cases, the depths of seismic discontinuities can be determined that are also sensitive to the water content (e.g., Deuss, 2009; Shearer, 2000). Consequently, there have been some attempts to use seismic wave velocities (e.g., Jacobsen et al., 2004, 2008; Jacobsen and Smyth, 2006) and/or the depth of seismic discontinuities to infer the water content. Particularly interesting is an approach used by Meier et al. (2009) and Suetsugu et al. (2006) where the anomalies in seismic wave velocities and in the depth of

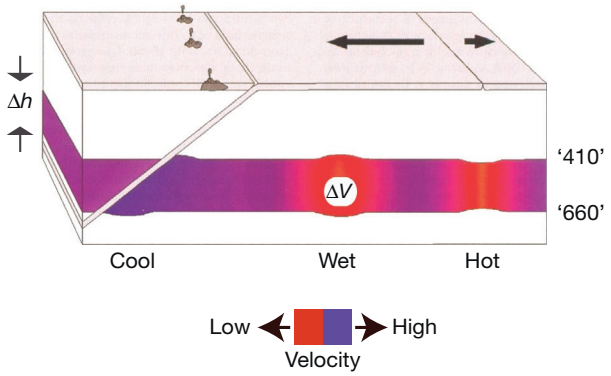

Figure 21 A schematic diagram showing how temperature and water may affect the seismic wave velocity and the topography of the 410 km and 660 km discontinuities (thickness of the transition zone). Temperature and water content affect seismic wave velocity and the topography of seismic discontinuities (or the transition zone thickness) differently. Therefore, by using the observations on the anomalies in seismic wave velocity and transition zone thickness, one can determine the anomalies in temperature and water content separately. However, in order for the method to work, temperature and water content must be the most important variables to affect seismic wave velocities and the topography of discontinuities. If some other variables such as the major element chemistry affect these properties more than the temperature and water content, this method will not work.

seismic discontinuities (thickness of the transition zone) are inverted together for the anomalies in temperature and water content (Figure 21):

$$\begin{pmatrix} \dfrac{\Delta V_{P,S}}{V_{P,S}} \\ \dfrac{\Delta h}{h} \end{pmatrix} = \begin{pmatrix} \dfrac{\partial \log V_{P,S}}{\partial T} & \dfrac{\partial \log V_{P,S}}{\partial C_W} \\ \dfrac{\partial \log h}{\partial T} & \dfrac{\partial \log h}{\partial C_W} \end{pmatrix} \begin{pmatrix} \Delta T \\ \Delta C_W \end{pmatrix} \qquad [14]$$

where $V_{P,S}$ is the seismic wave velocity, h is the thickness of the transition zone, T is the temperature, C_W is the water content, and ΔX is the anomaly of X. In such a formulation, one has two unknowns (water content and temperature), and using two independent observations (anomalies in seismic wave velocity and anomalies in the depth of seismic discontinuity), one can uniquely determine the temperature and water content.

Although this method would work in principle, such an approach led to puzzling conclusions such as water-poor transition zone in eastern Asia and water-rich transition zone in the central Pacific when it is applied to a global scale (Meier et al., 2009). This suggests that the assumption that the anomalies of seismic wave velocity and the topography of discontinuity (i.e., the thickness of the transition zone) depend primarily on water content and temperature is not appropriate. As seen from Figures 14 and 15, both seismic wave velocity and the topography of the seismic discontinuity depend only weakly on water content under typical (hot) mantle conditions. In other words, in the case of seismic wave velocity and the thickness of the transition zone, the influence of ξ in eqn [14] is so strong that the variation in $X(C_W, T; \xi)$ is mostly caused by that of ξ (major element chemistry) rather than the water content (C_W). In these cases, rather than the anomalies in the water content, ΔC_W, one should use another variable such as the variation in major element chemistry and temperature (ξ, T) as unknowns. Even in these cases, water content could be inferred if major element chemistry is very precisely known. This is almost impossible because in order to detect ~0.1 wt% of water, one needs to know the iron content better than ~0.1%, for example. I conclude that it is difficult to infer water content from seismic wave velocity and/or the topography of the mantle discontinuities.

There are other types of seismological observations that provide better constraints on the water content. The first is seismic wave attenuation and the second is seismic anisotropy. When seismic wave attenuation is well resolved, the observed attenuation can be used to infer water content (and temperature). Such an attempt was made for the Earth by Shito et al. (2006) who found water-rich regions in the deep (~300 km) wedge mantle in the western Pacific. Similarly, Karato (2013a) applied such a method to the Moon using the inferred tidal dissipation and electrical conductivity as constraints. He found evidence of a substantial amount of water in the deep lunar mantle similar to the upper mantle of the Earth. The limitations with this approach are that the relation between seismic wave attenuation (or tidal dissipation) and water content is not precisely constrained and that geophysical observations on attenuation have large uncertainties (e.g., Dalton et al., 2009; Romanowicz and Durek, 2000). In contrast, tidal dissipation is determined by the geodetic measurements of the shape of planets and can be determined precisely (errors less than ~10%) (e.g., Ray et al., 2001; Williams et al., 2001). However, tidal dissipation is a property of the whole planet, and one needs a model for the depth-dependent attenuation to interpret tidal dissipation (Karato, 2013a).

Deformation microstructures such as the LPO of olivine depend on the water content and other parameters such as temperature and stress (**Section 9.05.3.3**; **Figure 16**; Karato et al., 2008). Consequently, for a given flow geometry, seismic anisotropy depends on the water content (and other factors). Therefore, when flow geometry and other factors such as temperature are well known, one can infer the distribution of water content from seismic anisotropy. For example, anomalous seismic anisotropy in the central Pacific (Ekström and Dziewonski, 1998) was explained by the redistribution of water caused by deep partial melting associated with the Hawaiian plume (Karato, 2008b). Kneller et al. (2005) explained the complex pattern of anisotropy in the wedge mantle (mantle above a subducting slab) by the variation in LPO caused by the variation in stress, temperature, and water content. An obvious limitation of this approach is that the location of seismic anisotropy is not easily constrained particularly when one uses the body waves (e.g., SKS; Savage, 1999; Silver, 1996). Also, some laboratory studies suggest more complex behavior of LPO in olivine (e.g., Ohuchi and Irifune, 2013).

9.05.4.2.2 From electrical conductivity

Electrical conductivity in a planet can be inferred from the observations of electromagnetic induction (e.g., Banks, 1969; Hood et al., 1982; Kelbert et al., 2009; Rikitake, 1966). Temporal variations of an external magnetic field induce electrical currents in a planet that in turn induce magnetic field. By measuring the electromagnetic field on the planetary surface, one can determine the ratio of the external and internal field. The induced current is proportional to electrical conductivity,

and hence by determining the ratio of induced field to external field, one can infer the electrical conductivity. The depth variation of electrical conductivity can be inferred from the frequency dependence of electromagnetic induction. In many cases, the lateral variation in electrical conductivity is large comparable with the depth variation (e.g., Baba et al., 2010; Banks, 1969; Evans et al., 2011; Hood et al., 1982). This suggests the strong sensitivity of electrical conductivity to some parameters that change laterally such as temperature and the water content.

The resolution of electrical conductivity estimate is not as high as that of seismological observations. However, it is important to understand that the range of the water content we may have in a terrestrial planet is broad, from ~1 ppm wt or less (nearly completely dry) to ~1 wt% (nearly saturated). Consequently, if one can infer water content within one order of magnitude, this will be an important progress. Electrical conductivity observations have enough resolution for this purpose.

Figure 22 compares the conductivity–depth profile models corresponding to various water contents with geophysically inferred conductivity–depth profiles (Karato, 2011). Such a comparison suggests strongly layered water content in the Earth's mantle, ~0.01 wt% in the upper mantle (asthenosphere) and ~0.1 wt% in the transition zone (Figure 23). These results also show a large regional variation in the water content: a high water content in the transition zone in East Asia (Ichiki et al., 2006), a low water content in the transition zone in eastern/southern Europe (Tarits et al., 2004), and a low water content in the asthenosphere in the western Pacific (Baba et al., 2010). Currently, there are no constraints on the water content of the lower mantle because there are no laboratory data on the influence of the water content on the electrical conductivity of lower mantle minerals.

A similar study was made for the Moon where geophysically inferred electrical conductivity–depth profile was interpreted by a combination of temperature–water content (Karato, 2013a). Combining the constraints from tidal dissipation, which also provides a constraint on the temperature–water content combination, with electrical conductivity, Karato (2013a) estimated the temperature and water content separately and concluded that the presence of water similar to the upper mantle of the Earth (~0.01–0.001 wt%) is needed to explain these observations.

9.05.4.2.3 From rheological properties

Given the sensitivity of rheological properties to water content summarized in Section 9.05.3.2, one might consider that the variation of rheological properties (viscosity) of the mantle might be used to infer the water content. Such an approach is, however, hampered by the poor spatial resolution of the geophysical estimate of rheological properties and by the strong trade-off between the water and temperature effects. For example, Cadek and Fleitout (2003) and Nakada and Lambeck (1991) presented evidence for the lateral variation in viscosity, and Dixon et al. (2004) interpreted some of geophysical observations in terms of the lateral variation in water content. However, the results of these studies are subject to large uncertainties due to the strong trade-off between the temperature and water effects.

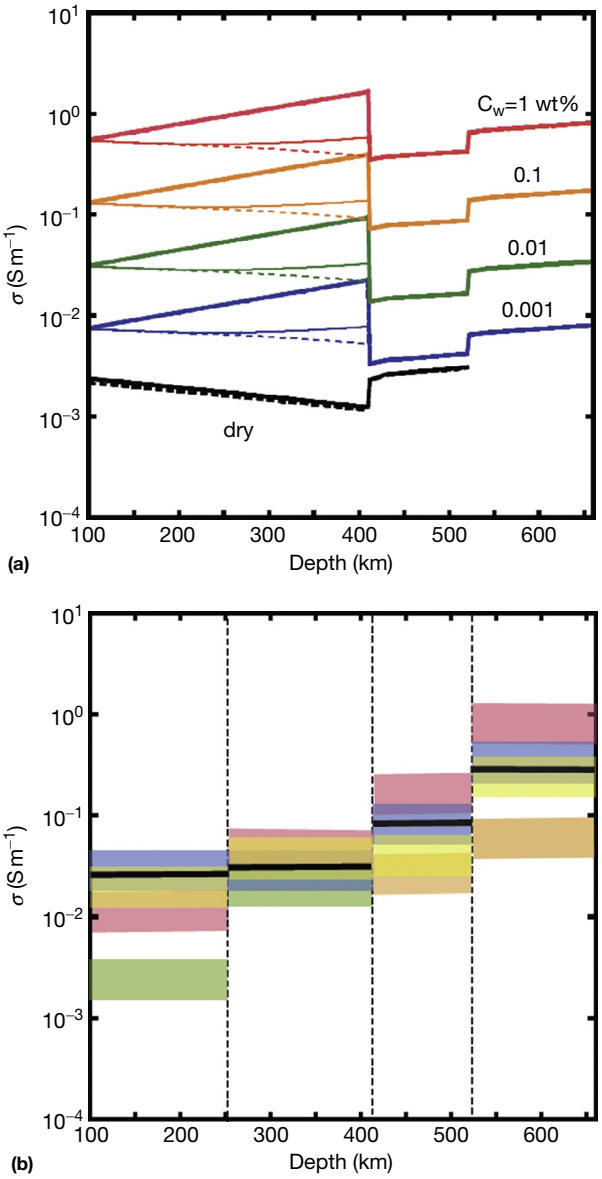

Figure 22 (a) Models of electrical conductivity versus depth relations in the Earth's upper mantle and transition zone (Karato, 2011). Water content is assumed to be independent of depth. The depth variation in conductivity is caused mainly by depth variation in temperature and mineralogy (phase transformations). (b) Geophysically inferred electrical conductivity in the upper mantle and transition zone (Karato, 2011). Different colors correspond to the conductivity in different regions (for details, see Karato, 2011).

9.05.4.3 Other Volatile Elements

Similar to hydrogen, the concentration of carbon in the mantle can be inferred from the composition of basaltic rocks (Dasgupta and Hirschmann, 2010; Hirschmann and Dasgupta, 2009; Wood et al., 1996). Both hydrogen and carbon are modest to highly incompatible elements, and a majority of them move to melts upon partial melting. However, there are two important differences in the behavior of carbon and hydrogen upon partial melting. First, carbon is more incompatible than

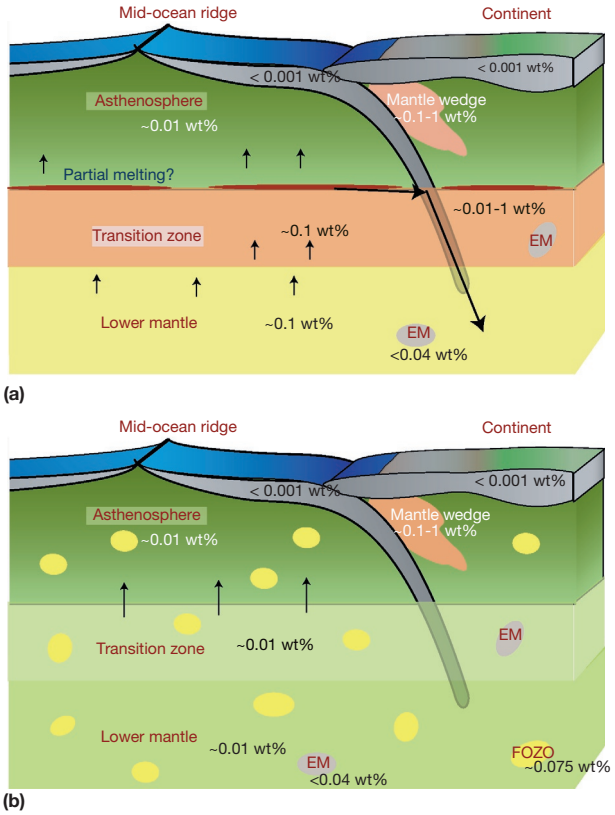

Figure 23 Models of water distribution in the Earth's mantle. (a) A layered water content model. Most geophysical models to explain electromagnetic induction observations require a substantial increase in electrical conductivity at ~410 km. This implies the increase in water content across the 410 km discontinuity. This model is consistent with the geochemical observations on the rare gases (Marty, 2012). (b) A raisin bread model. A model of patchy water-rich regions in the deep mantle proposed by Rüpke et al. (2006) and Korenaga (2008) is not consistent with the electrical conductivity and the rare gas observations (Marty, 2012). Reproduced from Karato S (2011) Water distribution across the mantle transition zone and its implications for global material circulation. *Earth and Planetary Science Letters* 301: 413–423.

hydrogen (Shcheka et al., 2006). Second, the diffusion coefficient of carbon in minerals is generally much slower than that of hydrogen. These two factors make carbon depletion more efficient upon partial melting. If indeed the upper mantle (asthenosphere) were formed as a result of partial melting at ~410 km, then the C/H ratio would be higher in the transition zone (and lower mantle) than that in the upper mantle.

Using the carbon and hydrogen contents in MORB and OIB, Hirschmann and Dasgupta (2009) inferred that the H/C ratio of the deep mantle (transition zone and the lower mantle) is substantially smaller than that in the upper mantle. The inferred difference in the H/C ratio between the upper mantle and the deep mantle is difficult to explain if there is no major mass segregation in between these two regions. However, because of the different behaviors of C and H upon partial melting, the inferred variation in the H/C ratio is naturally attributed to the effect of partial melting and melt-solid segregation at (near) 410 km. The abundance of other volatile elements is reviewed by Marty (2012) (**Table 2(b)**).

9.05.4.4 Water Content in Other Planetary Bodies

The water contents in some meteorites were measured and the water contents of comets were estimated (Jarosewich, 1990; Marty and Yokochi, 2006). Comets are volatile-rich (~50 wt%), so are carbonaceous chondrites (~10 wt%). Ordinary chondrites have ~0.1 wt% of water. The most depleted meteorite is enstatite chondrite that has less than 0.1 wt% of water. Most of ordinary chondritic meteorites are considered to come from the inner asteroid belt (2.1–2.5 AU; AU, the astronomical unit (the distance between the Earth and the Sun), 1.50×10^8 km from the Sun), whereas carbonaceous chondrites are from the outer region of the asteroid belt (~3 AU) (Gradie and Tedesco, 1982). This suggests that materials within the snow line (~2.7 AU; see **Section 9.05.5.1.2**) have enough water to be an important, perhaps dominant, source of the Earth's water.

Water contents of the Moon were inferred from the lunar samples, resulting in a wide range of values. Among them, the most robust is the measurements on basaltic inclusions in olivine that showed the water content similar to that in mid-ocean ridge basalt (Hauri et al., 2011) (see also Hui et al., 2013; Saal et al., 2013). Geophysical observations suggesting the Earth-like water content in the lunar mantle are reviewed by Karato (2013a). He used the geophysically inferred electrical conductivity–depth profile and the tidal dissipation to infer the water content (and temperature) to conclude that the water content of the lunar mantle is similar to that of the upper mantle of the Earth, a conclusion similar to that obtained

from the geochemical study by Hauri et al. (2011). Saal et al. (2013) also provided isotopic observations suggesting that water in the Moon is indigenous and the water and other volatiles in the Moon likely have similar origin as those in the Earth.

Water content in the Martian mantle can be inferred from the composition of the Martian meteorites (e.g., McSween et al., 2001; Mysen et al., 1998). However, the interpretation of observed water contents of these samples is not unique and different models were proposed (McSween et al., 2001; Mysen et al., 1998). Similar to the Moon, geophysical observations would provide additional constraints on the water content in the Martian mantle. The tidal dissipation of Mars was determined from the analysis of the orbits of its satellites (Lainey et al., 2007). If the electrical conductivity of Mars were inferred from electromagnetic induction measurements, it would be possible to infer the water distribution in Mars. For Venus, no data on tidal dissipation nor electrical conductivity are available. It is often discussed that the Venusian mantle is likely water-poor based on the observed positive correlation between topography and gravity (Kaula, 1990) and the composition of the atmosphere (e.g., Chapter 4 of de Pater and Lissauer, 2010). However, there is some suggestion that Venus had a large amount of hydrogen in the past (e.g., Donahue et al., 1982; Grinspoon, 1987; Kasting and Pollack, 1983). Because plate tectonics does not operate on Venus at least in the recent ~500 Myr, degassing is less efficient and Venusian mantle might contain a substantial amount of water (see also Halliday, 2013).

9.05.5 Volatiles During Planetary Formation

Planets are formed as a by-product of star formation, which is caused by the gravitational collapse of a molecular cloud (Shu et al., 1987). By gravitational collapse, such a cloud will be heated up (these materials will also be heated up by the radiation of the mother star). Most of the materials of the molecular cloud go to the center of the cloud from which a star is formed. However, there will be some leftover materials, from which planets are formed. The composition of these materials is initially similar to that of the molecular cloud from which the star was formed. In fact, recent search for exoplanets shows that a large fraction of the stars (>40%) have planets (Howard et al., 2010).

During the cooling of the nebula associated with the strong radiation generated by the early-stage star ('T Tauri' star, a star in the later stage of the Hayashi contraction phase; Hayashi, 1961), most of the volatile components in the gas will be blown off to define the initial composition of a terrestrial planet. In the later stage of planetary formation, extensive heating will occur by collisions that can result in the volatile loss. (In a giant impact, most materials are gravitationally bound and not much volatile loss will occur. However, if temperature exceeds the vaporization temperature, then planets (satellites) formed from the once vaporized materials will be depleted of volatiles to some extent during condensation (see, e.g., Karato, 2013b).) Collisions also lead to orbital scattering that enhances the mixing of materials with different volatile contents (e.g., Kokubo and Ida, 2000; Morbidelli et al., 2000). And finally, in the late stage of planetary formation, magma ocean and atmosphere will be formed that redistribute volatile elements (e.g., Abe and Matsui, 1985; Abe et al., 2000; Elkins-Tanton and Grove, 2011). After a planet is formed, some volatiles will be lost through the outer layer of the atmosphere (e.g., Abe et al., 2011; Hunten et al., 1989), but there will be a long-term circulation of volatiles involving degassing and regassing associated with mantle convection and core cooling (e.g., Franck and Bounama, 2001; McGovern and Schubert, 1989; Rüpke et al., 2006). The timescales of these processes are summarized in **Table 3**, showing that most of these stages have markedly different timescales so that some of them can be discussed separately. However, there are a few cases where the mutual feedback of two processes may be important including the formation of a satellite associated with a giant impact.

Table 3 Timescale of various planetary processes

Process	*Timescale (Myr)*
Nebular collapse, cooling	$\sim 10^{-4}$–10^{-3}
T Tauri stage (Hayashi contraction phase)	$\sim 10^{-2}$–1
Planetary formation	~10–10^{2}
Planetary evolution	~10^{3}–10^{4}

9.05.5.1 Acquisition and/or Loss of Volatile Elements in the Early Stage of Planetary Formation

9.05.5.1.1 General introduction

Terrestrial planets are made of condensed materials. Therefore, condensation from a hot gas is the first stage by which the volatile content of terrestrial planet is controlled. Upon cooling, refractory materials are condensed in the early hot stage and volatile materials are condensed later in the cool stage. The condensed materials not only will sink to the equatorial plane of the nebula and eventually form planets but also may migrate toward or away from the star. When gaseous phases are blown off by the strong solar wind at the T Tauri stage of the mother star, condensation will cease and the condensed materials at this stage will become the source materials of terrestrial planets (strong radiation will blow off most of the solar nebula composition gas from terrestrial planets, but not from giant planets because of the strong gravity for the latter). (Large impact could also blow off the preexisting atmosphere, but the timing of a large impact is 10 s of Myr after the formation of the Sun, and therefore, it will be after the blowoff of the primary atmosphere by the solar radiation during the T Tauri stage.)

Assuming this scenario, the composition of the condensed materials that will become terrestrial planets can be calculated from the temperature of the nebula at the time of the T Tauri phase. Whenever the timing of the T Tauri stage is, the temperature in the nebula at any distance from the mother star decreases with distance. Consequently, there will be a gradient in chemical composition of the condensed matter. Lewis (1972) proposed that the composition of the terrestrial planets can be explained by the condensation temperatures of various materials. Similarly, Gradie and Tedesco (1982) reported that the composition of asteroids inferred from the reflection

spectroscopy varies systematically as a function of the distance from the Sun. This is consistent with the condensation model. They also discussed that this observation suggests that there is not much orbital scattering of these bodies after their formation. However, recently, DeMeo and Carry (2014) showed a more complex compositional distribution in the asteroid belt, suggesting the importance of mixing. Also, Cassen (1996) developed a model to explain the variation of moderately volatile elements in some carbonaceous meteorites using such a model where radial transport of matter is also considered.

9.05.5.1.2 The snow line

There will be a critical distance from the mother star at which temperature becomes cooler than the condensation temperature of ice when the mother star is at the T Tauri stage of evolution. This critical distance (line) is called the snow line (Hayashi, 1981; or the 'frost line' or the 'ice line'). Hayashi (1981) estimated that the location of the snow line for the solar nebula is ~2.7 AU (uncertainties in such an estimate will be discussed later). Beyond the snow line, it is often argued that a large amount of volatile-rich materials is condensed that makes it possible to nucleate a core quickly on which a giant planet could be formed. (The formation of giant planets also needs a large amount of materials. Therefore, the distribution of giant planets is also controlled by the distribution of materials (the surface density) in the solar nebula.) The concept of the snow line provides a natural explanation of the presence of two classes of planets: terrestrial planets within the snow line (<2 AU) and gaseous planets away from the snow line (>4 AU).

It is often assumed that the condensed materials within the snow line are completely dry. If this were true, then in order for terrestrial planets formed within the snow line (e.g., the Earth) to acquire any water (hydrogen), substantial orbital scattering to increase the eccentricity would be needed (e.g., Albaréde, 2009; Morbidelli et al., 2000; Raymond et al., 2007). Because the orbital scattering becomes large only in the later stage of planetary accretion (Kokubo and Ida, 2000; Morbidelli et al., 2000), such a model would imply that water on Earth was acquired in the late stage of its accretion, say, ~50–100 Myr after the formation of the solar nebula (Albaréde, 2009) when the core was already formed (~30 Myr after the formation of the Sun; Kleine and Rudge, 2011). Wood et al. (2010), however, presented geochemical observations (abundance of moderately volatile and siderophile elements) suggesting that a substantial amount of volatile elements was present on Earth at the time of core formation. If most of volatile elements such as H were acquired after core formation, the core would not have much volatile elements. In contrast, if a substantial amount of volatile elements were acquired before core formation, then the core will have some volatile elements.

The location of the snow line depends on the opacity of the nebula and the radiation from the star at the time of the T Tauri stage of a star, both of which have large uncertainties. First, the temperature distribution in the nebula depends strongly on the opacity that in turn depends on poorly constrained amount of condensed matter (Cameron and Pine, 1973). In fact, Sasselov and Lecar (2000) proposed a model where dust grains play an important role in the thermal structure and suggested that the snow line is at ~1 AU for the solar system. Second, the condensation temperature of ice depends on the total pressure of the nebula that is model-dependent (see eqn [2]). The total pressure depends on the mass of the nebula and is different between the minimum mass model of Hayashi et al. (1985) and a model by Cameron (1988) where the mass of the nebula is considered to be the same as the mass of the Sun. This leads to a large uncertainty in the condensation temperature (see eqn [2]) and hence in the locations of the snow line.

9.05.5.1.3 Water (hydrogen) within the snow line?

When the concept of the snow line is used in its simplest form, the formation of hydrous minerals such as serpentine is not considered based on the simple collision theory of the kinetics of chemical reaction (e.g., Fegley, 2000). However, based on some experimental observations, Ganguly and Bose (1995) pointed out that the kinetics of formation of hydrous minerals might be much faster (more than 10^{14} times of magnitude faster!) than Fegley (2000) calculated (see also Jug et al. (2007)and Mejias et al. (1999) for the fast kinetics of hydrous mineral formation). If these experimental observations can be applied to the solar system, then the formation of hydrous minerals within the snow line would be possible. For these reasons, the concept of the snow line should be used with caution in the discussion of volatile acquisition in a growing terrestrial planet.

Another possibility was proposed by Muralidharan et al. (2008) who suggested that the surface adsorption of volatiles on dust grains might contribute to the volatile budget of terrestrial planets. In such a case, even materials within the ice line will acquire some volatiles. However, in order to explain an appreciable amount of volatiles by this mechanism, they need to assume large surface area caused by irregular morphology of grains. The validity of such an assumption is unclear. Recently, Vattuone et al. (2013) reported a more detailed experimental and theoretical study on water adsorption. Again, however, the amount of water that could be kept in these materials by adsorption depends strongly on the size of grains that is not well constrained.

The observed finite amount of water in chondrite suggests that there is some water within the snow line although the processes by which such a finite amount of water (and other volatiles) was acquired are not well understood.

9.05.5.1.4 Gas → solid versus gas → liquid condensation

Condensation occurs during nearly isobaric cooling (small reduction in pressure occurs during cooling). Therefore, whether gas → solid or gas → liquid condensation occurs is essentially determined by the relative position of the triple point pressure P_c and the actual total pressure (**Figure 3**).

Most previous discussions on the condensation of volatile elements in cosmochemistry have been made assuming the gas ↔ solid reactions (vaporization and condensation; Grossman and Larimer, 1974). As shown in **Figure 3**, such reactions are relevant at low pressures. In most of the environments in the primitive solar nebula, the gas pressure is low (Cameron and Pine, 1973; Hayashi, 1981) and such a model is appropriate. However, under some conditions where the total pressure was high, liquids will play an important role.

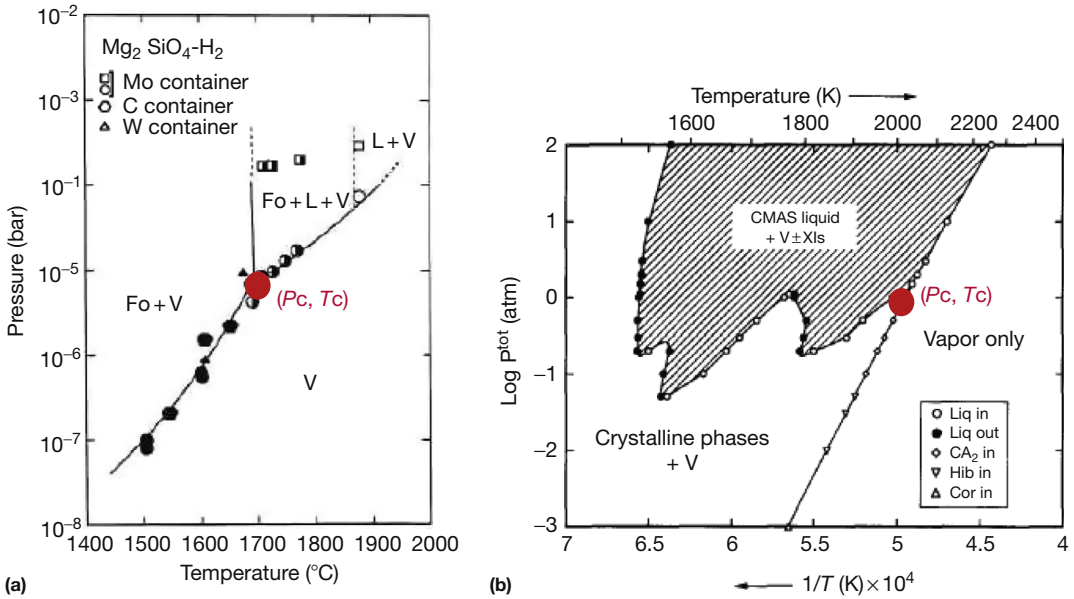

Figure 24 Phase diagrams of two systems in the cosmochemical environment. (a) The H_2–Mg_2SiO_4 system (Mysen and Kushiro, 1988). (b) The CaO–MgO–Al_2O_3–SiO_2+H_2 and other volatile systems (Yoneda and Grossman, 1995) (a substantial fraction of refractory elements is in the dusts). Condensation occurs during cooling that is nearly isobaric (pressure decreases slightly with cooling). For the solar nebula (low pressures), condensation occurs as gas → solid, whereas for a lunar disk (high pressures), it occurs as gas → liquid. A change in composition during condensation may also promote condensation of liquid phases (e.g., Ebel and Grossman, 2000).

Figure 24 shows phase diagrams relevant to planetary formation through condensation. Condensation occurs through (nearly) isobaric cooling. Consequently, the sequence of condensation depends strongly on the relative value of the triple point pressure P_c and the total pressure of the system. If the total pressure exceeds P_c, then condensation forms liquids first. This critical pressure (and temperature) depends on the composition of the system. P_c of a system H_2 and Mg_2SiO_4 (Mysen and Kushiro, 1988) is smaller than that of a system CaO–MgO–Al_2O_3–SiO_2+hydrogen and other volatiles where a substantial fraction of refractory elements are in the dusts (Yoneda and Grossman, 1995). The study of Mysen and Kushiro (1988) is an experimental study, whereas that of Yoneda and Grossman (2005) is a model. (The difference may also be due to the uncertainties in the model calculation by Yoneda and Grossman (2005).) In the solar nebula, a typical pressure is ~10–10^2 Pa, whereas in the Moon-forming disk, the pressure is much higher (10^4–10^7 Pa; Karato, 2013b). Condensation under relatively high pressure may also occur during the collisions of planetesimals as inferred from the chemistry of some meteorites (e.g., Campbell et al., 2002). Also, cooling after heating by a shock wave will involve gas → liquid condensation that is a possible mechanism of chondrule formation (e.g., Galy et al., 2000).

The gas → liquid condensation is important in relation to the volatile acquisition in a growing terrestrial planet. When only the gas → solid condensation is considered, what matters most is the condensation of volatile-rich minerals such as ice. However, when liquid phases are formed by condensation, they can store a much larger amount of volatiles than solids (Figure 25). Karato (2013a) explained the inferred high water content of the Moon (similar to that of the Earth's upper mantle) by the condensation to liquid phases and subsequent rapid accretion.

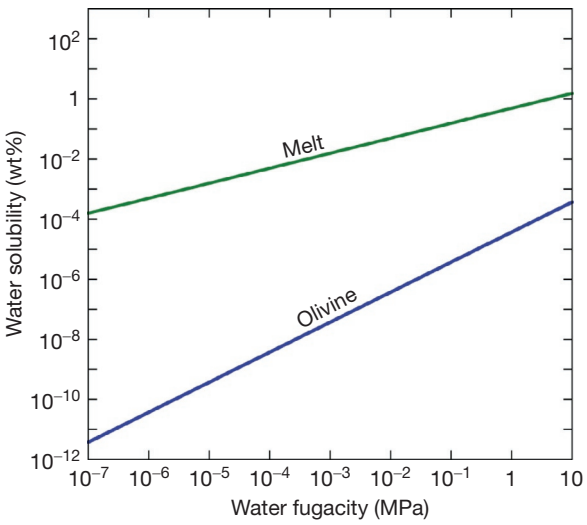

Figure 25 A comparison of solubility of hydrogen in melt (basalt) and solid (olivine). Hydrogen solubility in both basalt (silicate melt) and olivine increases with water fugacity (pressure). However, hydrogen solubility in basalt is much higher than that in olivine in all geologically plausible conditions.

9.05.5.2 Behavior of Volatiles During the Later Stage of Planetary Formation

9.05.5.2.1 Collision-induced melting and vaporization

Terrestrial planets grow as a result of collisions of small planetary bodies ('planetesimals') formed after condensation (e.g., Safronov, 1972). Once some volatile elements are acquired in the condensed matter (planetesimals) during the cooling of

the nebula, the next process that will redistribute volatile elements is the collision of planetesimals. The current models of planetary formation suggest that the average size of planetesimals increases with time, and in the later stage of planetary formation, relatively large bodies collide (e.g., Wetherill, 1990). Collisions of large bodies release a large amount of energy during a short time and hence produce high degree of heating and resultant redistribution of volatile elements.

There have been experimental studies (e.g., Lange and Ahrens, 1982; Tyburczy et al., 1986, 2001) as well as theoretical modeling (e.g., Ahrens and O'Keefe, 1972; Canup, 2004b; Pritchard and Stevenson, 2000; Stevenson, 1987) on these processes. The essential cause of impact-induced melting and/or vaporization is heating by the release of gravitational energy. Therefore, the degree of heating increases with the size of colliding (and collided) materials. The *maximum* (assuming no kinetic energy when bodies are far apart) temperature at the surface of a growing planet can be calculated assuming that all the gravitational energy is converted to heat, that is,

$$(\Delta T)_{\max} = \frac{4\pi R_{\mathrm{P}}^2 G\rho}{3C_{\mathrm{P}}} \qquad [15]$$

where G is the gravitational constant, R_{P} is the radius of a planet, ρ is the (average) density of a planet, and C_{P} is the specific heat. For the melting temperature of typical silicates at low pressure ($\sim$1500 K), one finds that the radius of $R_{\mathrm{P}} > 2000$ km will be needed. Therefore, in the later stage of planetary accretion, the surface of a growing planet will be melted if the size exceeds $\sim$1/3 of the Earth and if the gravitational energy is efficiently converted to heat. In other words, if a small planet such as the Moon ($R_{\mathrm{P}} = 1740$ km) was extensively melted when short-lived radioactive isotope such as ^{26}Al is not available (more than $\sim$10 Myr after the formation of the solar system), energy source other than its own gravitational energy must be present. The gravitational energy of the Earth (i.e., a giant impact to the Earth) is an obvious possibility to have caused extensive melting during the formation of the Moon.

The temperature given by eqn [15] is the maximum temperature for two reasons. First, in a realistic case, some of the energy is lost by radiation that reduces the temperature (e.g., Hanks and Anderson, 1969). It is understood that in the later stage of planetary accretion, the degree of radiative energy loss is small because of the short timescale of mass addition (due to the collisions of large bodies) and the blanketing effects of debris and/or the atmosphere (e.g., Hayashi et al., 1979; Kaula, 1979; Safronov, 1978). Second, some of the energy will be stored as an internal energy and only a fraction of energy changes to heat. Using a thermodynamic model of shock compression, one can analyze the degree of heating upon a collision. The heating associated with a collision is caused by the adiabatic heating and the entropy production due to compression (shock compression is not isoentropic) and is given by

$$\mathrm{d}T = -\frac{T\gamma}{V}\mathrm{d}V + \frac{1}{2C_v}[(P - P_{\mathrm{o}})\mathrm{d}V + (V_{\mathrm{o}} - V)\mathrm{d}P] \qquad [16]$$

where γ is the Grüneisen parameter, C_v is the specific heat, V is the volume at pressure P, and V_{o} is the volume at pressure P_{o} (Carter et al., 1975). The first term represents the adiabatic heating and the second term corresponds to the heating due to the excess entropy produced by shock deformation. Both of these terms are sensitive to the material properties such as the bulk modulus and the Grüneisen parameter (including its volume dependence) and hence the temperature increase due to a collision depends strongly on the compressional properties of materials (**Figure 26**) (Karato, 2014a). Because the compressional properties are markedly different between liquids and solids (e.g., Jing and Karato, 2011), the consequence of a giant impact will be different if the surface of a planet that is hit has a surface magma ocean or not. Sensitivity of collisional heating on material properties likely affects the composition of materials ejected by a giant impact. In examining the thermal and chemical aspects of a giant impact, the influence of compressional properties (equation of state) of materials involved must be examined carefully (for a discussion of shock heating, see also Ahrens and O'Keefe, 1972; Stevenson, 1987).

Some of the ejected materials by a giant impact is trapped by the gravity of a mother planet (e.g., the Earth) and is confined to a relatively small space (less than 5–10 RE (the Earth's radius) in the case of the Moon formation; Canup, 2004a). As a result, the pressure of the gas (+some condensed matter) is high in comparison with the pressure in the solar nebula, and the condensation in such a case occurs as gas → liquid rather than

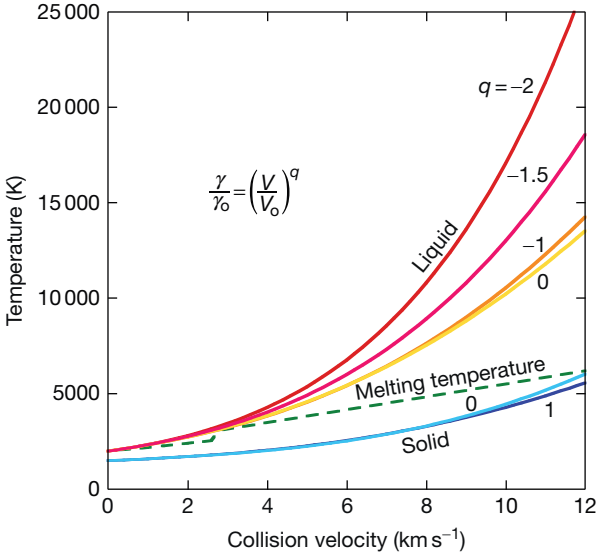

Figure 26 Temperature increase due to a collision as a function of collision velocity (from Karato, 2014a). The collision of a liquid (a planet covered with a magma ocean (proto-Earth)) and a solid at a planar interface is considered. Plausible collision velocity is the escape velocity, $\sim$10–11 km s^{-1} (for the collision to the proto-Earth). A larger degree of heating in liquids than solids is caused by the larger degree of compression for liquids than solids (due to the difference in the bulk modulus) and by the difference in the volume dependence of the Grüneisen parameter $\left(\gamma = \left(\frac{\partial \log T}{\partial \log \rho}\right)_{\mathrm{ad}}\right)$ that represents the efficiency of adiabatic heating (the Grüneisen parameter in silicate melts increases with compression, whereas the Grüneisen parameter in silicate minerals decreases with compression). As a consequence, vaporization due to a collision will occur mostly from the preexisting magma ocean if the proto-Earth was covered with a magma ocean. Heating in the solid planet unlikely exceeds the melting temperature.

gas → solid (see Figure 3). In these cases, a substantial amount of volatile elements can be dissolved in the condensed matter (liquid). If accretion is fast in comparison with the cooling timescale of the disk, then a substantial fraction of volatiles dissolved in the liquid phase could be preserved in the satellite (the Moon) (Karato, 2013a).

9.05.5.2.2 Formation of the atmosphere and the ocean

When the mass of a growing planet is large, it can acquire some gas from the surrounding nebula. However, geochemical observations, particularly those on heavy rare gases (e.g., Ne, Ar, and Xe), show that the amount of this primary gas (the solar gas) trapped by a terrestrial planet is small (e.g., Marty, 2012; Ozima and Igarashi, 1989). The majority of the volatile elements on a terrestrial planet are there as a consequence of outgassing from the planetary interior (e.g., Rubey, 1951).

Abe and Matsui developed a model of formation of the atmosphere and the ocean in the late stage of planetary formation (Abe and Matsui, 1985, 1988; Matsui and Abe, 1986a,b). They emphasized the role of impact-induced degassing and the chemical equilibrium at the interface between the growing magma ocean and the atmosphere. They found that the amount of water contained in the primitive atmosphere formed by the degassing during the formation of the Earth is $\sim 1.2 \times 10^{21}$ kg, which agrees well with the current ocean mass on Earth (1.4×10^{21} kg). They also showed that the predicted ocean mass is only weakly dependent on the amount of water contained in the source materials due to the large capacity of magma ocean to buffer the water content of the atmosphere. The near agreement of the predicted value of the ocean mass with the actual ocean mass on Earth is remarkable, and they suggested that water contained in the impact-induced atmosphere might be the source of the ocean water. If this model were correct, the Earth's interior would be essentially dry.

However, this model has some limitations, and it is not clear if this model explains the amount of volatiles in a planet. First, in their model, volatile elements dissolved in the magma ocean were not considered as a source of volatiles in the atmosphere and ocean. Because the solubility of volatile elements (such as hydrogen and carbon) in the magma is large (Figure 25), the magma ocean can contain a large amount of volatiles, and neglecting the volatile elements dissolved in the magma ocean is difficult to justify. Elkins-Tanton (2008) developed a different model for the atmosphere and the ocean formation on a terrestrial planet where the role of volatile elements dissolved in the magma ocean is emphasized. This model contains some details of the consequence of solidification, and similar to the model by the Abe and Matsui, this model predicts a dense primitive atmosphere exceeding ~10 MPa (~100 bars). In this model, the amount of water in the mantle (at the time of completion of magma ocean solidification) is determined by the amount of initial water content in the magma ocean and the solubility of water (hydrogen) in mantle minerals. Also, such a model predicts compositional stratification including the volatile content (e.g., Elkins-Tanton and Grove, 2011; Ohtani, 1985). However, the degree of stratification depends on the details of crystal settlements in a convecting magma ocean (e.g., Solomatov, 2009), and convection after the complete solidification could also destroy the initial stratification (e.g., Sleep, 1988). Hamano et al. (2013) recently investigated the consequence of magma ocean solidification and emphasized the importance of the cooling rate that determines the amount of water retained in a planet after the solidification of the magma ocean.

Second, Genda and Abe (2005) showed that when a large collision occurs on a planet with preexisting magma ocean, almost all the preexisting atmosphere will be blown off. If this happens, then the volatile content in the initial atmosphere would not play an important role in the long-term evolution of the volatile budget.

Regardless of the details, all models predict the presence of a hot initial atmosphere that helps maintain the surface temperature high enough to melt silicates. Such a high temperature lasts only through the period in which the rate of accretion is high and the large energy release occurs in a growing planet. As the rate of accretion (energy input) reduces, the atmosphere will cool down to allow surface ocean to exist if the greenhouse effect of the atmosphere is limited. The time for cooling depends on the energy release from a growing planet and is estimated to be on the order of 1 Myr for the Earth (e.g., Sleep, 2001). This means that the ocean is likely formed in the very early stage of evolution of a terrestrial planet.

9.05.5.2.3 Influence of core formation

Core formation (i.e., Fe–silicate separation) on Earth and other terrestrial planets occurred in the early stage of planetary evolution (<50 Myr; Kleine and Rudge, 2011). Fe–silicate separation occurs efficiently when the surface of a growing planet is covered with a magma ocean (e.g., Karato and Murthy, 1997; Stevenson, 1990). The core formation has important influence on the distribution of volatiles because iron can dissolve a large amount of volatiles at high pressure and temperature conditions (Section 9.05.2.3).

Two issues are critical in estimating how much volatiles might be in the core. First, in order for a substantial amount of volatiles to be dissolved in the core, the core formation must occur in a growing planet that already has acquired some volatiles. If the volatile acquisition were late as suggested by Albaréde (2009), then not much volatiles would be in the core. Second, even if the core formation occurred after a substantial amount of volatiles is already acquired in a growing planet, the degree to which separating iron captures the volatiles depends on the processes of core formation. Wood and Halliday (2010) presented evidence that a substantial amount of volatiles was already present when the core–mantle separation occurred on Earth. On the other hand, Karato and Murthy (1997) suggested that much of the iron–silicate separation occurs by merging of preexisting cores without chemical equilibrium. In such a case, the amount of volatiles in the core will be small. Dissolved volatiles will affect various physical properties of the core including density, seismic wave velocity, and electrical (and thermal) conductivity (e.g., Shibazaki et al., 2012).

Although currently no constraints are available for the water (and other volatile elements) concentration in the core, it is likely that the core has less than the solubility limits of these volatile elements. This is because the volatile solubility increases with pressure and the core–mantle equilibrium during core formation is likely established at the pressure lower than the current core–mantle boundary pressure (e.g., Karato and Murthy, 1997; Rubie et al., 2007). This means that even if

the core could contain a large amount of volatiles (e.g., water; Figure 7), it likely serves as a *sink* for the mantle water rather than the *source* for the mantle water as far as the degree of undersaturation is larger in the core than in the mantle.

9.05.6 Evolution of the Ocean and the Atmosphere

9.05.6.1 Observational Constraints

Vigorous degassing during the late stage of planetary accretion is a natural consequence of the oligarchic growth of planets. This suggests the formation of the atmosphere and the ocean on a terrestrial planet in the early stage of its evolution (the late stage of planetary accretion). There are a number of observations supporting this view. For example, Hamano and Ozima (1978) used $^{40}Ar/^{36}Ar$ to suggest massive degassing in the early history of the Earth. (The primordial gas does not have much ^{40}Ar, and most of ^{40}Ar comes from the radioactive decay of 40 K in the Earth's interior. Therefore, the abundance of ^{40}Ar (relative to ^{36}Ar) provides a measure of degassing from the Earth's interior.) Using the similar observations, Sarda et al. (1985) estimated the effective time of atmospheric formation of ~4.4 Gyr BP. Allègre et al. (1986/1987) also reported geochemical evidence (the absence of the anomalies in ^{129}Xe) suggesting that the source regions of OIB (presumably the deep mantle) were not as much degassed as the source region of MORB (the asthenosphere) in the early stage of the Earth's evolution.

As with the ocean, using the evidence of low-temperature (~1000 K) crystallization of ~4.3 Gyr old zircon, Watson and Harrison (2005) presented evidence for the presence of the surface ocean in the very early stage of the Earth's evolution. Similarly, based on the oxygen isotopic observation of ~4.3 Gyr old zircon, Mojzsis et al. (2001) presented more indirect inference to reach the same conclusion. Considering the timescale of cooling of hot protoatmosphere of ~1 Myr (Sleep, 2001) and the lifetime of the magma ocean of ~10–100 Myr (e.g., Abe, 1997; Solomatov, 2009), such a short timing for the appearance of the surface ocean is not surprising although the spatial extent of an early ocean is unknown.

After the formation of the primitive atmosphere and ocean in less than the first few 100 million years, a slow evolution of both the atmosphere and the ocean followed for several billions of years. Based on the inferred rate of chemical reactions between volatiles and rocks, Rubey (1951) presented a strong case that the ocean and atmosphere of the Earth must have been formed through the processes involving long-term degassing from the solid Earth, and hence, the ocean mass is maintained by the dynamic balance of these processes. There is a range of observations to suggest the change in the chemistry of both the atmosphere and the ocean during this period (e.g., Berner, 1994; Holland, 2003; Holland et al., 1986; Kasting, 1993), implying the presence of active chemical reactions between the atmosphere–ocean and the solid Earth.

If extensive chemical reactions occur between the atmosphere–ocean and the solid Earth during this period, how did the mass of the ocean and atmosphere change? There are no well-established methods to estimate the history of the atmospheric mass directly. ($^{40}Ar/^{36}Ar$ ratio provides indirect evidence for the evolution of the atmosphere.) Som et al. (2012) used the size of raindrop imprints to infer the air pressure at the end of the Archean period (~2.7 Gyr ago) to conclude that the air pressure on the Earth's surface, that is, the atmospheric mass, at ~2.7 Gyr ago, was not much larger (less than a factor of two difference) than it is today. The D/H ratio also provides some clue as to the extent of atmospheric loss because H is preferentially removed from the atmosphere than D due to a large difference in mass. For instance, the observed much higher D/H for the atmosphere of Venus is considered to be the evidence for a large degree of hydrogen loss (Donahue et al., 1982; Grinspoon, 1987; Kasting and Pollack, 1983).

We have better constraints on the history of the ocean mass. The history of the ocean mass could be inferred from the height of the continental shoreline ('continental freeboard'). If the areas of continent and ocean remain the same and if the average age of the ocean is also constant, then by measuring the height of the shoreline, one can infer the volume (mass) of the ocean. However, the validity of both of these assumptions is unclear, and in fact, some authors used the observed variation of continental freeboard to infer the growth rate of continents using a model of variation of average age of the ocean with time and assuming the ocean mass remained constant (e.g., Reymer and Schubert, 1984).

To understand the reasons for the different conclusions from the same observations (sea-level changes), let us first write an equation among the ocean mass, the relative sea level, and the fraction of continents (Figure 27) (The sea-level equation must include the influence of the ice sheet melting. However, the timescale of climate change (ice age) is much shorter (~1 Myr) than the timescale of ocean volume change that we consider here, so the influence of ice sheet melting is averaged out in this equation except for the period of snowball Earth):

$$[h(t) + X(t) - \bar{z}(t)][1 - f(t)] \cdot S = V(t) \qquad [17]$$

where $h(t)$ is the sea level at the continental margin (continental 'freeboard'), $X(t)$ is the dynamic topography of the continent (topography change of the continent caused by the

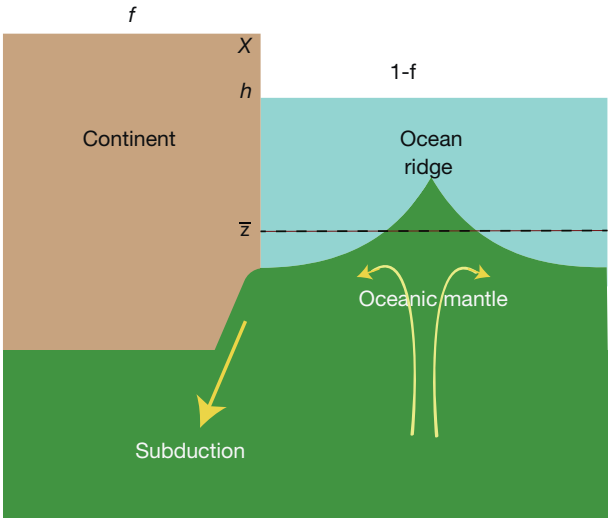

Figure 27 A cartoon showing the definitions of various terms in eqn [17].

convection current beneath (positive upward)), $\bar{z}(t)$ is the average depth of the ocean that depends on the average age of the oceanic mantle, $f(t)$ is the fraction of the surface covered by the continents, S is the surface area of the Earth, and $V(t)$ is the volume of the ocean. I assume that the temperature variation occurs only in the shallow mantle, and therefore, the surface area S remains approximately constant. Equation [17] contains five variables ($h(t)$,$X(t)$, $f(t)$, $\bar{z}(t)$, $V(t)$), and hence, if one were to infer the ocean mass history, $V(t)$, from one observation, $h(t)$, one needs to know the history of the continental area, $f(t)$; the history of the mean ocean depth, $\bar{z}(t)$; and the dynamic topography, $X(t)$.

The continental growth curve, $f(t)$, is controversial but most models suggest that the variation in $f(t)$ is less than ~30% during the whole Proterozoic period (~2.5 Gyr to ~600 Myr BP; e.g., Reymer and Schubert, 1984; Stein and Ben-Avraham, 2007). If one focuses on the Phanerozoic period (~600 Myr ago to the present) where reliable observations on the sea level, $h(t)$, are available, the change in $f(t)$ and its uncertainties are less than 10%, and hence, the influence of this term on the ocean volume is less than ~3%. The change in the mean ocean depth, $\bar{z}(t)$, could be calculated from the decay of heating by radioactivity using the boundary layer theory of internally heated fluid (e.g., Turcotte and Schubert, 1982). For the last ~1 Gyr, the heating rate changed ~15% that translates to a change in $\bar{z}(t)$ of ~4%. Sleep (1992) suggested even a smaller change in the plate velocity with time. However, the short-term fluctuation in the average age of the ocean floor and hence $\bar{z}(t)$ can be larger (e.g., Richards et al., 2000). (In addition to the change in average sea level (eustatic sea-level change), the local effects near the continental margins such as the dynamic topography associated with subduction will also contribute to the observed sea-level changes (e.g., Gurnis, 1993).) In fact, the observed sea-level variations do show large short-term fluctuations (**Figure 28**; e.g., Eriksson et al., 2006; Galer and Mezger, 1998; Hallam, 1992; Parai and Mukhopadhyay, 2012; Wise, 1974). In terms of the absolute rate of sea-level changes, the short-term sea-level change rate is up to ~10 times larger than the long-term sea-level change rate (~10% variation in ~1 Gyr and ~10% variation in ~100 Myr). The influence of dynamic topography on the sea level can be large (several 100 ms) but is sensitive to the viscosity–depth structure and will be discussed later.

The inferred long-term stability of the ocean mass on Earth (near-constant ocean mass for ~1 Gyr or more) is critical for the evolution of life (e.g., Langmuir and Broecker, 2012). However, considering potential causes to destabilize the ocean mass including the climate change and the changes in the degassing and/or regassing rates associated with the changes in plate velocities or the distribution of the continents,

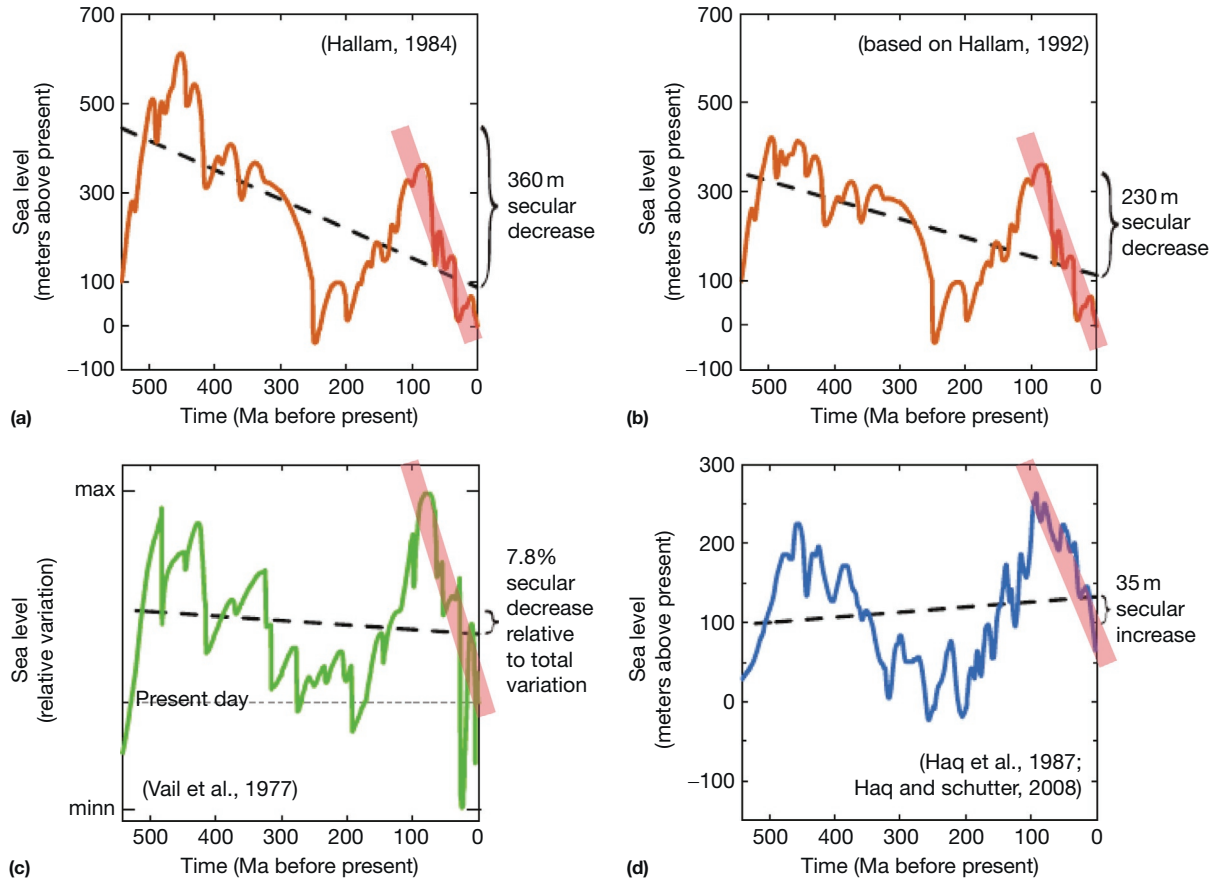

Figure 28 Phanerozoic sea levels compiled by Parai and Mukhopadhyay (2012). In addition to the secular change, large fluctuations are observed. The long-term variation in the sea level is small (less than ~5%/gigayear; black broken lines), whereas short-term variation is large (~5%/100 Myr in the recent ~100 Myr; red thick lines).

the inferred stability of ocean mass is remarkable and requires some explanation. In the following, I will review our current understanding of the long-term stability of ocean mass from two aspects: (i) the stability of atmospheric mass (and temperature) and (ii) the stability of ocean mass through the ocean–solid Earth interactions. However, since the stability of the atmosphere including hydrogen loss from the atmosphere and the conditions for the stable climate has been discussed extensively (e.g., Abe et al., 2011; Hunten and Donahue, 1976; Hunten et al., 1989; Kasting, 1989; Kasting and Catling, 2003; Kasting et al., 1993), I will make only a brief summary on it and focus on the second issue that has not been discussed in detail.

9.05.6.2 Stability of the Atmosphere and the Hydrogen (Water) Loss from the Atmosphere

For the ocean to be present for billions of years, the clement atmosphere must exist for a long time that allows the escape of water (hydrogen) from the atmosphere to be small. For this, a key is the concentration of greenhouse gases such as carbon dioxide and water vapor. Emphasizing the role of carbon dioxide, Walker et al. (1981) proposed that the interaction between the atmosphere and the solid Earth through the formation of carbonates may stabilize the climate: if the concentration of carbon dioxide is high in the atmosphere, then temperature will increase leading to the increased rate of reaction to form carbonate that in turn will reduce the concentration of carbon dioxide in the atmosphere. Conversely, if much of the atmospheric carbon dioxide is stored in carbonate (low carbon dioxide in the atmosphere) and if subduction occurs by plate tectonics, then a large amount of subducted carbonate will increase the outgassing from the magma to increase the amount of atmospheric carbon dioxide. Such a *negative feedback* will stabilize the atmospheric concentration of carbon dioxide and hence the atmospheric temperature (climate). Other factors such as albedo (reflectivity) and the fraction of continents that affects near-surface water content also control the stability of atmospheric temperatures (e.g., Abe et al., 2011; Kasting et al., 1993). Abe et al. (2011) found that for a reasonable range of solar radiation, conditions favoring the presence of oceans could last ~10 Gyr or more.

Important conclusions from these studies are as follows: (i) there are some conditions under which atmosphere with modest temperature to support the surface oceans exists for more than ~10 Gyr, but (ii) under other conditions, substantial atmospheric (or hydrogen) escape occurs. When significant but selective atmospheric loss occurs, there will be an isotopic signature (Hunten et al., 1989; Pepin, 1997; Robert et al., 2003). In particular, the change in the D/H ratio will be large when effective atmospheric loss occurs because hydrogen (H) is easier to escape than deuterium (D) because of the large difference in the mass (Robert et al., 2003). In the following, I will assume that the conditions of the stable presence of atmosphere of modest temperature for the liquid water to exist are met and ask how the fluctuations in degassing and/or regassing rates could affect the ocean mass.

9.05.6.3 Evolution of the Ocean Mass: Models of Global Water (Volatile) Circulation

Under the assumption that the water loss from the atmosphere is negligible, the total amount of water in the ocean and the Earth's interior (mantle) is fixed. Then, the evolution of the ocean mass is the history of exchange of water between the ocean and the solid Earth (mantle), that is,

$$X^{\text{total}} = X^{\text{mantle}} + X^{\text{ocean}} (= \text{constant}) \quad [18]$$

and

$$\frac{dX^{\text{ocean}}}{dt} = \Gamma_D - \Gamma_R \equiv F(X^{\text{ocean}}) \quad [19]$$

where X^{ocean} is the ocean mass, X^{mantle} is the water mass in the mantle (X^{total}: total water mass), Γ_D is the rate of water transport from the mantle to the ocean (*degassing* rate), and Γ_R is the rate of water transport from the ocean to the mantle (*regassing* rate) (Table 4).

Figure 29 illustrates the processes of degassing and regassing. Degassing is caused by partial melting near the surface and most of the volatiles in the mantle rocks are removed to

Table 4 Inferred degassing and regassing rate (global integrated values)[a]

	Values	*References*
Degassing rate[b]	1.5×10^{11} kg year^{-1}	Data compiled by Parai and Mukhopadhyay (2012)
Regassing rate[c]	0.7×10^{12} kg year^{-1}	Jarrard (2003)
	1.1×10^{12} kg year^{-1}	van Keken et al. (2011)
	1.3×10^{12} kg year^{-1}	Hacker (2008)
	$(0.9–1.8) \times 10^{12}$ kg year^{-1}	Rüpke et al. (2004)
	$(2.0–2.9) \times 10^{12}$ kg year^{-1}	Schmidt and Poli (1998)

[a]The estimated values correspond to near recent processes. Degassing rate is likely much faster in the early stage of the Earth's evolution (see **Figure 31**). The current ocean mass is 1.4×10^{21} kg. If this much water were to be transported in 1 Gyr, the rate of transportation would be 1.4×10^{12} kg year^{-1}. With the inferred degassing rate in the early stage of the Earth's evolution (~10^{13} kg year^{-1}), one ocean mass could have been produced in ~100 Myr.

[b]The rate of transportation of water-containing materials to the volcanic regions (e.g., mid-ocean ridges) is well constrained (with the uncertainties of ~50%). In some studies, all of water in these rocks is assumed to degass (e.g., Franck and Bounama, 2001; McGovern and Schubert, 1989; Parai and Mukhopadhyay, 2012), whereas in other studies, only a fraction of it is considered to degass (e.g., Rüpke et al., 2006).

[c]Among various estimates of regassing rate, Jarrard (2003) provided the lowest rate while Schmidt and Poli (1998) showed the highest rate. Jarrard (2003) considered only the sediments and the oceanic crust, whereas Schmidt and Poli (1998) considered the deep oceanic crust and the upper mantle as well including the dense hydrous phases such as phase A. A wide variation in the estimated regassing rate is partly caused by the assumed mineralogy.

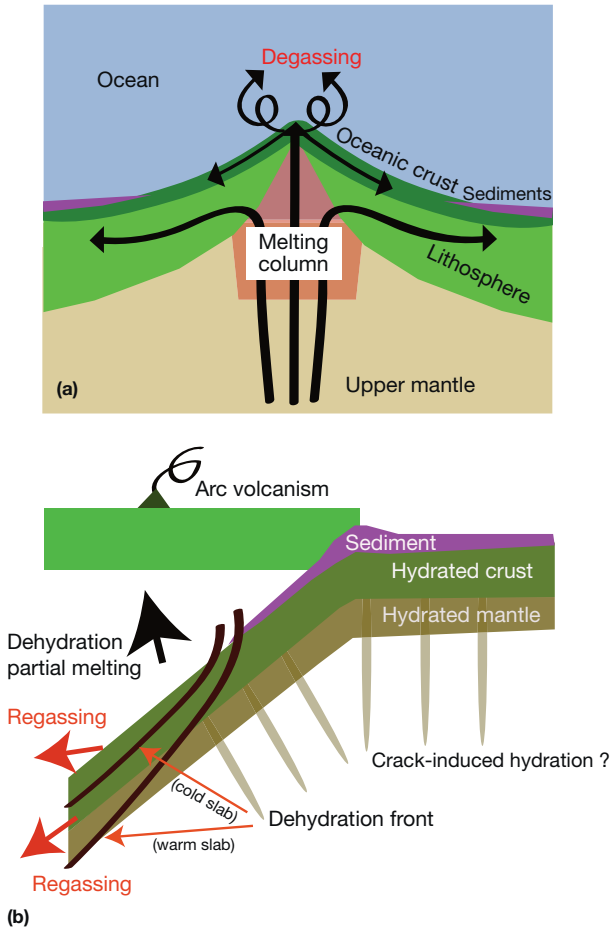

Figure 29 (a) A schematic drawing of processes of degassing at mid-ocean ridges. Water-bearing mantle materials rise nearly adiabatically below volcanoes (e.g., mid-ocean ridges) leading to partial melting. Volatiles go mostly to the melt, and when melt is frozen, some of the dissolved volatiles go to the ocean and atmosphere ('degassing'). (b) A schematic drawing of processes of regassing in the subduction zone. Volatiles such as hydrogen and carbon react with rocks to form hydrous minerals or carbonates. Hydrous minerals (including sediments) and carbonates on the oceanic lithosphere go back to the mantle upon subduction ('regassing'). The rate of regassing depends on the degree of hydration (carbonation) and the degree of dehydration (decarbonation) by heating (**Table 4**).

the molten rock (basalt). When basaltic rocks cool down, most of the volatiles will go to the ocean or to the atmosphere. One uncertainty is the fraction of volatiles in basalt that goes to the ocean (and atmosphere). Some of the volatiles will remain in the deep oceanic crust (gabbro).

Regassing involves more complicated processes than degassing. The regassing occurs at trenches where hydrated oceanic lithosphere carries water (and other volatiles) into the Earth's interior by subduction. The rate of regassing is therefore dependent on the degree of hydration of the oceanic lithosphere and the degree to which hydrated materials survive dehydration by heating after subduction. The degree of hydration of the oceanic lithosphere is controversial. Hydration caused by the hydrothermal activities near mid-ocean ridges is down to ~5 km (e.g., Lowell et al., 1995). In addition to near-ridge hydration, evidence of deep (to ~20 km) hydration by cracking near trenches is reported (Faccenda et al., 2009; Garth and Rietbrock, 2014; Ranero et al., 2003; Van Avendonk et al., 2011) although such processes may not be global. When volatiles subduct deep into the mantle, heating will dehydrate them, and only a fraction of volatiles goes into the deep mantle. However, the degree to which dehydration occurs depends on several parameters including (i) the temperature distribution near the slab/mantle interface that depends on a number of parameters including the age of subducting lithosphere and the degree of mechanical coupling between the slab and the wedge mantle (e.g., Rüpke et al., 2004; van Keken et al., 2011) and (ii) the depth of hydration. Both of which likely depend on various tectonic setting and are expected to vary from one region to another.

Both degassing and regassing rates are proportional to the rate at which materials circulate in the Earth's mantle. Therefore, these models must be combined with a model of evolution of mantle convection (thermal history). In thermal history modeling, the interplay between temperature (and water content)-dependent rheological properties and cooling plays an important role.

There have been several studies to investigate the history of the ocean mass through these approaches (e.g., Crowley et al., 2011; Franck and Bounama, 2001; Korenaga, 2011; McGovern and Schubert, 1989; Rüpke et al., 2006; Wallmann, 2001). In most of these studies, one develops some models for the degassing and regassing rates (Γ_D, Γ_R) and integrates eqn [19] together with the thermal evolution equation.

The ocean mass evolution depends essentially on $\Gamma_D - \Gamma_R$ and the results of such modeling depend entirely on this value. Therefore, subtle variations in either the degassing or the regassing rate (or both) could change the results of such a model drastically. Because a large number of parameters and assumptions are involved in these models, the results of these models must be compared to observations carefully. However, the interpretation of observations is not straightforward. In the following, I will discuss some of the key issues in the study of evolution of the ocean mass.

Most models show initially high degassing rate, $\sim 10^{13}$ kg year^{-1}, that decreases with time as a result of secular cooling (**Figure 30(a)** and **30(b)**). This fast initial degassing rate implies that one ocean mass could have been created in ~100 Myr by degassing from the interior (in addition to water from the condensation of the moist protoatmosphere (Abe and Matsui, 1985) and/or from the solidification of the water-bearing magma ocean (Elkins-Tanton, 2008; Hamano et al., 2013)). One of the large differences among different models is the treatment of the regassing rate. In some models, the dependence of regassing rate on the (average) slab age is not included and the regassing rate and the mantle water content change with time monotonically (e.g., Franck and Bounama, 2001; McGovern and Schubert, 1989, **Figure 30(a)**; Crowley et al., 2011, **Figure 30(c)**). In contrast, Rüpke et al. (2006) included the high sensitivity of the regassing rate on the (average) slab age (temperature) in their model and found that substantial regassing starts only in the later stage of the Earth's history where cold slabs subduct, leading to nonmonotonic variation of mantle water content with time (**Figure 30(b)**). The large influence of regassing parameter on the history of the ocean

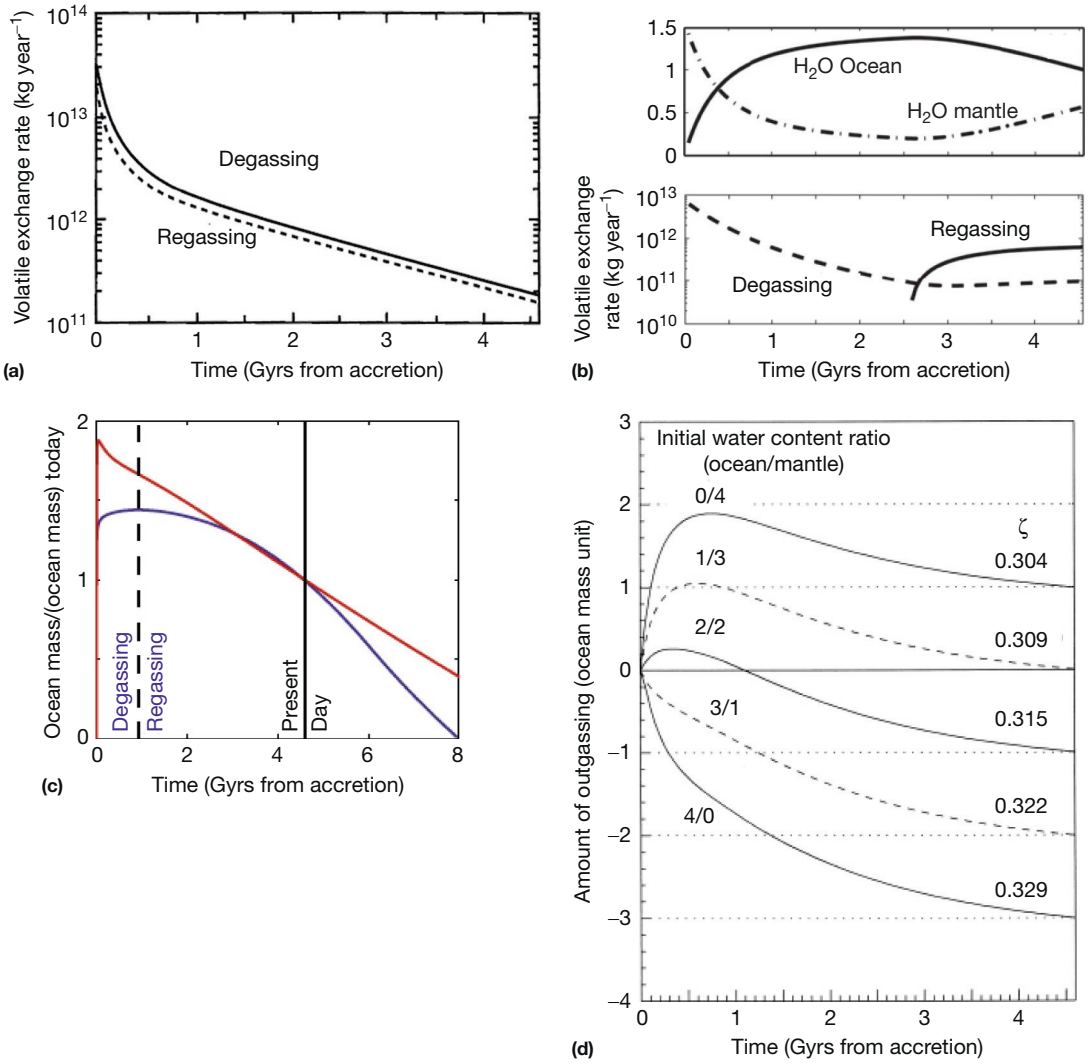

Figure 30 An example of water history (degassing/regassing rate and ocean mass) calculation on Earth. (a) In this model, degassing rate is always higher than regassing rate leading to the increase in the ocean mass (reproduced from McGovern PJ and Schubert G (1989) Thermal evolution of the Earth: Effects of volatile exchange between atmosphere and interior. *Earth and Planetary Science Letters* 96: 27–37). (b) In this model, an efficient regassing occurs only after the Earth has cooled enough. Therefore, the ocean mass increases with time initially but decreases later (reproduced from Rüpke LH, Phipps Morgan J, and Dixon JE (2006) Implications of subduction rehydration for Earth's deep water cycle. In: Jacobsen SD and Lee Svd (eds), *Earth's Deep Water Cycle*, pp. 263–276. Washington, DC: American Geophysical Union). (c) Ocean mass history for water-dependent rheology (blue line) and for water-independent rheology (red line). Regassing efficiency is assumed to be constant (reproduced from Crowley JW, Gérault M, and O'Connell RJ (2011) On the relative role of influence of heat and water transport on planetary dynamics. *Earth and Planetary Science Letters* 310: 380–388). (d) The amount of total outgassed water is plotted against time for various initial ocean water mass/initial mantle water. ζ is a fraction of subducted water that goes into the mantle. This result shows high sensitivity of ocean mass history to the regassing rate (reproduced from Franck S and Bounama C (2001) Global water cycle and Earth's thermal evolution. *Journal of Geodynamics* 32: 231–246).

mass was also shown by Franck and Bounama (2001) (**Figure 30(d)**).

A common approach in these studies is to identify a range of parameter set that explains the 'observed' long-term (~1 Gyr) ocean mass evolution (water circulation between the ocean and the mantle). Therefore, the 'stability' of the ocean mass is a part of the assumptions in these models, and the cause for the stability was never considered. However, the choice (or the interpretation) of 'observational constraints' is not trivial. The issues on the estimated mantle water content are discussed in **Section 9.05.4**. Rüpke et al. (2006) chose a small water content in the mantle (~30% ocean mass) consistent with a model by Dixon et al. (2002), but Franck and Bounama (2001) chose a higher water content (approximately three times ocean mass) based on the discussion by Ringwood (1975). As I discussed in **Section 9.05.4**, both geochemical and geophysical observations favor a high water content in the mantle (approximately three times ocean mass or higher).

Perhaps more important is the interpretation of the short-term variations of the sea level. Given the high sensitivity of the ocean mass evolution to the regassing rate and given the sensitivity of regassing rate on a number of variables (processes),

one may expect a large fluctuation in the ocean mass. Indeed, the reported sea level (continental freeboard) history shows very large short-term (~100 Myr) variations (Figure 28). In most of previous studies, however, the reported short-term sea-level variations were attributed to some 'tectonic' effects (effects due to $\bar{z}(t)$, $X(t)$ in eqn [17]), and they considered that the ocean mass did not change appreciably. For instance, Gurnis (1993) and Worsley et al. (1984) noted a good correlation between the distribution of continents and the sea level versus time curve and argued that the observed fluctuation of the sea level is largely due to the influence of the change in the distribution of continents. In more detail, Gurnis (1993) noted that the dynamic topography near subduction zones plays an important role in the observed sea-level changes and could explain the observed sea-level variation assuming that the viscosity–depth profile in these regions is the same as other regions. However, Billen and Gurnis (2001) showed that the low viscosity–depth structure of the upper mantle in these regions substantially reduces the amplitude of dynamic topography. I conclude that if low viscosity in these regions is included, then it will be difficult to explain the observed large sea-level variation by the dynamic topography. It is likely that at least a part of these short-term sea-level fluctuations is caused by the change in the ocean mass.

Considering these uncertainties, it is worthwhile to discuss some possible mechanisms to 'stabilize' the ocean mass physically. Emphasizing the role of regassing on the ocean mass, Kasting and Holm (1992) proposed that the ocean mass may be stabilized due to the influence of ocean mass (pressure at the bottom of the ocean) on the degree of hydration near the mid-ocean ridges. Hydration of the oceanic lithosphere occurs mostly by the hydrothermal circulation near mid-ocean ridges (e.g., Lister, 1980) and the degree to which hydration occurs is sensitive to the properties of aqueous fluids. Kasting and Holm (1992) noted that the pressure and temperature of hydrothermal fluids at the present time are close to the critical conditions of water where water can carry unusually high amount of heat. Consequently, the depth extent to which hydrothermal circulation penetrates is largest under the current conditions, leading to a negative feedback when the ocean depth is below the current value. However, if the ocean mass exceeds the current level, the ocean mass would increase and will not be stabilized. In addition, even if the degree of hydration is controlled by this mechanism, the regassing rate also depends on the near-surface temperature of subducting plate where substantial dehydration occurs. Therefore, even if the degree of hydration is stabilized, a large fluctuation in the degree of dehydration will cause the large fluctuation in the regassing rate. Alternatively, the ocean mass might be regulated by the negative feedback between ocean mass and the degassing efficiency. The degassing efficiency depends on the pressure at which degassing occurs from the erupted magma. When the ocean mass increases, then pressure increases leading to less efficient degassing that causes the decrease in the ocean mass and vice versa.

One of the major limitations of the most previous models of global water circulation is the assumption that the mantle acts as a single reservoir (Figure 31(a)). In such a case, the reaction of the mantle to a change in regassing rate is direct. In contrast, when there are internal processes to redistribute water, then the reaction of the mantle to the variation in the regassing rate is indirect and, under some cases, reduces the sensitivity of the mantle water content to the change in the regassing rate. One example is the role of midmantle partial melting (Figure 31(b)). Partial melting buffers the water content in the residual mantle (see Figure 12) and hence the sensitivity of the mantle water content to the fluctuation in the regassing rate. The observational support for midmantle partial melting and its consequence on the global water circulation were discussed by Karato (2011). Water-promoted melting could occur also below the '660 km' discontinuity in or near the subduction zone. Partial melting below '660 km' discontinuity is expected to be limited to near the subduction zone. Seismological tests of the presence of partial melting below the '660 km' discontinuity is limited (e.g., Schmandt et al., 2011) compared with a layer above the '410 km' discontinuity (e.g., Bagley et al., 2009; Coutier and Revenaugh, 2007; Tauzin et al., 2010). Internal processes such as midmantle partial melting are a consequence of the presence of a peak in water solubility in the midmantle as shown in Figure 7. If indeed such internal processes as deep partial melting were essential for the long-term presence of the surface ocean, it would imply that the planetary size would need to be large enough to cause such partial melting (pressure in the mantle needs to exceed ~15 GPa). Numerical modeling combined with some observational constraints will be helpful to understand these potentially important processes.

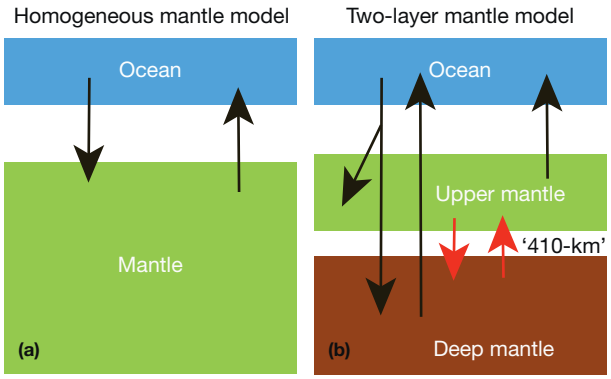

Figure 31 A schematic diagram showing the processes of water circulation in Earth. (a) A single-layer mantle model. (b) A two-layer mantle model where partial melting at '410 km' redistributes water.

9.05.7 Origin of Volatiles on Earth and Other Terrestrial Planets

Where did volatile elements (such as H) on Earth and other terrestrial planets come from? Are the volatile elements acquired by the Earth mostly from materials in or close to the current Earth's orbit (1 AU from the Sun)? Or was there substantial mixing of materials during planetary formation such that the Earth acquired its volatiles mostly from materials away from its current orbit?

The isotopic compositions provide important constraints on the origin of volatiles. Figure 32 summarizes isotopic compositions of two light elements (H and N; from Marty, 2012; Saal et al., 2013). It is seen that comets, meteorites, and

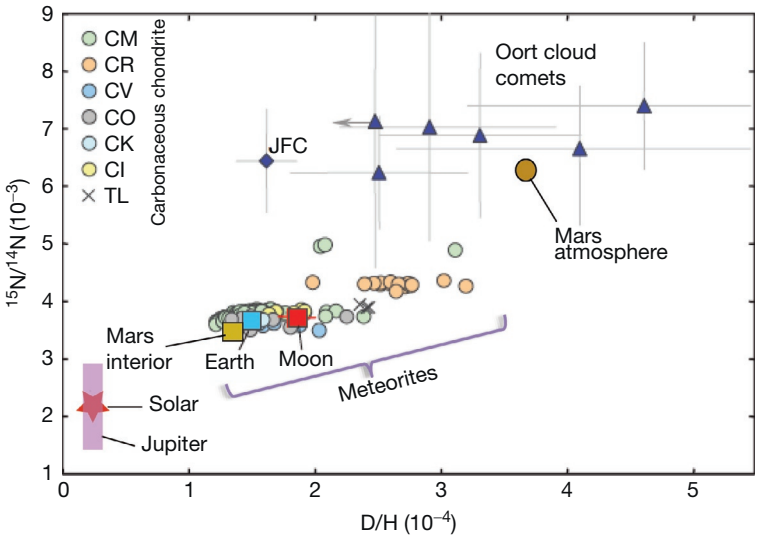

Figure 32 Isotopic compositions of volatile elements H and N of various planetary bodies (after Marty, 2012; Saal et al., 2013). Isotopic compositions of H and N for the Earth, the Moon, and Mars (interior) are similar to the average of meteorites but differ significantly from those of comets. Most of terrestrial planets (the Earth, the Moon, and Mars) are likely formed from materials similar to meteorites. Small contributions from solar component and from comet-like materials are also suggested (e.g., Halliday, 2013; Marty, 2012). CM, CR, CV, CO, CK, CI, and TL represent various types of carbonaceous chondrite. JFC represents Jupiter family comets.

terrestrial planetary bodies (the Earth, the Moon, and Mars) have isotopic compositions distinct from the solar composition, and each terrestrial body has different isotopic compositions. This indicates that terrestrial bodies acquired these light elements whose isotopic compositions were modified from the solar values after the formation of the Sun. Small but clear differences in the isotopic composition between Mars (1.5 AU) and the Earth (1 AU) are noted (see also Pahlevan and Stevenson, 2007), suggesting that the isotopic ratios of these elements strongly depend on the location of these bodies in the solar system.

From such a plot, it is clear that most comet-like materials cannot be a major source of volatiles for the terrestrial planets. (Halliday (2013), however, argued that a contribution from comet-like materials is needed to explain some heavy rare gas (e.g., Kr) observations.) Isotopic signatures of volatile elements of the Earth and other terrestrial planets are close to those of carbonaceous chondrites. However, both Drake and Righter (2002) and Marty (2012) concluded that the contribution from carbonaceous chondrite should be less than ~2%; otherwise, some other geochemical observations cannot be explained (e.g., Os isotopic ratios). Currently, materials similar to carbonaceous chondrites are identified in the outer region of the asteroid belt (~2.5–4.5 AU) (Gradie and Tedesco, 1982). Carbonaceous chondrite-like materials could provide volatiles to the Earth if substantial mixing (due to orbital scattering) occurred in the later stage of planetary formation (~100 Myr after the formation of the Sun) (e.g., Albaréde, 2009; Morbidelli et al., 2000). However, Wood et al. (2010) and Wood and Halliday (2010) presented discussions against the late acquisition of volatiles based on the abundance of siderophile (iron-loving) element abundance pattern and on the different interpretation of the lead isotope data.

I conclude that volatile-rich carbonaceous chondrite-type materials are good candidate from which terrestrial planets acquired volatile elements but that the geochemical observations summarized in the preceding text do not require carbonaceous chondrite-type materials as a source for volatiles. And in fact, there are some geochemical observations suggesting that volatiles were acquired in the early stage of planetary accretion where extensive mixing caused by large orbital scattering is unlikely. Most ordinary chondrites have enough (~0.1 wt%) water (and other volatiles) to make a planet like the Earth with ocean and other volatiles. Based on the Os isotopic observations, Drake (2005) argued against the 'late veneer' origin of volatiles and proposed a possible mechanism to acquire a small amount of volatiles within the snow line through the surface adsorption. By the same token, Marty (2012) showed the presence of the 'solar component' in the Earth's mantle, suggesting that a small amount of the solar gas was trapped in the building block of the Earth. But he also discussed that the volatile (including the rare gas) composition suggests that the volatiles in the terrestrial bodies are made of a mixture of the solar component and the chondritic component.

9.05.8 Summary and Outlook

In this article, I have reviewed the current understanding of the role of water (and other volatile elements) in the evolution of the Earth and other terrestrial planets including the processes of planetary formation and the long-term evolution through global volatile circulation. Studies in such an area require an integration of methodologies and observations in the vast areas such as astronomy, planetary science, geophysics, geochemistry, and materials science (mineral physics). There has been major progress in these areas including (i) the improved understanding of the properties of volatile elements under broad planetary conditions, (ii) the improved

observations to shed some insights into the behavior of volatiles in the planetary environment, and (iii) the development of models where the results of these areas are integrated. However, much needs to be done to answer our major question of why is the Earth so unique in having a modest amount of water on its surface for a geologically long time (billions of years), but not on other terrestrial planets. Let me list some issues that deserve further investigation:

(1) Volatiles in planetary formation

Spectroscopic observations on volatiles on planetary nebulae will help obtain some ideas about the distribution of volatiles in the planetary nebulae under a variety of conditions (e.g., Hrivnak et al., 2000; Miranda et al., 2001).

Previous condensation modeling ignored much of the chemical reactions including volatile elements. Improved modeling based on the experimental data on the equilibrium and kinetic properties (kinetics of chemical reactions) of volatile-bearing materials will be useful.

(2) Water distribution in the deep Earth

Water distribution in Earth has been inferred only for the shallow mantle (upper mantle and transition zone). It is important to infer the water content in the lower mantle and in the core. To do this, experimental studies need to be made to determine the behavior of water (hydrogen) under these conditions, and one must identify and develop methods of remote sensing to infer the water content in these regions.

(3) Volatile distribution in other terrestrial planets

Volatile (water) distribution in Earth (and the Moon) has been inferred using electrical conductivity and tidal dissipation. These properties can be inferred for other planets using remote sensing. It will be important to infer water content (distribution) in Mars, Mercury, and Venus using these techniques.

(4) Modeling volatile circulation and evolution

Only a simplified version of global volatile circulation has been used in most previous studies where the mantle is treated as a single unit. Recent geophysical and geochemical studies summarized here suggest that the Earth's mantle has more complex chemical structure including a layered structure. The nature of water (volatiles) circulation is quite different between a homogeneous mantle model and a layered mantle model. Much effort needs to be focused on modeling in such a realistic system in combination with the improved observations. Particularly important observational constraints include (i) the history of the ocean mass (as discussed in this article) and (ii) the history of the water content in the mantle that might be inferred from the isotopic analysis of ancient MORB.

Acknowledgment

I thank David Evans, Lindy Elkins-Tanton, Bernard Marty, Shigenori Maruyama, Sujoy Mukhopadhyay, Hiroko Nagahara, Masao Nakada, Kazuhito Ozawa, Kaveh Pahlevan, Alberto Saal, and Slava Solomatov for their helpful discussions and Dave Stevenson for inviting me to write this review and for his valuable comments. This work is partially supported by NSF.

References

Abe Y (1997) Thermal and chemical evolution of terrestrial magma ocean. *Physics of Earth and Planetary Interiors* 100: 27–39.

Abe Y, Abe-Ouchi A, Sleep NH, and Zahnle KJ (2011) Habitable zone limits for dry planets. *Astrobiology* 11: 443–460.

Abe Y and Matsui T (1985) Formation of an impact-generated H_2O atmosphere and its implications for the early thermal history of the Earth. *Journal of Geophysical Research* 90: 545–559.

Abe Y and Matsui T (1988) Evolution of an impact-generated H_2O–CO_2 atmosphere and formation of a hot proto-ocean on Earth. *Journal of Atmospheric Sciences* 45: 3081–3101.

Abe Y, Ohtani E, Okuchi T, Righter K, and Drake MJ (2000) Water in the early Earth. In: Canup RM and Righter K (eds.) *Origin of the Earth and Moon*, pp. 413–433. Tucson: University of Arizona Press.

Ahrens TJ and O'Keefe JD (1972) Shock melting and vaporization of lunar rocks and minerals. *The Moon* 4: 214–249.

Aizawa Y, Barnhoorn A, Faul UH, Fitz Gerald JD, Jackson I, and Kovács I (2008) Seismic properties of Anita Bay dunite: An exploratory study of the influence of water. *Journal of Petrology* 49: 841–855.

Albaréde F (2009) Volatile accretion history of the terrestrial planets and dynamic implications. *Nature* 461: 1227–1233.

Allègre CJ, Hofmann AW, and O'Nions K (1996) The argon constraints on mantle structure. *Geophysical Research Letters* 23: 3555–3557.

Allègre CJ, Staudacher T, and Sarda P (1986/1987) Rare gas systematics: Formation of the atmosphere, evolution and structure of the Earth's mantle. *Earth and Planetary Science Letters* 81: 127–150.

Baba K, Chave AD, Evans RL, Hirth G, and Randall L (2006) Mantle dynamics beneath the East Pacific Rise at 17°S: Insights from the Mantle Electromagnetic and Tomography (MELT) experiments. *Journal of Geophysical Research* 111. http://dx.doi.org/10.1029/2004JB003598.

Baba K, Utada H, Goto T, Kasaya T, Shimizu H, and Tada N (2010) Electrical conductivity imaging of the Philippine Sea upper mantle using seafloor magnetotelluric data. *Physics of the Earth and Planetary Interiors* 183: 44–62.

Bagley B, Coutier AM, and Revenaugh J (2009) Melting in the deep upper mantle oceanward of the Honshu slab. *Physics of the Earth and Planetary Interiors* 175: 137–144.

Banks RJ (1969) Geomagnetic variations and the electrical conductivity of the upper mantle. *Geophysical Journal of Royal Astronomical Society* 17: 457–487.

Baxter EF (2010) Diffusion of noble gases in minerals. *Reviews in Mineralogy and Geochemistry* 72: 509–557.

Bell DR and Rossman GR (1992) Water in Earth's mantle: The role of nominally anhydrous minerals. *Science* 255: 1391–1397.

Bercovici D and Karato S (2003) Whole mantle convection and transition-zone water filter. *Nature* 425: 39–44.

Berner RA (1994) 3GEOCARB II: A revised model for atmospheric CO_2 over Phanerozoic time. *American Journal of Science* 294: 56–91.

Billen MI and Gurnis M (2001) A low viscosity wedge in subduction zones. *Earth and Planetary Science Letters* 193: 227–236.

Blacic JD (1972) Effects of water in the experimental deformation of olivine. In: Heard HC, Borg IY, Carter NL, and Raleigh CB (eds.) *Flow and Fracture of Rocks*, pp. 109–115. Washington, DC: American Geophysical Union.

Bolfan-Casanova N (2005) Water in the Earth's mantle. *Mineralogical Magazine* 69: 229–257.

Bowen NL (1928) *The Evolution of Igneous Rocks*. Princeton: Princeton University Press, 334 pp.

Burbidge EM, Burbidge GR, Fowler WA, and Hoyle F (1957) Synthesis of the elements in stars. *Review of Modern Physics* 4: 547–650.

Cadek O and Fleitout L (2003) Effect of lateral viscosity variation in the top 300 km on the geoid and dynamic topography. *Geophysical Journal International* 152: 566–580.

Cameron AGW (1988) Origin of the solar system. *Annual Review of Astronomy and Astrophysics* 26: 441–472.

Cameron AGW and Pine MR (1973) Numerical models of the primitive solar nebula. *Icarus* 18: 377–406.

Campbell AJ, Humayun M, and Weisberg MK (2002) Siderophile element constraints on the formation of metal in the metal-rich chondrites Bencubbin, Weatherford, and Gujba. *Geochimica et Cosmochimica Acta* 66: 647–660.

Canup RM (2004a) Dynamics of lunar formation. *Annual Review of Astronomy and Astrophysics* 42: 441–475.

Canup RM (2004b) Simulation of a late lunar-forming impact. *Icarus* 168: 433–456.

Carmichael ISE, Turner FJ, and Verhoogen J (1974) *Igneous Petrology*, p. 739. New York: McGraw-Hill.

Carter WJ, Fritz JN, Marsh SP, and McQueen RG (1975) Hugoniot equation of state of the lanthanides. *Journal of Physics and Chemistry of Solids* 36: 741–752.

Cassen P (1996) Models for the fractionation of moderately volatile elements in the solar system. *Meteoritics and Planetary Sciences* 31: 793–806.

Cemič L, Will G, and Hinze E (1980) Electrical conductivity measurements on olivines Mg_2SiO_4–Fe_2SiO_4 under defined thermodynamic conditions. *Physics and Chemistry of Minerals* 6: 95–107.

Chakraborty S (2010) Diffusion coefficients in olivine, wadsleyite and ringwoodite. *Reviews in Mineralogy and Geochemistry* 72: 603–639.

Chen S, Hiraga T, and Kohlstedt DL (2006) Water weakening of clinopyroxene in the dislocation creep regime. *Journal of Geophysical Research* 111. http://dx.doi.org/10.1029/2005JB003885.

Chen J, Inoue T, Yurimoto H, and Weidner DJ (2002) Effect of water on olivine-wadsleyite phase boundary in the (Mg, $Fe)_2SiO_4$ system. *Geophysical Research Letters* 29. http://dx.doi.org/10.1029/2001GRL014429.

Cherniak DJ and Dimanov A (2010) Diffusion in pyroxene, mica and amphibole. *Review in Mineralogy and Geochemistry* 72: 641–690.

Cooper RF and Kohlstedt DL (1982) Interfacial energies in the olivine–basalt system. In: Akimoto S and Manghnani MH (eds.) *High Pressure Research in Geophysics*, pp. 217–228. Tokyo: Venter for Academic Publication.

Costa F and Chakraborty S (2008) The effect of water on Si and O diffusion rates in olivine and implications for transport properties and processes in the upper mantle. *Physics of the Earth and Planetary Interiors* 166: 11–29.

Coutier AM and Revenaugh J (2006) A water-rich transition zone beneath the eastern United States and Gulf of Mexico from multiple ScS reverberations. In: Jacobsen SD and van der Lee S (eds.) *Earth's Deep Water Cycle*, pp. 181–193. Washington, DC: American Geophysical Union.

Coutier AM and Revenaugh J (2007) Deep upper-mantle melting beneath the Tasman and Coral Seas detected with multiple ScS reverberations. *Earth and Planetary Science Letters* 259: 66–76.

Crowley JW, Gérault M, and O'Connell RJ (2011) On the relative role of influence of heat and water transport on planetary dynamics. *Earth and Planetary Science Letters* 310: 380–388.

Dai L and Karato S (2009a) Electrical conductivity of orthopyroxene: Implications for the water content of the asthenosphere. *Proceedings of the Japan Academy* 85: 466–475.

Dai L and Karato S (2009b) Electrical conductivity of pyrope-rich garnet at high temperature and pressure. *Physics of the Earth and Planetary Interiors* 176: 83–88.

Dai L and Karato S (2009c) Electrical conductivity of wadsleyite under high pressures and temperatures. *Earth and Planetary Science Letters* 287: 277–283.

Dai L and Karato S (2014) Highly anisotropic electrical conductivity of the asthenosphere caused by hydrogen diffusion in olivine. *Earth and Planetary Science Letters*, in press.

Dalton CA, Ekström G, and Dziewonski AM (2009) Global seismological shear velocity and attenuation: A comparison with experimental observations. *Earth and Planetary Science Letters* 284: 65–75.

Dasgupta R and Hirschmann MM (2006) Melting in the Earth's deep mantle caused by carbon dioxide. *Nature* 440: 659–662.

Dasgupta R and Hirschmann MM (2010) The deep carbon cycle and melting in Earth's interior. *Earth and Planetary Science Letters* 298: 1–13.

de Pater I and Lissauer JJ (2010) *Planetary Sciences*, 2nd edn., p. 647. Cambridge: Cambridge University Press.

DeMeo FE and Carry B (2014) Solar system evolution from compositional mapping of the asteroid belt. *Nature* 505: 629–634.

Demouchy S, Jacobsen SD, Gaillard F, and Stern CR (2006) Rapid magma ascent recorded by water diffusion profiles in mantle olivine. *Geology* 34: 429–432.

Deuss A (2009) Global observations of mantle discontinuities using SS and PP precursors. *Surveys in Geophysics* 30: 301–326.

Dixon JE, Dixon TH, Bell DR, and Malservisi R (2004) Lateral variation in upper mantle viscosity: Role of water. *Earth and Planetary Science Letters* 222: 451–467.

Dixon JE, Leist L, Langmuir J, and Schiling JG (2002) Recycled dehydrated lithosphere observed in plume-influenced mid-ocean-ridge basalt. *Nature* 420: 385–389.

Dobson D (2003) Oxygen ionic conduction in $MgSiO_3$ perovskite. *Physics of the Earth and Planetary Interiors* 139: 55–64.

Dobson DP and Brodholt JP (2000) The electrical conductivity of the lower mantle phase magnesiowüstite at high temperatures and pressures. *Journal of Geophysical Research* 105: 531–538.

Donahue TM, Hoffman JH, Hodges RR Jr., and Watson AJ (1982) Venus was wet: A measurement of the ratio of deuterium to hydrogen. *Science* 216: 630–633.

Drake MJ (2005) Origin of water in the terrestrial planets. *Meteoritics and Planetary Sciences* 40: 519–527.

Drake MJ and Righter K (2002) Determining the composition of the Earth. *Nature* 416: 39–44.

Duba A and Shankland TJ (1982) Free carbon and electrical conductivity in the Earth's mantle. *Geophysical Research Letters* 9: 1271–1274.

Dziewonski AM (2000) Global seismic tomography: Past, present and future. In: Boschi E, Ekström G, and Morelli A (eds.) *Problems in Geophysics for the Next Millennium*, pp. 289–349. Roma: Editorice Compositori.

Ebel DS and Grossman L (2000) Condensation in dust-enriched systems. *Geochimica et Cosmochimica Acta* 64: 339–366.

Ekström G and Dziewonski AM (1998) The unique anisotropy of the Pacific upper mantle. *Nature* 394: 168–172.

Elkins-Tanton LT (2008) Linked magma ocean solidification and atmospheric growth for Earth and Mars. *Earth and Planetary Science Letters* 271: 181–191.

Elkins-Tanton L and Grove TL (2011) Water (hydrogen) in the lunar mantle: Results from petrology and magma ocean modeling. *Earth and Planetary Science Letters* 307: 173–179.

Eriksson PG, Mazumder R, Catuneau O, Bumby AJ, and Ilondo BO (2006) Precambrian continental freeboard and geologic evolution: A time perspective. *Earth Science Reviews* 79: 165–204.

Evans RL, Jones AG, Garcia X, et al. (2011) Electrical lithosphere beneath the Kaapvaal craton, southern Africa. *Journal of Geophysical Research* 116. http//dx.doi.org/10.1029/2010JB007883.

Faccenda M, Gerya TV, and Burlini L (2009) Deep slab hydration induced by bending-related variations in tectonic pressure. *Nature Geoscience* 2: 790–793.

Farver JR (2010) Oxygen and hydrogen diffusion in minerals. *Reviews in Mineralogy and Geochemistry* 72: 447–507.

Fegley B (2000) Kinetics of gas-grain reactions in the solar nebula. *Space Science Reviews* 92: 177–200.

Fei H, Wiedenbeck M, Yamazaki D, and Katsura T (2013) Small effect of water on upper-mantle rheology based on silicon self-diffusion coefficients. *Nature* 498: 213–216.

Fiquet G, Guyot F, Kunz M, Matas J, Andrault D, and Hanfland M (2002) Structural refinements of magnesite at very high pressure. *American Mineralogist* 87: 1261–1265.

Franck S and Bounama C (2001) Global water cycle and Earth's thermal evolution. *Journal of Geodynamics* 32: 231–246.

Frost DJ and Dolejš D (2007) Experimental determination of the effect of H_2O on the 410-km seismic discontinuity. *Earth and Planetary Science Letters* 256: 182–195.

Fukai Y and Suzuki T (1986) Iron–water interaction under high pressure and its implications in the evolution of the Earth. *Journal of Geophysical Research* 91: 9222–9230.

Gaillard F, Malki M, Iacono-Maziano G, Pichavant M, and Scaillet B (2008) Carbonatite melts and electrical conductivity in the asthenosphere. *Science* 322: 1363–1365.

Galer SJG and Mezger K (1998) Metamorphism, denudation and sea level in the Archean and cooling of the Earth. *Precambrian Research* 92: 389–412.

Galy A, Young ED, Ash RD, and O'Nions RK (2000) The formation of chondrules at high gas pressures in the solar nebula. *Science* 290: 1751–1753.

Gando A, et al. (2011) Partial radiogenic heat model for Earth revealed by geoneutrino measurements. *Nature Geoscience* 4: 647–651.

Ganguly J and Bose K (1995) Kinetics of formation of hydrous phyllosilicates in the solar nebula. In: *Proceedings of the Lunar Science Conference, vol. XXVI*, pp. 441–442.

Gao W, Matzel E, and Grand SP (2006) Upper mantle seismic structure beneath eastern Mexico determined from P and S waveform inversion and its implications. *Journal of Geophysical Research* 111. http://dx.doi.org/10.1029/2006JB004304.

Garcia RF, Gagnepain-Beyneix J, Chevrot S, and Lognonné P (2011) Very preliminary reference Moon model. *Physics of the Earth and Planetary Interiors* 188: 96–113.

Garth T and Rietbrock A (2014) Order of magnitude increase in subducted H_2O due to hydrated normal faults within the Wadati-Benioff zone. *Geology* 42: 207–210.

Genda H and Abe Y (2005) Enhanced atmospheric loss on protoplanets at the giant impact phase in the presence of oceans. *Nature* 433: 842–844.

Gradie J and Tedesco E (1982) Compositional structure of the asteroid belt. *Science* 216: 1405–1407.

Griggs DT and Blacic JD (1965) Quartz: Anomalous weakness of synthetic crystals. *Science* 147: 292–295.

Grinspoon DH (1987) Was Venus wet? Deuterium reconsidered. *Science* 238: 1702–1704.

Grossman L (1972) Condensation in the primitive solar nebula. *Geochemica and Cosmochemica Acta* 36: 597–619.

Grossman L and Larimer JW (1974) Early chemical history of the solar system. *Review of Geophysics and Space Physics* 12: 71–101.
Gurnis M (1993) Phanerozoic marine inundation of continents driven by dynamic topography above subducting slabs. *Nature* 364: 589–593.
Hacker BR (2008) H_2O subduction beyond arcs. *Geochemistry, Geophysics, Geosystems* 9. http://dx.doi.org/10.1029/2007GC001707.
Haggerty SE and Sautter V (1990) Ultra deep (>300 km) ultramafic, upper mantle xenoliths. *Science* 248: 993–996.
Hallam A (1992) *Phanerozoic Sea-Level Changes*, p. 266. New York: Columbia University Press.
Halliday AN (2013) The origins of volatiles in the terrestrial planets. *Geochimica et Cosmochimica Acta* 105: 146–171.
Hamano K, Abe Y, and Genda H (2013) Emergence of two types of terrestrial planet on solidification of magma ocean. *Nature* 497: 607–610.
Hamano Y and Ozima M (1978) Earth-atmosphere evolution model based on Ar isotopic data. In: Alexander JEC and Ozima M (eds.) *Terrestrial Rare Gases*, pp. 155–171. Tokyo: Japan Scientific Society Press.
Hanks TC and Anderson DL (1969) The early thermal history of the Earth. *Physics of the Earth and Planetary Interiors* 2: 19–29.
Harte B (2010) Diamond formation in the deep mantle: The record of mineral inclusions and their distribution in relation to mantle dehydration zones. *Mineralogical Magazine* 74: 189–215.
Hauri EH, Gaetani GA, and Green TH (2006) Partitioning of water during melting of the Earth's upper mantle at H_2O-undersaturated conditions. *Earth and Planetary Science Letters* 248: 715–734.
Hauri EH, Weinreich T, Saal AE, Rutherford MC, and Van Orman JA (2011) High pre-eruptive water contents preserved in lunar melt inclusions. *Science* 333: 213–215.
Hayashi C (1961) Stellar evolution in early phases of gravitational contraction. *Publications of the Astronomical Society of Japan* 13: 450–458.
Hayashi C (1981) Structure of the solar nebula, growth and decay of magnetic fields and effects of magnetic and turbulent viscosities on the nebula. *Progress of Theoretical Physics Supplement* 70: 35–53.
Hayashi C, Nakazawa K, and Mizuno H (1979) Earth's melting due to the blanketing effect of the primordial dense atmosphere. *Earth and Planetary Science Letters* 43: 22–28.
Hayashi C, Nakazawa K, and Nakagawa Y (1985) Formation of the solar system. In: Black DC and Matthews MS (eds.) *Protoplanets and Planets II*, pp. 1100–1153. University of Arizona Press.
Hirschmann MM (2006) Water, melting, and the deep Earth H_2O cycle. *Annual Review of Earth and Planetary Sciences* 34: 629–653.
Hirschmann MM (2010) Partial melt in the oceanic low velocity zone. *Physics of the Earth and Planetary Interiors* 179: 60–71.
Hirschmann MM and Dasgupta R (2009) The H/C ratio of Earth's near-surface and deep reservoirs, and consequences for deep Earth volatile cycles. *Chemical Geology* 262: 4–16.
Hofmann AW (1997) Mantle geochemistry: The message from oceanic volcanism. *Nature* 385: 219–228.
Holland HD (2003) The geologic history of seawater. In: Turekian KK and Holland HD (eds.) *Treatise on Geochemistry*, pp. 1–46. Amsterdam: Elsevier.
Holland HD, Lazar B, and McGaffrey M (1986) Evolution of the atmosphere and oceans. *Nature* 320: 27–33.
Hood LL, Herbert F, and Sonett CP (1982) The deep lunar electrical conductivity profile: Structural and thermal inferences. *Journal of Geophysical Research* 87: 5311–5326.
Howard AW, Marcy GW, Johnson JA, et al. (2010) The occurrence and mass distribution of close-in super-Earths, Neptunes, and Jupiters. *Science* 330: 653–655.
Hrivnak BJ, Volk K, and Kwok S (2000) 2–45 micron infrared spectroscopy of carbon-rich proto-planetary nebulae. *The Astrophysical Journal* 535: 275–292.
Huang X, Xu Y, and Karato S (2005) Water content of the mantle transition zone from the electrical conductivity of wadsleyite and ringwoodite. *Nature* 434: 746–749.
Huebner JS, Wiggins LB, and Duba AG (1979) Electrical conductivity of pyroxene which contains trivalent cations: Laboratory measurements and the lunar temperature profiles. *Journal of Geophysical Research* 84: 4652–4656.
Hui H, Peslier AH, Zhang Y, and Neal CR (2013) Water in lunar anorthosites and evidence for a wet early Moon. *Nature Geoscience* 6: 177–180.
Hunten DM and Donahue TM (1976) Hydrogen loss from the terrestrial planets. *Annual Review of Earth and Planetary Sciences* 4: 265–292.
Hunten DM, Donahue TM, Walker JCG, and Kasting JF (1989) Escape of atmospheres and loss of water. In: Atreya SK, Pollack JB, and Matthews MS (eds.) *Origin and Evolution of Planetary and Satellite Atmospheres*, pp. 386–422. Tuscon: The University of Arizona Press.
Ichiki M, Baba K, Obayashi M, and Utada H (2006) Water content and geotherm in the upper mantle above the stagnant slab: Interpretation of electrical conductivity and seismic P-wave velocity models. *Physics of the Earth and Planetary Interiors* 155: 1–15.
Ingrin J and Skogby H (2000) Hydrogen in nominally anhydrous upper-mantle minerals: Concentration levels and implications. *European Journal of Mineralogy* 12: 543–570.
Inoue T (1994) Effect of water on melting phase relations and melt composition in the system Mg_2SiO_4–$MgSiO_3$–H_2O up to 15 GPa. *Physics of Earth and Planetary Interiors* 85: 237–263.
Inoue T, Wada T, Sasaki R, and Yurimoto H (2010) Water partitioning in the Earth's mantle. *Physics of the Earth and Planetary Interiors* 183: 245–251.
Ito E, Harris DM, and Anderson AT (1983) Alteration of oceanic crust and geologic cycling of chlorine and water. *Geochemica and Cosmochemica Acta* 47: 1613–1624.
Iwamori H (1993) Dynamic disequilibrium melting model with porous flow and diffusion-controlled chemical equilibration. *Earth and Planetary Science Letters* 114: 301–313.
Jacobsen SD (2006) Effect of water on the equation of state of nominally anhydrous minerals. In: Keppler H and Smyth JR (eds.) *Water in Nominally Anhydrous Minerals*, pp. 321–342. Washington, DC: Mineralogical Society of America.
Jacobsen SD, Jiang F, Mao Z, et al. (2008) Effects of hydration on the elastic properties of olivine. *Geophysical Research Letters* 35. http://dx.doi.org/10.1029/2008GL034398.
Jacobsen SD and Smyth JR (2006) Effect of water on the sound velocities of ringwoodite in the transition zone. In: Jacobsen SD and van der Lee S (eds.) *Earth's Deep Water Cycle*, pp. 131–145. Washington, DC: American Geophysical Union.
Jacobsen SD, Smyth JR, Spetzler HA, Holl CM, and Frost DJ (2004) Sound velocities and elastic constants of iron-bearing hydrous ringwoodite. *Physics of the Earth and Planetary Interiors* 143(144): 47–56.
Jarosewich E (1990) Chemical analyses of meteorites: A compilation of stony and iron meteorite analyses. *Meteoritics* 25: 323–337.
Jarrard RD (2003) Subduction fluxes of water, carbon dioxide, chlorine, and potassium. *Geochemistry, Geophysics, Geosystems* 4. http://dx.doi.org/10.1029/2002GC000392.
Jing Z and Karato S (2011) A new approach to the equation of state of silicate melts: An application of the theory of hard sphere mixtures. *Geochimica et Cosmochimica Acta* 75: 6780–6802.
Jones AG, Lazaeta P, Fergurson IJ, et al. (2003) The electrical structure of the Slave craton. *Lithos* 71: 505–527.
Jug K, Heidelberg B, and Bredow T (2007) Cyclic cluster study on the formation of brucite from periclase and water. *Journal of Physical Chemistry* C111: 13103–13108.
Karato S (1986) Does partial melting reduce the creep strength of the upper mantle? *Nature* 319: 309–310.
Karato S (1995) Effects of water on seismic wave velocities in the upper mantle. *Proceedings of the Japan Academy* 71: 61–66.
Karato S (2006a) Influence of hydrogen-related defects on the electrical conductivity and plastic deformation of mantle minerals: A critical review. In: Jacobsen SD and van der Lee S (eds.) *Earth's Deep Water Cycle*, pp. 113–129. Washington, DC: American Geophysical Union.
Karato S (2006b) Remote sensing of hydrogen in Earth's mantle. In: Keppler H and Smyth JR (eds.) *Water in Nominally Anhydrous Minerals*, pp. 343–375. Washington, DC: Mineralogical Society of America.
Karato S (2008a) *Deformation of Earth Materials: Introduction to the Rheology of the Solid Earth*, p. 463. Cambridge: Cambridge University Press.
Karato S (2008b) Insights into the nature of plume–asthenosphere interaction from central Pacific geophysical anomalies. *Earth and Planetary Science Letters* 274: 234–240.
Karato S (2010a) The influence of anisotropic diffusion on the high-temperature creep of a polycrystalline aggregate. *Physics of the Earth and Planetary Interiors* 183: 468–472.
Karato S (2010b) Rheology of the deep upper mantle and its implications for the preservation of the continental roots: A review. *Tectonophysics* 481: 82–98.
Karato S (2011) Water distribution across the mantle transition zone and its implications for global material circulation. *Earth and Planetary Science Letters* 301: 413–423.
Karato S (2012) On the origin of the asthenosphere. *Earth and Planetary Science Letters* 321(322): 95–103.
Karato S (2013a) Geophysical constraints on the water content of the lunar mantle and its implications for the origin of the Moon. *Earth and Planetary Science Letters* 384: 144–153.
Karato S (2013b) Theory of isotope diffusion in a material with multiple-species and its implications for hydrogen-enhanced electrical conductivity in olivine. *Physics of the Earth and Planetary Interiors* 219: 49–54.

Karato S (2014a) Asymmetric shock heating and the terrestrial magma ocean origin of the Moon. *Proceedings of the Japan Academy* B90: 97–103.

Karato S (2014b) Does partial melting explain geophysical anomalies? *Physics of the Earth and Planetary Interiors* 228: 300–306.

Karato S and Jung H (2003) Effects of pressure on high-temperature dislocation creep in olivine polycrystals. *Philosophical Magazine A* 83: 401–414.

Karato S, Jung H, Katayama I, and Skemer PA (2008) Geodynamic significance of seismic anisotropy of the upper mantle: New insights from laboratory studies. *Annual Review of Earth and Planetary Sciences* 36: 59–95.

Karato S and Murthy VR (1997) Core formation and chemical equilibrium in the Earth I. physical considerations. *Physics of Earth and Planetary Interiors* 100: 61–79.

Karato S, Paterson MS, and Fitz Gerald JD (1986) Rheology of synthetic olivine aggregates: Influence of grain-size and water. *Journal of Geophysical Research* 91: 8151–8176.

Karato S and Wang D (2013) Electrical conductivity of minerals and rocks. In: Karato S (ed.) *Physics and Chemistry of the Deep Earth*, pp. 145–182. New York: Wiley-Blackwell.

Kasting JF (1989) Long-term stability of the Earth's climate. *Paleogeography Paleoclimate Paleoecology* 75: 83–96.

Kasting JF (1993) Earth's early atmosphere. *Science* 259: 920–926.

Kasting JF and Catling D (2003) Evolution of a habitable planet. *Annual Review of Astronomy and Astrophysics* 41: 429–463.

Kasting JF and Holm NG (1992) What determines the volume of ocean? *Earth and Planetary Science Letters* 109: 507–515.

Kasting JF and Pollack JB (1983) Loss of water from Venus. I. Hydrodynamic escape of hydrogen. *Icarus* 53: 479–508.

Kasting JF, Whitmire DP, and Reynolds RT (1993) Habitable zones around main sequence stars. *Icarus* 101: 108–128.

Katayama I and Karato S (2008a) Effects of water and iron content on the rheological contrast between garnet and olivine. *Physics of the Earth and Planetary Interiors* 166: 59–66.

Katayama I and Karato S (2008b) Low-temperature high-stress rheology of olivine under water-rich conditions. *Physics of the Earth and Planetary Interiors* 168: 125–133.

Katsura T, Sato K, and Ito E (1998) Electrical conductivity of silicate perovskite at lower-mantle conditions. *Nature* 395: 493–495.

Kaula WM (1979) Thermal evolution of Earth and Moon growing by planetesimal impacts. *Journal of Geophysical Research* 84: 999–1008.

Kaula WM (1990) Venus: A contrast in evolution to Earth. *Science* 247.

Kawazoe T, Ohuchi T, Nishihara Y, Nishiyama N, Fujino K, and Irifune T (2013) Seismic anisotropy in the mantle transition zone induced by shear deformation of wadsleyite. *Physics of the Earth and Planetary Interiors* 216: 91–98.

Kelbert A, Schultz A, and Egbert G (2009) Global electromagnetic induction constraints on transition-zone water content variations. *Nature* 460: 1003–1006.

Keppler H and Bolfan-Casanova N (2006) Thermodynamics of water solubility and partitioning. In: Keppler H and Smyth JR (eds.) *Water in Nominally Anhydrous Minerals*, pp. 193–230. Washington, DC: Mineralogical Society of America.

Keppler H, Wiedenbeck M, and Shcheka SS (2003) Carbon solubility in olivine and the mode of carbon storage in the Earth's mantle. *Nature* 424: 414–416.

Kleine T and Rudge JF (2011) Chronometry of meteorites and the formation of the Earth and Moon. *Elements* 7: 41–46.

Kneller EA, van Keken PE, Karato S, and Park J (2005) B-type olivine fabric in the mantle wedge: Insights from high-resolution non-Newtonian subduction zone models. *Earth and Planetary Science Letters* 237: 781–797.

Kohlstedt DL (2002) Partial melting and deformation. In: Karato S and Wenk H-R (eds.) *Plastic Deformation of Minerals and Rocks*, pp. 121–135. Washington, DC: Mineralogical Society of America.

Kohlstedt DL (2009) Properties of rocks and minerals – Constitutive equations, rheological behavior, and viscosity of rocks. In: Price GD (ed.) *Treatise on Geophysics*, pp. 389–417. Amsterdam: Elsevier.

Kohlstedt DL, Keppler H, and Rubie DC (1996) Solubility of water in the α, β and γ phases of $(Mg, Fe)_2SiO_4$. *Contributions to Mineralogy and Petrology* 123: 345–357.

Kokubo E and Ida S (2000) Formation of protoplanets from planetesimals in the solar nebula. *Icarus* 143: 15–27.

Konopliv AS, Asmar SW, Carranza E, Sjogren WL, and Yuan DN (2001) Recent gravity models as a result of the Lunar Prospector mission. *Icarus* 150: 1–18.

Korenaga J (2008) Plate tectonics, flood basalts and the evolution of Earth's ocean. *Terra Nova* 20: 419–439.

Korenaga J (2011) Thermal evolution with a hydrating mantle and the initiation of plate tectonics in the early Earth. *Journal of Geophysical Research* 116. http://dx.doi.org/10.1029/2011JB008410.

Kushiro I (2001) Partial melting experiments on peridotite and origin of mid-ocean ridge basalt. *Annual Review of Earth and Planetary Sciences* 29: 71–107.

Kushiro I, Syono Y, and Akimoto S (1968) Melting of a peridotite nodule at high pressures and high water pressures. *Journal of Geophysical Research* 73: 6023–6029.

Lainey V, Dehant V, and Pätzold M (2007) First numerical ephemerides of the Martian moons. *Astronomy and Astrophysics* 465: 1075–1084.

Lange MA and Ahrens TJ (1982) The evolution of impact-generated atmosphere. *Icarus* 51: 96–120.

Langmuir CH and Broecker WS (2012) *How to Build a Habitable Planet*, 2nd edn., p. 718. Princeton: Princeton University Press.

Larimer JW (1967) Chemical fractionations in meteorites – I. Condensation of the elements. *Geochemica et Cosmochemica Acta* 31: 1215–1238.

Lauretta DS (2011) A cosmochemical view of the solar system. *Elements* 7: 11–16.

Leahy G and Bercovici D (2007) On the dynamics of hydrous melt layer above the transition zone. *Journal of Geophysical Research* 112. http://dx.doi.org/10.1029/2006JB004631.

Lewis JS (1972) Metal/silicate fractionation in the solar system. *Earth and Planetary Science Letters* 15: 286–290.

Lewis JS (1974) Chemical composition of the solar system. *Scientific American* 230: 50–65.

Lifshitz IM and Shikin VB (1965) The theory of diffusional viscous flow of polycrystalline solids. *Soviet Physics, Solid State* 6: 2211–2218.

Lister CRB (1980) Heat flow and hydrothermal circulation. *Annual Review of Earth and Planetary Sciences* 8: 95–117.

Litasov KD and Ohtani E (2007) Effect of water on the phase relations in Earth's mantle and deep water cycle. In: Ohtani E (ed.) *Advances in High-Pressure Mineralogy*, pp. 115–156. Geological Society of America.

Lowell RP, Rona PA, and von Herzen RP (1995) Seafloor hydrothermal systems. *Journal of Geophysical Research* 100: 327–352.

Mao Z, Jacobsen SB, Jiang F, et al. (2008) Single-crystal elasticity of wadsleyite, β-Mg_2SiO_4, containing 0.37–1.66 wt.% H_2O. *Earth and Planetary Science Letters* 266: 78–89.

Marty B (2012) The origins and concentrations of water, carbon, nitrogen and noble gases on Earth. *Earth and Planetary Science Letters* 313(314): 56–66.

Marty B and Yokochi R (2006) Water in early Earth. In: Keppler H and Smyth JR (eds.) *Water in Nominally Anhydrous Minerals*, pp. 421–450. Washington, DC: Mineralogical Society of America.

Maruyama S, Ikoma M, Genda H, Hirose K, Yokoyama T, and Santosh M (2013) The naked planet Earth: Most essential pre-requisite for the origin and evolution of life. *Geoscience Frontiers* 4: 141–165.

Matsui T and Abe Y (1986a) Evolution of an impact-induced atmosphere and magma ocean on the accreting Earth. *Nature* 319: 303–305.

Matsui T and Abe Y (1986b) Impact-induced atmospheres and oceans on Earth and Venus. *Nature* 322: 526–528.

McCarthy C, Takei Y, and Hiraga T (2011) Experimental study of attenuation and dispersion over a broad frequency range: 2. The universal scaling of polycrystalline materials. *Journal of Geophysical Research* 116. http://dx.doi.org/10.1029/2011JB008384.

McGovern PJ and Schubert G (1989) Thermal evolution of the Earth: Effects of volatile exchange between atmosphere and interior. *Earth and Planetary Science Letters* 96: 27–37.

McKenzie D (1984) The generation and compaction of partially molten rocks. *Journal of Petrology* 25: 713–765.

McMillan PF (1994) Water solubility and speciation models. In: Carroll MR and Holloway JR (eds.) *Volatiles in Magmas*, pp. 131–156. Washington, DC: Mineralogical Society of America.

McSween HYJ, Grove TL, Lentz RCF, et al. (2001) Geochemical evidence for magmatic water within Mars from pyroxenes in the Shergotty meteorite. *Nature* 409: 487–490.

Mei S and Kohlstedt DL (2000a) Influence of water on plastic deformation of olivine aggregates, 1. Diffusion creep regime. *Journal of Geophysical Research* 105: 21457–21469.

Mei S and Kohlstedt DL (2000b) Influence of water on plastic deformation of olivine aggregates, 2. Dislocation creep regime. *Journal of Geophysical Research* 105: 21471–21481.

Meier U, Trampert J, and Curtis A (2009) Global variations of temperature and water content in the mantle transition zone from higher mode surface waves. *Earth and Planetary Science Letters* 282: 91–101.

Mejias JA, Berry AJ, Refson K, and Fraser DG (1999) The kinetics and mechanism of MgO dissolution. *Chemical Physics Letters* 314: 558–563.

Miranda LF, Gómez Y, Anglada G, and Torrelles JM (2001) Water-maser emission from a planetary nebula with a magnetized torus. *Nature* 414: 284–286.

Mojzsis SJ, Harrison TM, and Pidgeon RT (2001) Oxygen-isotope evidence from ancient zircons for liquid water at the Earth's surface 4,300 Myr ago. *Nature* 409: 178–181.
Morbidelli A, Chambers JE, Lunine JI, Petit JM, Valsecchi GB, and Cyr K (2000) Source regions and timescales for the delivery of water to the Earth. *Meteoritics and Planetary Sciences* 35: 1309–1320.
Muralidharan K, Deymier P, Stimfl M, de Leeuw NH, and Drake MJ (2008) Origin of water in the inner Solar System: A kinetic Monte Carlo study of water adsorption on forsterite. *Icarus* 198: 400–407.
Mysen BO and Kushiro I (1988) Condensation, evaporation, melting, and crystallization in the primitive solar nebula: Experimental data in the system MgO–SiO_2–H_2 to 10^{-9} bar and 1870 °C with variable oxygen fugacity. *American Mineralogist* 73: 1–19.
Mysen BO, Virgo D, Popp RK, and Bertka CM (1998) The role of H_2O in Martian magmatic systems. *American Mineralogist* 83: 942–946.
Naif S, Key K, Constable S, and Evans RL (2013) Melt-rich channel observed at the lithosphere–asthenosphere boundary. *Nature* 495: 356–359.
Nakada M and Lambeck K (1991) Late Pleistocene and Holocene sea-level change: Evidence for lateral mantle viscosity variation? In: Sabadini R, Lambeck K, and Boschi E (eds.) *Glacial Isostasy, Sea Level and Mantle Rheology*, pp. 79–94. Dortrecht: Kluwer Academic.
Ni H and Keppler H (2013) Carbon in silicate melts. *Reviews in Mineralogy & Geochemistry* 75: 251–287.
Ni H, Keppler H, and Behrens H (2011) Electrical conductivity of hydrous basaltic melts: Implications for partial melting in the upper mantle. *Contributions to Mineralogy and Petrology* 162: 637–650.
Nishihara Y, Shinmei T, and Karato S (2008) Effects of chemical environments on the hydrogen-defects in wadsleyite. *American Mineralogist* 93: 831–843.
Ohtani E (1985) The primordial terrestrial magma ocean and its implications for stratifications of the mantle. *Earth and Planetary Science Letters* 78: 70–80.
Ohtani E (2005) Water in the mantle. *Elements* 1: 25–30.
Ohtani E, Hirano N, Kondo T, Ito M, and Kikegawa T (2005) Iron–water interaction at high pressure and temperature, and hydrogen transport to the core. *Physics and Chemistry of Minerals* 32: 77–82.
Ohtani E, Litasov K, Hosoya T, Kubo T, and Kondo T (2004) Water transport into the deep mantle and formation of a hydrous transition zone. *Physics of the Earth and Planetary Interiors* 143(144): 255–269.
Ohuchi T and Irifune T (2013) Development of A-type olivine fabric in water-rich upper mantle. *Earth and Planetary Science Letters* 362: 20–30.
Okuchi T (1997) Hydrogen partitioning into molten iron at high pressure: Implications for Earth's core. *Science* 278: 1781–1784.
Otsuka K and Karato S (2013) The influence of ferric iron and hydrogen on Fe–Mg interdiffusion in ferropericlase in the lower mantle. *Physics and Chemistry of Minerals,* in press.
Otsuka K, Longo M, McCammon CA, and Karato S (2013) Ferric iron content of ferropericlase as a function of composition, oxygen fugacity, temperature and pressure: Implications for redox conditions during diamond formation in the lower mantle. *Earth and Planetary Science Letters* 365: 7–16.
Ozima M and Igarashi G (1989) Terrestrial noble gases: Constraints and implications on atmospheric evolution. In: Atreya SK, Pollack JB, and Matthews MS (eds.) *Origin and Evolution of Planetary and Satellite Atmospheres*, pp. 306–327. Tuscon: The University of Arizona Press.
Pahlevan K and Stevenson DJ (2007) Equilibration in the aftermath of the lunar-forming giant impact. *Earth and Planetary Science Letters* 262: 438–449.
Parai R and Mukhopadhyay S (2012) How large is the subducted water flux? New constraints on mantle regassing rates. *Earth and Planetary Science Letters* 317–318: 396–406.
Pearson DG, et al. (2014) Hydrous mantle transition zone indicated by ringwoodite included within diamond. *Nature* 507: 221–224.
Pepin RO (1997) Evolution of Earth's noble gases: Consequence of assuming hydrodynamic loss driven by giant impact. *Icarus* 126: 148–156.
Peslier AH (2010) A review of water contents of nominally anhydrous natural minerals in the mantles of Earth, Mars and the Moon. *Journal of Volcanology and Geothermal Research* 197: 239–258.
Peslier AH, Woodland AB, Bell DR, and Lazarov M (2010) Olivine water contents in the continental lithosphere and the longevity of cratons. *Nature* 467: 78–83.
Peyronneau J and Poirier J-P (1989) Electrical conductivity of the material of the Earth's lower mantle. *Nature* 365: 537–539.
Post AD, Tullis J, and Yund RA (1996) Effects of chemical environment on dislocation creep of quartzite. *Journal of Geophysical Research* 101: 22143–22155.
Pritchard ME and Stevenson DJ (2000) Thermal aspects of a lunar origin by giant impact. In: Canup RM and Righter K (eds.) *Origin of the Earth and Moon*, pp. 179–196. Tuscon: The University of Arizona Press.
Raj R (1975) Transient behavior of diffusion-induced creep and creep rupture. *Metallurgical Transactions* 6A: 1499–1509.
Raj R and Ashby MF (1971) On grain boundary sliding and diffusional creep. *Metallurgical Transactions* 2: 1113–1127.
Ranero CR, Phipps Morgan J, McIntosh KD, and Reichert C (2003) Bending, faulting, and mantle serpentinization at the Middle America trench. *Nature* 425: 367–373.
Ray RD, Eanes RJ, and Lemoine FG (2001) Constraints on energy dissipation in the Earth's body tide from satellite tracking and altimetry. *Geophysical Journal International* 144: 471–480.
Raymond SN, Quinn T, and Lunine JI (2007) High-resolution simulations of the final assembly of Earth-like planets. 2. Water delivery and planetary habitability. *Astrobiology* 7: 66–84.
Reymer A and Schubert G (1984) Phanerozoic addition rates to the continental crust and crustal growth. *Tectonics* 3: 63–77.
Ribe NM (1985) The generation and compaction of partial melts in the earth's mantle. *Earth and Planetary Science Letters* 73: 361–376.
Richard G, Monnereau M, and Ingrin J (2002) Is the transition zone an empty water reservoir? Inference from numerical model of mantle dynamics. *Earth and Planetary Science Letters* 205: 37–51.
Richards MA, Bunge H-P, and Lithgow-Bertelloni C (2000) Mantle convection and plate motion history: Toward general circulation models. In: Richards MA, Gordon RG, and Hilst RDvd (eds.) *The History and Dynamics of Global Plate Motions*, pp. 289–308. Washington, DC: American Geophysical Union.
Richter FM and McKenzie D (1984) Dynamical models for melt segregation from a deformable matrix. *The Journal of Geology* 92: 729–740.
Rikitake T (1966) *Electromagnetism and the Earth's Interior*. Amsterdam: Elsevier, 308 pp.
Ringwood AE (1975) *Composition and Structure of the Earth's Mantle*, p. 618. New York: McGraw-Hill.
Ringwood AE (1979) *Origin of the Earth and Moon*, p. 295. Berlin: Springer-Verlag.
Ritsema J, Deuss A, van Heijst HJ, and Woodhouse JH (2011) S40RTS: A degree-40 shear-velocity model for the mantle from new Rayleigh wave dispersion, teleseismic traveltime and normal-mode splitting function measurements. *Geophysical Journal International* 184: 1223–1236.
Robert F, Gautier D, and Dubrulle B (2003) The solar system D/H ratio: Observations and theories. *Space Science Reviews* 92: 201–224.
Rohrbach A and Schmidt MW (2011) Redox freezing and melting in the Earth's mantle resulting from carbon–iron redox coupling. *Nature* 472: 209–214.
Romanowicz B and Durek JJ (2000) Seismological constraints on attenuation in the Earth: A review. In: Karato S, Forte AM, Liebermann RC, Masters G, and Stixrude L (eds.) *Earth's Deep Interior*, pp. 161–179. Washington, DC: American Geophysical Union.
Ross JV and Nielsen KC (1978) High-temperature flow of wet polycrystalline enstatite. *Tectonophysics* 44: 233–261.
Rubey W (1951) Geologic history of sea water, an attempt to state the problem. *Geological Society of America Bulletin* 62: 1111–1148.
Rubie DC, Nimmo F, and Melosh HJ (2007) Formation of Earth's core. In: Stevenson D (ed.) *Evolution of the Earth*, pp. 51–90. Amsterdam: Elsevier.
Rüpke LH, Phipps Morgan J, and Dixon JE (2006) Implications of subduction rehydration for Earth's deep water cycle. In: Jacobsen SD and Lee Svd (eds.) *Earth's Deep Water Cycle*, pp. 263–276. Washington, DC: American Geophysical Union.
Rüpke LH, Phipps Morgan J, Hort M, and Connolly JAD (2004) Serpentine and the subduction zone water cycle. *Earth and Planetary Science Letters* 223: 17–34.
Saal AE, Hauri EH, Van Orman JA, and Rutherford MC (2013) Hydrogen isotopes in lunar volcanic glasses and melt inclusions reveal a carbonaceous chondrite heritage. *Science* 340: 1317–1320.
Safronov VS (1972) *Evolution of the Protoplanetary Cloud and Formation of the Earth and Planets*, p. 212. Jerusalem: Keter Publishing House.
Safronov VS (1978) The heating of the earth during its formation. *Icarus* 33: 3–12.
Sarda P, Staudacher T, and Allègre CJ (1985) $^{40}Ar/^{36}Ar$ in MORB glasses: Constraints on atmosphere and mantle evolution. *Earth and Planetary Science Letters* 72: 357–375.
Sasselov DD and Lecar M (2000) On the snow line in dusty protoplanetary disks. *The Astrophysical Journal* 528: 995–998.
Savage MK (1999) Seismic anisotropy and mantle deformation: What have we learned from shear wave splitting? *Review of Geophysics* 37: 65–106.
Schmandt B, Dueker K, Hansen SM, Jabinsek JJ, and Zhang Z (2011) A sporadic low-velocity layer atop the western U.S. mantle transition zone and short-wavelength variations in transition zone discontinuities. *Geochemistry, Geophysics, Geosystems* 12. http://dx.doi.org/10.1029/2011GC003668.
Schmidt MW and Poli S (1998) Experimentally based water budgets for dehydrating slabs and consequences for arc magma generation. *Earth and Planetary Science Letters* 163: 361–379.

Shankland TJ, Peyronneau J, and Poirier J-P (1993) Electrical conductivity of the Earth's lower mantle. *Nature* 399: 453–455.

Shcheka SS, Wiedenbeck M, Frost DJ, and Keppler H (2006) Carbon solubility in mantle minerals. *Earth and Planetary Science Letters* 245: 730–742.

Shearer PM (2000) Upper mantle discontinuities. In: Karato S, Forte AM, Liebermann RC, Masters G, and Stixrude L (eds.) *Earth's Deep Interior: Mineral Physics and Tomography from the Atomic to the Global Scales*, pp. 115–131. Washington, DC: American Geophysical Union.

Shibazaki Y, et al. (2012) Sound velocity measurements in dhcp-FeH to 70 GPa with inelastic X-ray scattering: Implications for the composition of the Earth's core. *Earth and Planetary Science Letters* 313(314): 79–85.

Shito A, Karato S, Matsukage KN, and Nishihara Y (2006) Toward mapping water content, temperature and major element chemistry in Earth's upper mantle from seismic tomography. In: Jacobsen SD and Lee Svd (eds.) *Earth's Deep Water Cycle*, pp. 225–236. Washington, DC: American Geophysical Union.

Shu FH, Adams FC, and Lizano S (1987) Star formation in molecular clouds: Observations and theory. *Annual Review of Astronomy and Astrophysics* 25: 23–81.

Sifré D, Gardés E, Massuyeau M, Hashin L, Hier-Majumder CA, and Gaillard F (2014) Electric conductivity during incipient melting in the oceanic low-velocity zone. *Nature* 509: 81–85.

Silver PG (1996) Seismic anisotropy and mantle deformation: Probing the depths of geology. *Annual Review of Earth and Planetary Sciences* 24: 385–432.

Sleep NH (1988) Gradual entrainment of a chemical layer at the base of the mantle by overlying convection. *Geophysical Journal of Royal Astronomical Society* 95: 437–447.

Sleep NH (1992) Archean plate tectonics: What can be learn from continental geology? *Canadian Journal of Earth Sciences* 29: 2066–2071.

Sleep NH (2001) Initiation of clement surface conditions on the earliest Earth. *Proceedings of National Academy of Sciences* 98: 3666–3672.

Smyth JR and Frost DJ (2002) The effect of water on the 410-km discontinuity: An experimental study. *Geophysical Research Letters* 29. http://dx.doi.org/10.129/2001GL014418.

Solomatov VS (2009) Magma oceans and primordial mantle differentiation. In: Stevenson DJ (ed.) *Evolution of the Earth*, pp. 91–119. Amsterdam: Elsevier.

Som SM, Catling DC, Harnmeijer JP, Polivka PM, and Buick R (2012) Air density 2.7 billion years ago limited to less than twice modern levels by fossil raindrop imprints. *Nature* 484: 359–362.

Stein M and Ben-Avraham Z (2007) Mechanisms of continental crust growth. In: Stevenson D (ed.) *Evolution of the Earth*, pp. 171–195. Amsterdam: Elsevier.

Stevenson DJ (1987) Origin of the moon—The collision hypothesis. *Annual Review of Earth and Planetary Sciences* 15: 271–315.

Stevenson DJ (1990) Fluid dynamics of core formation. In: Jones HENaJH (ed.) *Origin of the Earth*, pp. 231–249. Oxford: Oxford University Press.

Suetsugu D, Inoue T, Yamada A, Zhao D, and Obayashi M (2006) Towards mapping three-dimensional distribution of water in the transition zone from P-wave velocity tomography and 660-km discontinuity depths. In: Jacobsen SD and Lee Svd (eds.) *Earth's Deep Water Cycle*, pp. 237–249. Washington, DC: American Geophysical Union.

Takei Y (2002) Effect of pore geometry on Vp/Vs: From equilibrium geometry to crack. *Journal of Geophysical Research* 107. http://dx.doi.org/10.1029/2001JB000522.

Takei Y and Holtzman B (2009) Viscous constitutive relations of solid–liquid composites in terms of grain boundary contiguity: 1. Grain boundary diffusion control model. *Journal of Geophysical Research* 114. http://dx.doi.org/10.1029/2008JB005850.

Tarits P, Hautot S, and Perrier F (2004) Water in the mantle: Results from electrical conductivity beneath the French Alps. *Geophysical Research Letters* 31. http://dx.doi.org/10.1029/2003GL019277.

Tauzin B, Debayle E, and Wittingger G (2010) Seismic evidence for a global low-velocity layer within the Earth's upper mantle. *Nature Geoscience* 3: 718–721.

Tonks WB and Melosh HJ (1990) The physics of crystal settling and suspension in a turbulent magma ocean. In: Newsom HE and Jones JH (eds.) *Origin of the Earth*, pp. 151–174. New York: Oxford University Press.

Turcotte DL and Schubert G (1982) *Geodynamics: Applications of Continuum Physics to Geological Problems*, p. 450. New York: John Wiley & Sons.

Tyburczy JA, Frisch B, and Ahrens TJ (1986) Shock-induced volatile loss from a carbonaceous chondrite – Implications for planetary accretion. *Earth and Planetary Science Letters* 80: 201–207.

Tyburczy JA, Xu XM, Ahrens TJ, and Epstein S (2001) Shock-induced devolatilization and isotopic fractionation of H and C from Murchison meteorite: Some implications for planetary accretion. *Earth and Planetary Science Letters* 192: 23–30.

Ulmer P and Trommsdorff V (1995) Serpentine stability to mantle depths and subduction-related magmatism. *Science* 268: 858–861.

Urey HC (1952) *The Planets: Their Origin and Development*, p. 245. New Haven: Yale University Press.

Van Avendonk HJA, Holbrook WS, Lizarralde D, and Denyer P (2011) Structure and serpentinization of the subducting Cocos plate offshore Nicaragua and Costa Rica. *Geochemistry, Geophysics, Geosystems* 12. http://dx.doi.org/10.1029/2011GC003592.

van Keken PE, Hacker BR, Syracuse EM, and Abers GA (2011) Subduction factory 4: Depth-dependent flux of H_2O from subducting slabs worldwide. *Journal of Geophysical Research* 116. http://dx.doi.org/10.1029/2010JB007922.

van Thienen P, Benzerara K, Breuer D, et al. (2007) Water, life, and planetary geodynamical evolution. *Space Science Reviews* 129: 167–203.

Vattuone L, Smerieri M, Savio L, et al. (2013) Accretion disk origin of the Earth's water. *Philosophical Transactions of the Royal Society of London* A371. http://dx.doi.org/10.1098/rsta.2011.0585.

Walker JCG, Hays PB, and Kasting JF (1981) A negative feedback mechanism for the long-term stabilization of Earth's surface temperature. *Journal of Geophysical Research* 86: 9776–9782.

Wallmann K (2001) The geological water cycle and the evolution of marine $\delta^{18}O$ values. *Geochimica et Cosmochimica Acta* 65: 2469–2485.

Walter MJ, Kohn SC, Araujo D, et al. (2011) Deep mantle cycling of oceanic crust: Evidence from diamonds and their mineral inclusions. *Science* 334: 54–57.

Wang D, Karato S, and Jiang Z (2013) An experimental study of the influence of graphite on the electrical conductivity of olivine aggregate. *Geophysical Research Letters* 40: 2028–2032.

Wang D, Mookherjee M, Xu Y, and Karato S (2006) The effect of water on the electrical conductivity in olivine. *Nature* 443: 977–980.

Wang W and Takahashi E (2000) Subsolidus and melting experiments of K-doped peridotite KLB-1 to 27 GPa; Its geophysical and geochemical implications. *Journal of Geophysical Research* 105: 2855–2868.

Watson EB and Harrison TM (2005) Zircon thermometer reveals minimum melting conditions on earliest Earth. *Science* 308: 841–844.

Wetherill GW (1990) Formation of the Earth. *Annual Review of Earth and Planetary Sciences* 18: 205–256.

Williams JG, Boggs DH, Yoder CF, Ratcliff JT, and Dickey JO (2001) Lunar rotational dissipation in solid body and molten core. *Journal of Geophysical Research* 106: 27933–27968.

Williams Q and Hemley RJ (2001) Hydrogen in the deep Earth. *Annual Review of Earth and Planetary Sciences* 29: 365–418.

Wise DU (1974) Continental margins, freeboard and the volumes of continents and ocean through time. In: Burk CA and Drake CL (eds.) *Geology of Continental Margins*, pp. 45–58. New York: Springer.

Wood BJ and Halliday AN (2010) The lead isotopic age of the Earth can be explained by core formation alone. *Nature* 465: 767–771.

Wood BJ, Halliday A, and Rehkämper M (2010) Volatile accretion history of the Earth. *Nature* 567: E6–E7.

Wood BJ, Pawley AR, and Frost DR (1996) Water and carbon in the Earth's mantle. *Philosophical Transaction of Royal Society of London* 354: 1495–1511.

Worsley TR, Nance D, and Moody JB (1984) Global tectonics and eustasy for the past 2 billion years. *Marine Geology* 58: 373–400.

Wyllie PJ and Huang WL (1976) Carbonation and melting reactions in the system CaO–MgO–SiO_2–CO_2 at mantle pressure with geophysical and petrological applications. *Contributions to Mineralogy and Petrology* 54: 79–107.

Yang X (2012) Orientation-related electrical conductivity of hydrous olivine, clinopyroxene and plagioclase and implications for the structure of the lower continental crust and uppermost mantle. *Earth and Planetary Science Letters* 317(318): 241–250.

Yang X, Keppler H, McCammon C, and Ni H (2012) Electrical conductivity of orthopyroxene and plagioclase in the lower crust. *Contributions to Mineralogy and Petrology* 163: 33–48.

Yoneda S and Grossman L (1995) Condensation of CaO–MgO–Al_2O_3–SiO_2 liquids from cosmic gases. *Geochimica et Cosmochimica Acta* 59: 3413–3444.

Yoshino T, Nishihara Y, and Karato S (2007) Complete wetting of olivine grain-boundaries by a hydrous melt near the mantle transition zone. *Earth and Planetary Science Letters* 256: 466–472.

Yoshino T, Yamazaki D, and Mibe K (2009) Well-wetted olivine grain boundaries in partially molten peridotite in the asthenosphere. *Earth and Planetary Science Letters* 283: 167–173.

Young TE, Green HW II, Hofmeister AM, and Walker D (1993) Infrared spectroscopic investigation of hydroxyl in β-$(Mg, Fe)_2SiO_4$ and coexisting olivine: Implications for mantle evolution and dynamics. *Physics and Chemistry of Minerals* 19: 409–422.